



Recent progress in biologically active xanthenes

Arshdeep Singh^a, Navdeep Kaur^b, Sahil Sharma^{a*} and Preet Mohinder Singh Bedi^a

^aDepartment of Pharmaceutical Sciences, Guru Nanak Dev University, Amritsar, Punjab, India

^bDepartment of Chemistry, Guru Nanak Dev University, Amritsar, Punjab, India

ABSTRACT

Xanthone is a novel and pharmacologically important oxygen containing heterocyclic ring exhibiting variety of potent biological activities. This fused tricyclic ring is derived naturally from the plants of Bonnetiaceae and Clusiaceae family as well as synthesized by employing various synthetic protocols. Their wide range of reported therapeutic attributes include α -glucosidase inhibition, anti-cancer, anti-oxidant, anti-asthmatic, anti-convulsant, xanthine oxidase inhibition and anti-microbial. Among these attributes, anti-cancer and anti-oxidant potential are comprehensively studied as evidenced by number of research papers. Although, there is no marketed formulation containing xanthone derivatives except some herbal formulations, their medicinal properties can not be neglected at all. Promising activities revealed by these compounds chains their use and places them ahead as potential drug candidates for the future studies. Therefore, the present review article is entirely an assemblage of recent research work that has been done on xanthenes and their analogs as therapeutic agents. This review article can be reasonably encouraging for those engaged in the area of developing efficient and effective, single therapeutic agent exhibiting a wide range of biological activities involving xanthone as crucial and central nucleus.

Keywords: α -glucosidase inhibition, anti-cancer, anti-oxidant, anti-asthmatic, anti-convulsant, xanthine oxidase inhibition, anti-microbial

INTRODUCTION

Heterocycles coins an exceedingly important class of compounds that form the basis of many pharmaceutical, agrochemical and veterinary products [1-3]. Many natural drugs such as quinine, papaverine, emetine, theophylline, atropine, procaine, codeine, morphine and reserpine are heterocyclic in nature. There are large number of natural and synthetic heterocyclic compounds containing pyrrole, pyrrolidine, furan, thiophene, piperidine, pyridine and thiazole having important applications [4]. Some of the heterocyclic drugs possessing varied biological activities are shown in Figure 1.

Xanthone is a special class of oxygenated tricyclic compounds which exhibits various interesting biological activities depending upon the nature and pattern of substitutions [15-17]. Xanthenes are frequently valued as an effective pharmacophore in the field of medicinal chemistry [18]. Earlier, xanthenes were introduced as insecticide, larvicide and ovide codling moth eggs [19]. Later, it has been found in some scientific studies that xanthone derivatives can prevent the development of cancer cells and also possesses anti-inflammatory and anti-oxidant properties [20].

Xanthenes are derived naturally from the plants of Bonnetiaceae and Clusiaceae family and are also found in some species of Podostemaceae, Guttiferae and Gentianaceae family [21]. There are some herbal formulations in the market having xanthone derivative as one of their active ingredient:

- Xanthone Benefit Plus which is a herbal drink product [22].
- Xantho Plus capsules which is an anti-oxidant complex on the bases of Mangostin [23].
- MX3 (Mangostin Xanthone) capsules which is also a herbal product used as dietary supplement [24].

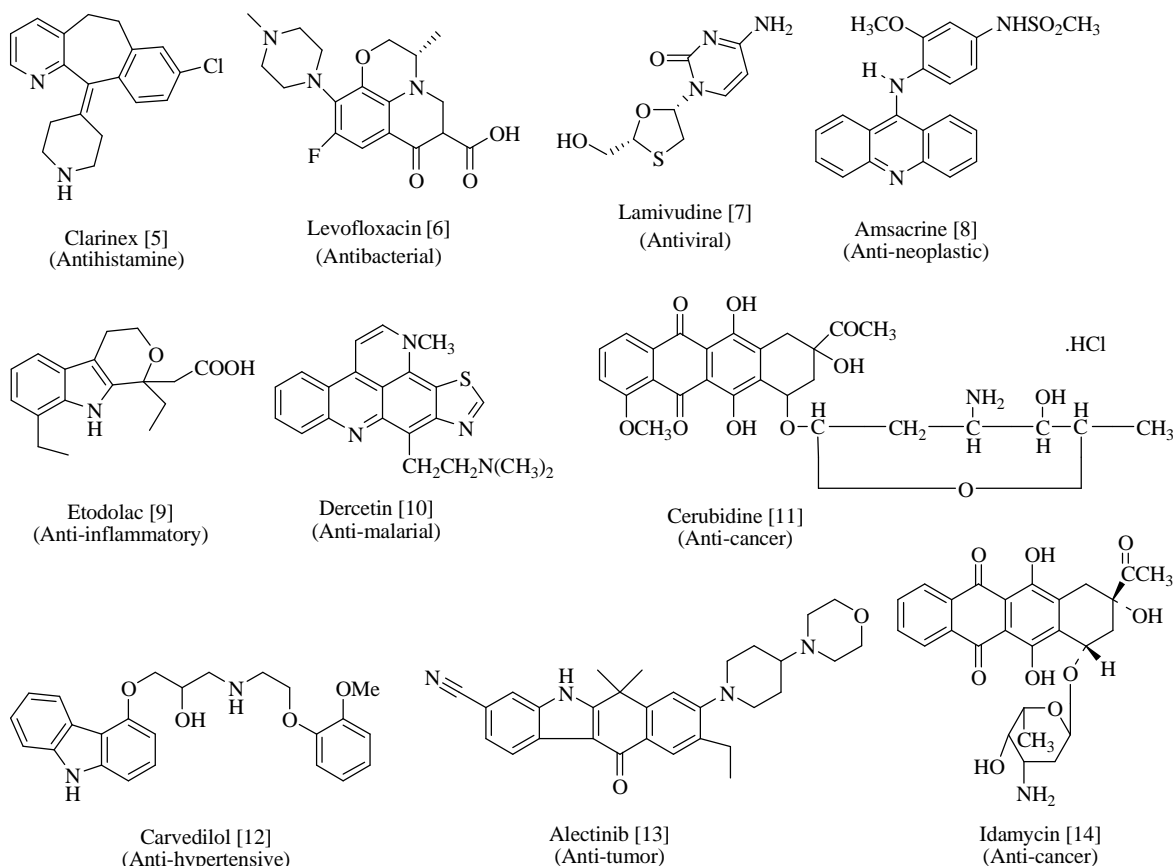


Figure 1. Heterocyclic based marketed drugs

The main component of these formulations is an extract from the well known fruit – Mangostin (*Garcinia mangostana*), which is also called the “Queen of fruits” mostly found in Malaysia and Southeast Asia. Mangostin extract contain xanthone derivatives i.e. 3-isomangostin, alpha mangostin, Gamma mangostin, Garcinone A, Garcinone B, C, D and E, maclurin, mangostenol (Figure 2). Over 200 naturally occurring xanthones which have been identified so far and approximately 40 of those are found in the mangostin.

In the early 80s, xanthone containing fruit, mangostin was used to treat diarrhea, dysentery, genitor-urinary infections, and also as a wash for aphthae of the mouth. Then in 90s xanthones were developed as insecticide. They also found use as ovicide, larvicide and in the preparation of xanthidrol, which is used in the determination of urea levels in the blood. In view of their therapeutic potential, lot of work has been done to explore the beneficial effects of this nucleus. Recent reports suggest that xanthones possess numerous medicinal properties such as, antiallergic, anti-inflammatory, antitubercular, antitumor, antiplatelet, anticonvulsant as well as β -adrenergic blocking property. These promising activities place xanthones ahead as potential drug candidates for the future studies.

Accordingly, xanthone moiety as a whole is active, possessing a number of biological activities already mentioned. One of the most common approaches to improve the therapeutic efficacy and the reduction of side effects is chemical medication which is of great interest at present. Xanthones are very restricted in occurrence, naturally and majority of them are found in just two families of higher plants – Guttiferae and Gentianaceae. Moreover, xanthones showed considerable biological potential, but surprisingly, none has an established use in medicine except some herbal medicines mentioned above. Presently, researchers are mainly focused on the synthetically modified xanthone derivatives having varied biological activities. Therefore, the present review article is entirely an assemblage of recent research work that has been done on xanthones and their analogs as therapeutic agents. This review article can be reasonably encouraging for those engaged in the area of developing efficient and effective, single therapeutic agent exhibiting a wide range of biological activities involving xanthone as crucial and central nucleus. The article would inevitably help the researchers to find some new xanthone derivative with good biological

activity and least side effects, which may, some day would help to bring new medicinal agents having xanthone as an active ingredient in market.

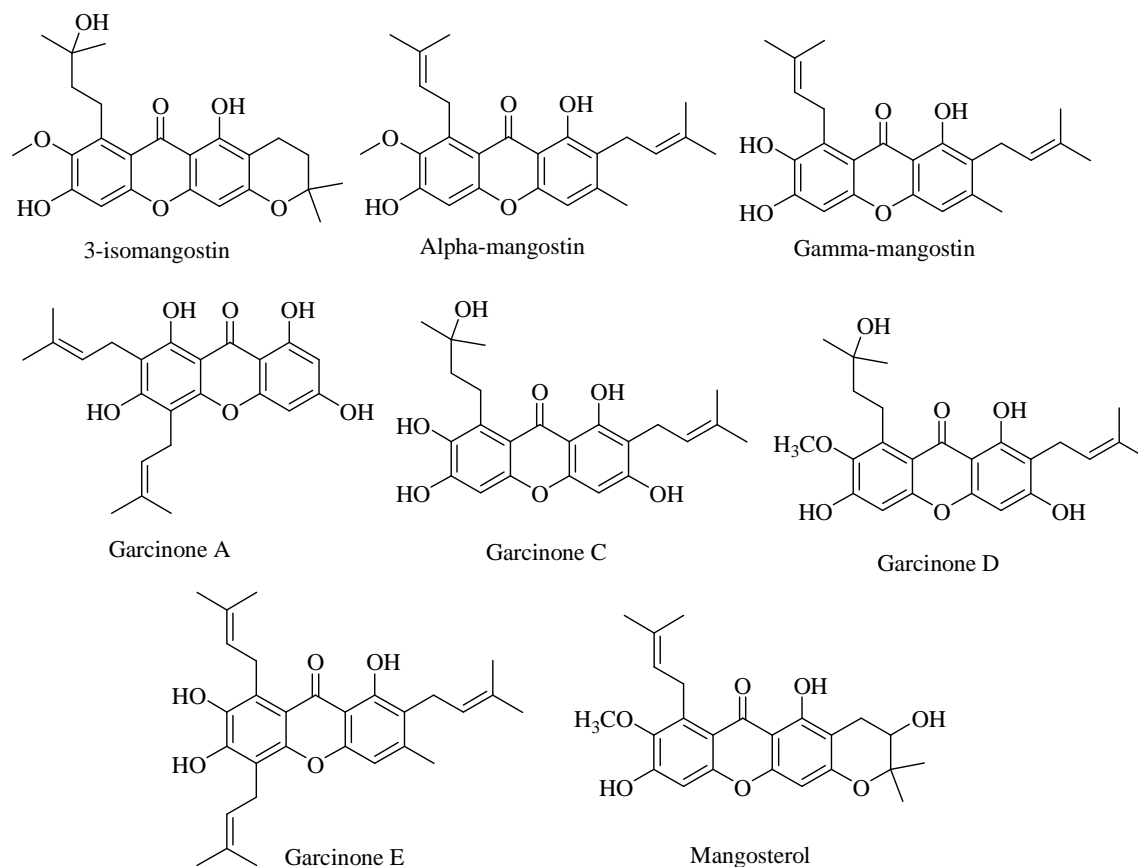


Figure 2. Xanthone derivatives present in marketed formulations

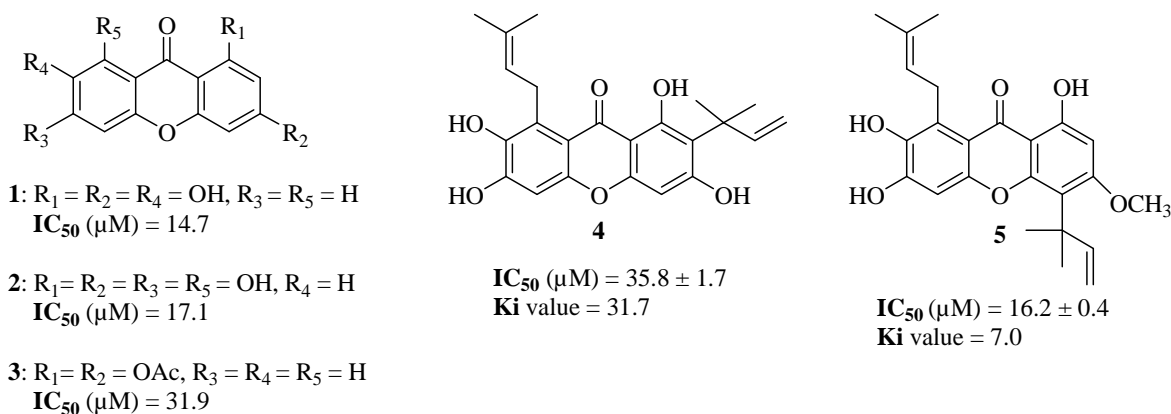
BIOLOGICAL ACTIVITIES OF XANTHONES

2-1. Xanthones as α -glucosidase inhibitors

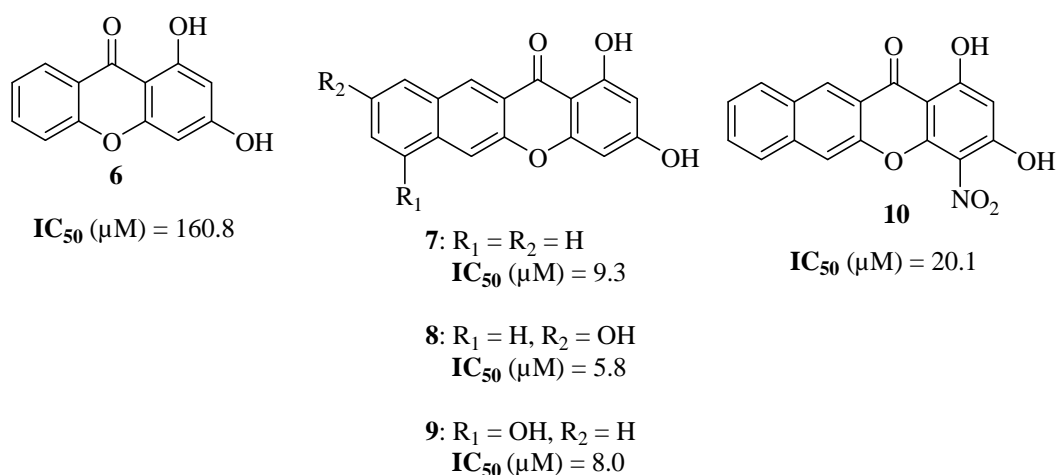
In 2006, Yan Liu *et al.* synthesized a series of hydroxyxanthones and their acetoxy and alkoxy derivatives **1**, **2**, **3** (Figure 3) and evaluated as α -glucosidase inhibitors. The results indicated that these xanthone derivatives were capable of inhibiting *in vitro* α -glucosidase with moderate to good activities. Among them, polyhydroxyxanthones exhibited the highest activities and thus may be exploitable as a lead compound for the development of potent α -glucosidase inhibitors [25].

The IC_{50} value was determined against yeast α -glucosidase in 50 μ M phosphate buffer (pH 6.8) at 37 $^{\circ}$ C (Figure 3). A classical α -glucosidase inhibitor, 1-deoxynojirimycin, was adopted as a positive control with an IC_{50} value of 26.4 μ M.

In 2007, Eun Jin Seo *et al.* proved that xanthones isolated from the root of *C.tricuspidata* possess highly potent α -glucosidase inhibition properties. Compound **4** and **5** was identified as a new isoprenylated tetrahydroxyxanthone; *1,3,6,7-tetrahydroxy-2-(3-methylbut-2-enyl)-8-(2-methylbut-3-en-2-yl)-9H-xanth en-9-one* **4**. These are the first natural xanthones documented to exhibit such inhibition. The IC_{50} values of compounds **4**, **5** inhibiting α -glucosidase activity were determined to be up to 16.2 μ M (Figure 3) [26].

Figure 3. Xanthenes exhibiting α -glucosidase inhibition properties

In 2007, Yan Liu *et al.* synthesized a series of novel xanthone derivatives with extended π -systems, that is, benzoxanthenes (Figure 4), and their structurally perturbed analogs as α -glucosidase inhibitors. Their inhibitory activities toward yeast's α -glucosidase were evaluated with the aim to enrich the structure–activity relationship. The results indicated that benzoxanthenes **7–9** were capable of inhibiting *in vitro* yeast's α -glucosidase 17 to 28 fold more strongly than xanthone derivative **6** that has smaller conjugated π -system. O-Methylation of 3-OH of benzoxanthone **10** and nitration at C4 position led to a large decrease in the activity. This indicates that 3-OH of benzoxanthone was crucial to the inhibitory activity, primarily as an H-bonding donor. The present results suggest that π – π stacking effect and H-bonding make substantial contributions to elicit the inhibitory activities of this general class of inhibitors [27]. Determined against yeast's α -glucosidase in 50 μM phosphate buffer (pH 6.8) containing 5% v/v DMSO at 37°C.

Figure 4. Xanthone derivatives with extended π -system

In 2008, Yan Liu *et al.* employed multiple linear regression (MLR) method to establish QSAR models for xanthone derivatives **11–25** (Figure 5), that have diverse structures, to provide deep insight into the correlation between inhibitory activities and structures of xanthenes. Among the 38 typical descriptors investigated, Hs (number of H-bond forming substituents), $N\pi$ (number of aromatic rings), and S (softness value) can be utilized to model the inhibitory activity. The Hs, $N\pi$, S and IC_{50} (Figure 5). Thus, inhibitory activities of xanthone derivatives can be regulated by H-bond forming substituents, π -stacking-forming aromatic rings and softness values on the xanthone skeleton [28].

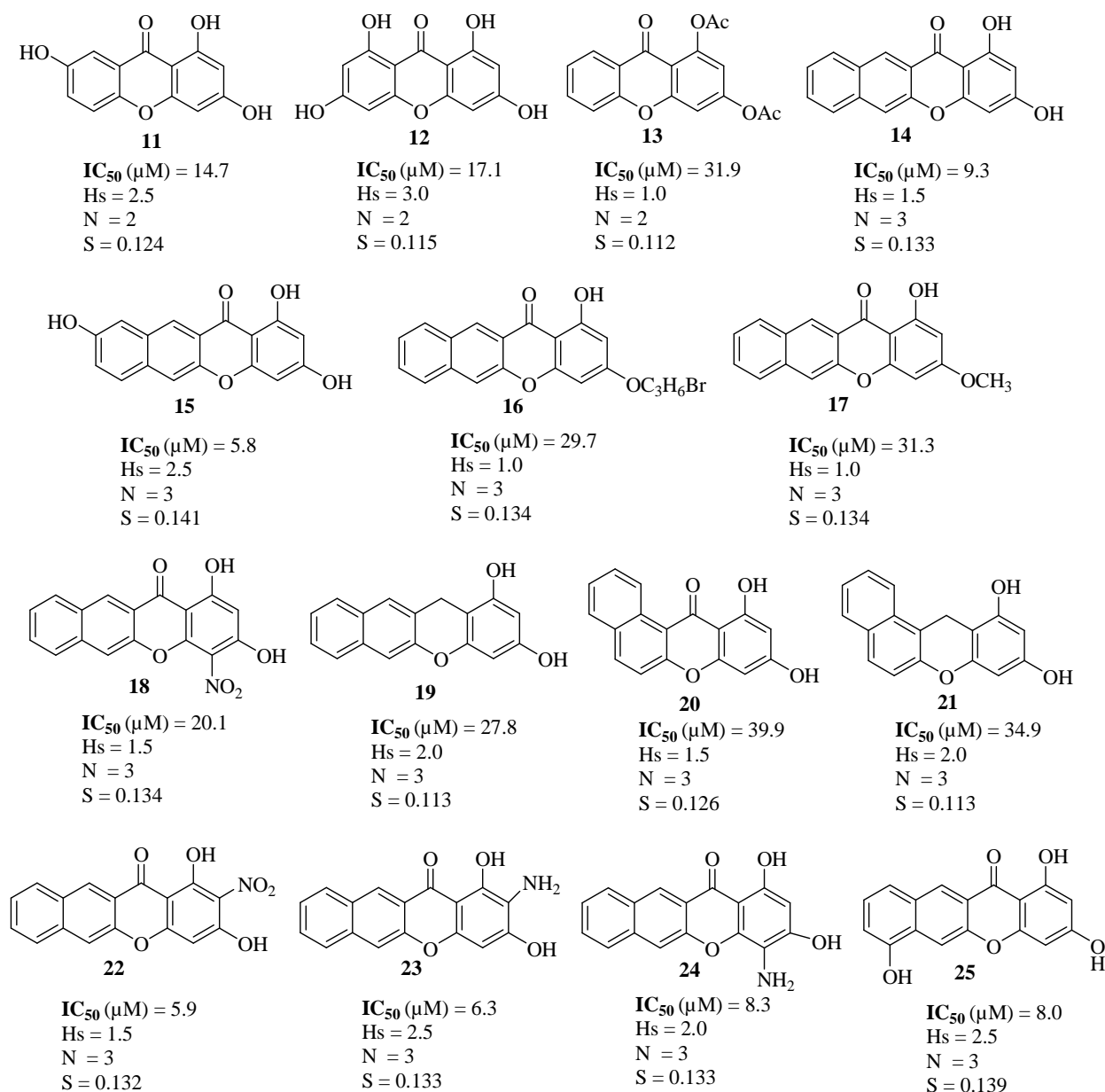


Figure 5. Xanthone derivatives and their H_s (number of h-bond forming substituents), N (π number of aromatic rings), and S (softness value)

In 2011, Gia Li Li *et al.* synthesized a series of novel xanthone derivatives **31-41** having non-coplanar and flexible structures as potent α -glucosidase inhibitors. Biological evaluation indicated that compounds **31-37** bearing one or two naphthol moieties exhibited up to 30-fold enhanced activities compared with their corresponding parent compounds **27-30**, whereas compounds **38-41** bearing one dihydroxynaphthalenyl group showed decreased activities compared with their corresponding analogs **31-34** having one naphthol group (Figure 6). Among them, compounds **32-33**, **35-37** and **40** were more active than 1-deoxynojirimycin, a well-known inhibitor for α -glucosidase. The structure-activity correlations suggested that inhibiting of α -glucosidase was a result of multiple interactions with the enzyme, including π -stacking, hydrophobic effect and conformational flexibility due to the structural non-coplanarity. In addition, compounds **29**, **33** and **40** showed non-competitive inhibition [29].

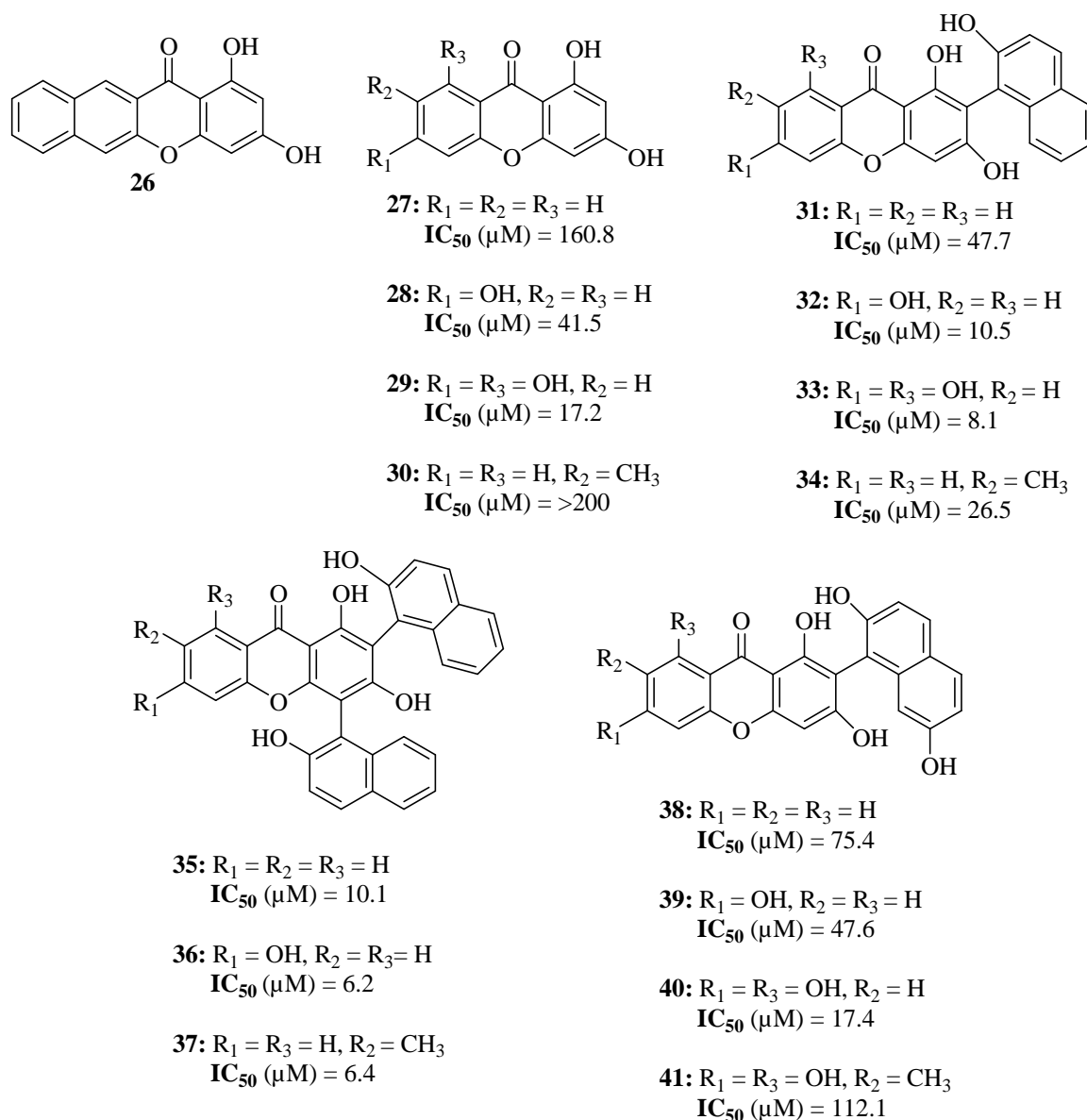


Figure 6. Xanthone derivatives having non-coplanar and flexible structures as potent α -glucosidase inhibitors

2-2. Anti-cancer xanthones

In 1991, Masahiro Aoki *et al.* reported Vinaxanthone **42** (Figure 7) a novel phospholipase C inhibitor, produced by *Penicillium vinaceum* Gilman and Abott NR6815. Its structure (MW 576, $C_{28}H_{16}O_{14}$) has been elucidated as a polycyclic xanthone with poly acidic functional groups based on various NMR studies including HMBC, COLOC, 2D-INADEQUATE and selective ID-INADEQUATE [30].

In 1998, Yuan-Jian Xu *et al.* discovered xanthone. A bioactivity-directed fractionation of the extracts of the Malaysian plant *Garcinia pavifolia* and a phytochemical study of *G. griffithii* led to the discovery of griffipavixanthone **43** (Figure 7), a novel cytotoxic bixanthone with cyclized prenyl groups providing the xanthone-xanthone linkage. Griffipavixanthone **43** showed high *in vitro* cytotoxicity against P388, LL/2 and Wehil64 cell lines with $ED_{50} = 3.40, 6.80$ and 4.60 $\mu g/ml$, respectively [31].

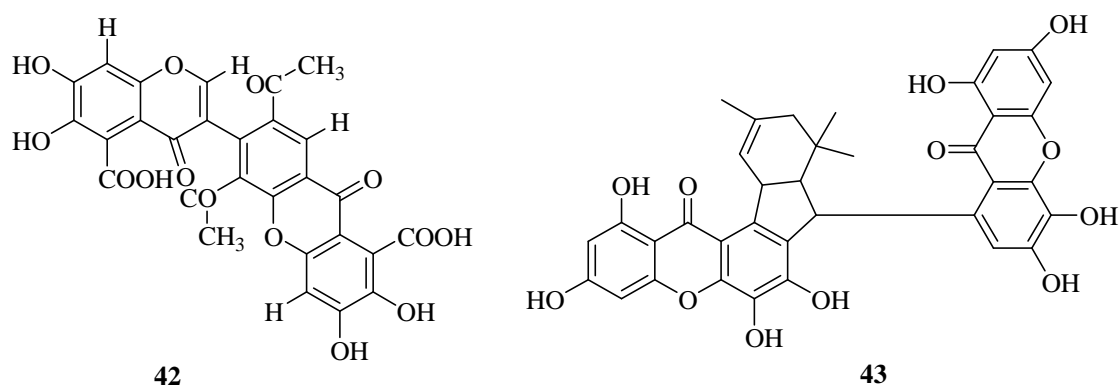
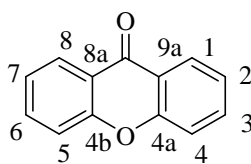


Figure 7. Vinaxanthone and Griffipavixanthone

In 2002, Madalena Pedro *et al.* evaluated xanthenes of Formula I **44-49** (Table 1) on the proliferation of human T-lymphocytes. Oxygenated xanthenes have been assessed for their capacity to inhibit *in vitro* the growth of three human cancer cell lines, MCF-7 (breast cancer), TK-10 (renal cancer) and UACC-62 (melanoma) (Table 1). Differences on their potency towards the effect on the growth of the human cancer cell lines as well as on the proliferation of human T-lymphocytes can be ascribed to the nature and positions of the substituents on the xanthonic nucleus [32].



Formula I

Table 1. Effects of xanthone derivatives of Formula I on the growth of human cancer cell lines and proliferation of human lymphocytes

Compounds		[GI ₅₀ (μM)]		[IC ₅₀ (μM)]	
		MCF-7 ^b (breast cancer)	TK-10 ^b (renal cancer)	UACC-62 ^b (melanoma)	Human lymphocytes ^c
44	Xanthone	>200	>200	>200	>200
45	1,2-Dihydroxy	38.4±2.7	65.8±5.1	14.0±0.3	73.3±2.2
46	1,7-Dihydroxy	57.1±11.0	60.1±9.6	51.3±9.6	20.2±0.2
47	2,3-Dihydroxy	40.6±1.3	61.4±4.3	31.7±3.7	31.3±1.5
48	3,4-Dihydroxy	40.5±1.5	59.2 ^a	21.6±2.6	12.2±1.3
49	2-Hydroxy-1-methoxy	24.1±3.0	35.2±7.6	39.3±10.6	11.6±0.8
50	5-Hydroxy-3-methoxy	66.1±12.6	30.9±2.3	37.7±6.7	111.2±8.3
51	1,3-Dihydroxy-2-methyl	21.9±0.4	34.3±3.8	20.0±0.5	84.4±12.4
52	2,3-Dihydroxy-4-methoxy	37.2 ^d	76.6±7.0	19.8±1.6	17.4±2.7

^aResults are expressed as GI₅₀ (concentrations of compounds that cause 50% inhibition of cancer cell growth) or IC₅₀ (concentrations that cause 50% inhibition of lymphocytes proliferation) and show means ±SEM of 3–6 independent observations performed in duplicate.

^bDoxorubicin was used as positive control in cancer cell lines growth (GI₅₀ MCF-7=42.8±8.2 nM; GI₅₀ TK-10=548.0±60.0 nM; GI₅₀ UACC-62=94.0±9.4 nM).

^cCyclosporin A was used as positive control in lymphocytes proliferation (IC₅₀=0.34±0.04 μM). ^dData based on two independently run duplicate experiments.

In 2002, Babita Madan *et al.* synthesised xanthenes bearing different functionalities, namely 1-hydroxyxanthone (**53**), 3-hydroxyxanthone (**54**), 1,4-dihydroxyxanthone (**55**), 2,6-dihydroxyxanthone (**56**), 1,2-diacetoxyxanthone (**57**), 2,6-diacetoxyxanthone (**58**), 3-methoxyxanthone (**59**), 1,3,7-trimethoxyxanthone (**60**) and 1,5-dihydroxy-6-methoxyxanthone (**61**) (Figure 8) and examined for their effect on nicotinamide adenine dinucleotide phosphate (NADPH)-catalysed liver microsomal lipid peroxidation and on tumour necrosis factor-α (TNF-α) induced expression of intercellular adhesion molecule-1 (ICAM-1) on endothelial cells, with a view to establish structure–activity relationship (Table 2). Hydroxy and acetoxy xanthenes showed potent inhibitory effects on NADPH-catalysed lipid peroxidation and TNF-α induced expression of ICAM-1 on endothelial cells (Table 3) [33].

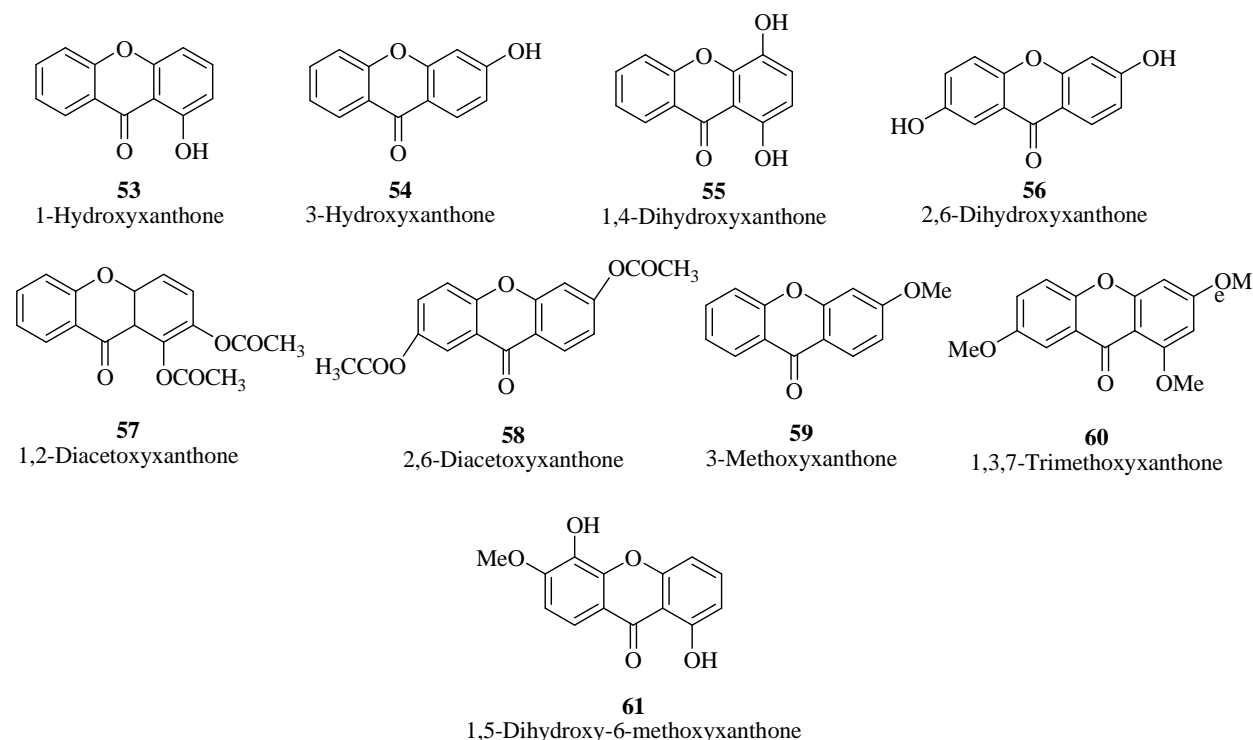


Figure 8. Xanthenes bearing different functionalities

Table 2. Effect of xanthenes on the TNF- α induced expression of ICAM-1 on endothelial cells

Serial No.	Compound name	Concentration ($\mu\text{g/mL}$) ^a	% Inhibition of ICAM-1 expression
53	1-Hydroxyxanthone	60	22.2
54	3-Hydroxyxanthone	66	13.7
55	1,4-Dihydroxyxanthone	65	86.0
56	2,6-Dihydroxyxanthone	18	40.9
57	1,2-Diacetoxymethoxyxanthone	75	42.4
58	2,6-Diacetoxymethoxyxanthone	100	23.8
59	3-Methoxyxanthone	46	0
60	1,3,7-Trimethoxyxanthone	13	0
61	1,5-Dihydroxy-6-methoxyxanthone	20	1.6

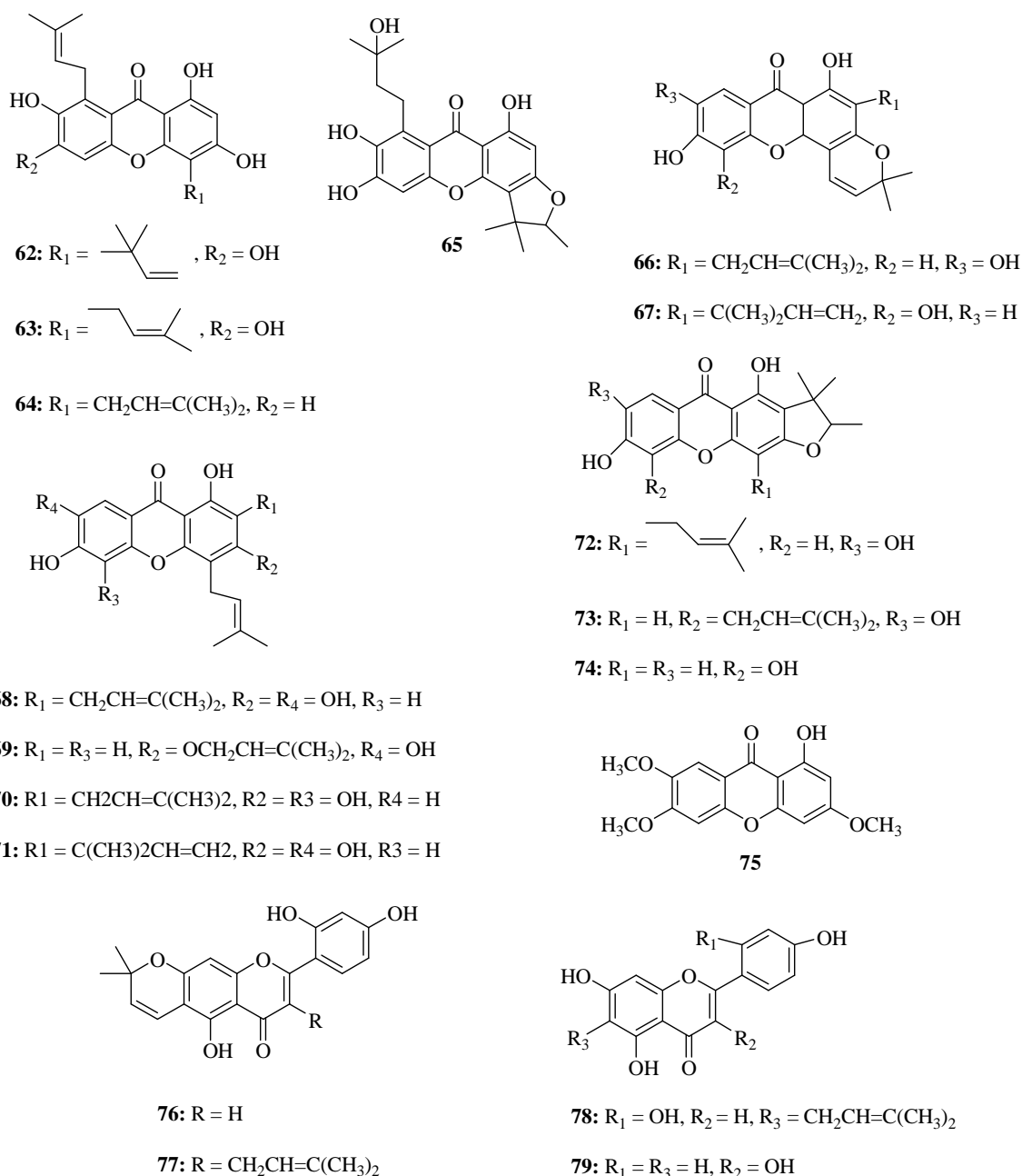
^aThe concentration levels of different compounds are based on their maximum tolerable concentrations by the cells.

Table 3. Effect of xanthenes on NADPH-dependent inhibition of lipid peroxidation initiation

SerialNo.	Compound name	NADPH-dependent lipid peroxidation initiation, percent of the control ^a
53	1-Hydroxyxanthone	28
54	3-Hydroxyxanthone	38
55	1,4-Dihydroxyxanthone	60
56	2,6-Dihydroxyxanthone	43
57	1,2-Diacetoxymethoxyxanthone	30
58	2,6-Diacetoxymethoxyxanthone	–
59	3-Methoxyxanthone	2
60	1,3,7-Tri-methoxyxanthone	0
61	1,5-Dihydroxy-6-methoxyxanthone	–

^aControl represents the assay in the absence of the test compounds and the values represent the average of four observations within an error range of 5.0%.

In 2004, Ying-Shu Zou *et al.* isolated eight new isoprenylated xanthenes, cudraticusxanthenes A–H (62–67), from the roots of *Cudrania tricuspidata*, together with ten known compounds, cudraxanthenes H (64) and M (73), xanthone V_{1a} (70), toxyloxanthone C (74), macluraxanthone B (71), 1-hydroxy-3, 6, 7-trimethoxyxanthone (75), cycloartocarpesin (76), artocarpesin (78), cudraflavone B (77), and kaempferol (79) (Figure 9). Their structures were characterized by spectroscopic methods. Xanthenes 68, 69, 73 and 74 showed inhibitory effects on four kinds of human digestive apparatus tumor cell lines (HCT-116, SMMC-7721, SGC-7901, and BGC-823) with IC₅₀ values of 1.6–11.8 $\mu\text{g/mL}$. Xanthenes 63, 66, and 70 displayed significant cytotoxicity against HCT-116, SMMC-7721 and SGC-7901 (IC₅₀=1.3–9.8 $\mu\text{g/mL}$). Flavonoids 76–77 were almost inactive (Table 4) [34].

Figure 9. Xanthones extracted from the roots of *Cudrania tricuspidata*Table 4. IC_{50} values ($\mu\text{g/ml}$) of compounds against human tumor cell lines

Compound	HCT-116	SMMC-7721	SGC-7901	BGC-823
Xanthones				
62	ND ^a	ND	ND	15.2
63	3.9	6.9	4.3	ND
64	ND	11.7	1.8	9.2
65	12.2	8.9	ND	ND
66	4.1	4.2	9.8	ND
68	4.7	4.2	5.4	1.6
69	1.8	2.7	3.4	1.6
70	1.3	6.2	3.4	ND
73	3.4	5.1	9.5	2.6
74	2.8	8.8	11.8	5.2
Flavonoids				
76	ND	ND	ND	ND
77	ND	ND	ND	7.2
78	ND	ND	ND	ND
Vincristine	0.0089	0.034	0.0029	19

^aND: not determined (IC_{50} values $>30 \mu\text{g/mL}$ not considered to be significant and not calculated).

In 2005, Kenji Matsumoto *et al.* investigated the anti-proliferative effects of four structurally similar prenylated xanthenes α -mangostin **80**, β -mangostin **81**, γ -mangostin **82**, and methoxy- β -mangostin **83** (Figure 10), in human colon cancer DLD-1 cells. These xanthenes differ in the number of hydroxyl and methoxy groups. Except for methoxy- β -mangostin, the other three xanthenes strongly inhibited cell growth at 20 μ M and their antitumor efficacy was correlated with the number of hydroxyl groups. Hoechst 33342 nuclear staining and nucleosomal DNA-gel electrophoresis revealed that the anti-proliferative effects of α - and γ -mangostin, but not that of β -mangostin, were associated with apoptosis. It was also shown that their anti-proliferative effects were associated with cell-cycle arrest by affecting the expression of cyclins, *cdc2*, and *p27*; G1 arrest was by α -mangostin and β -mangostin, and S arrest by γ -mangostin. These findings provide a relevant basis for the development of xanthenes as an agent for cancer prevention and combination therapy with anti-cancer drugs [35].

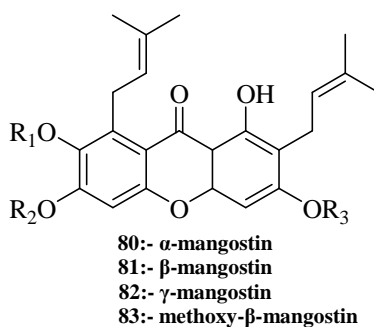


Figure 10. Prenylated xanthenes: α -mangostin, β -mangostin, γ -mangostin, and methoxy- β -mangostin

In 2006, E. M. Kithsiri Wijeratne *et al.* found new xanthenes. Bioassay-guided fractionation of a cytotoxic EtOAc extract of the fungal strain, *Chaetomium globosum*, inhabiting the rhizosphere of the Christmas cactus, *Opuntia leptocaulis*, of the Sonoran desert afforded a new dihydroxanthene, globosuxanthoneA **84**, a new tetrahydroxanthene, globosuxanthone B **85**, two new xanthenes, globosuxanthone C **86** and D **87** (Figure 11). Of the compounds encountered, **84** was found to exhibit strong cytotoxicity against a panel of seven human solid tumor cell lines, disrupt the cell cycle leading to the accumulation of cells in either G₂/M or S phase, and induce classic signs of apoptosis (Table 5) [36].

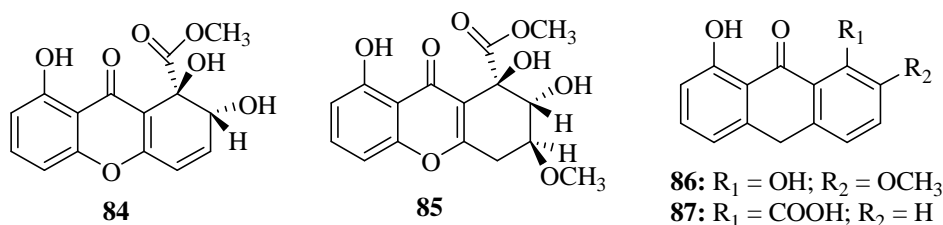


Figure 11. Dihydroxanthenes, tetrahydroxanthene and globosuxanthone

Table 5. Cytotoxicities (IC₅₀, μ M) of globosuxanthone (**84**) against a panel of seven human solid tumor cell lines

Cell line	NCI-H460	MCF-7	SF-268	PC-3	PC-3M	LNCaP	DU-145
84	3.6	1.3	1.1	0.65	1.1	1.5	1.2
Dox	0.01	0.07	0.04	ND	ND	ND	ND
Tax	0.01	0.01	0.02	ND	ND	ND	ND

Results are expressed as IC₅₀ values in μ M; ND, not determined.

NCI-H460, non-small cell lung cancer; MCF-7, breast cancer; SF-268, CNS cancer (glioma); PC-3, hormone- (androgen) independent prostate adenocarcinoma; PC-3M, highly metastatic variant of PC-3; LNCaP, hormone-sensitive prostate cancer; DU-145, hormone-independent prostate cancer.

Doxorubicin (Dox) and Taxol (Tax) were used as positive controls.

In 2007, Sangwook Woo *et al.* prepared some 3-(2',3'-epoxypropoxy)xanthenes and their epoxide ring opened halohydrin analogues **88-94** (Figure 12) and evaluated their cytotoxicity and topoisomerase II inhibition activity using doxorubicin and etoposide as references, respectively. Another xanthone compound **90**, 1,3-di(2',3'-epoxypropoxy)xanthone, was also synthesized and its DNA cross-linking property including other two biological activities investigated. The biological test results showed compound **90** possessed excellent cytotoxic and topoisomerase II inhibitory activity than other compounds tested (Table 6). It also exhibited significant DNA cross-linking activities [37].

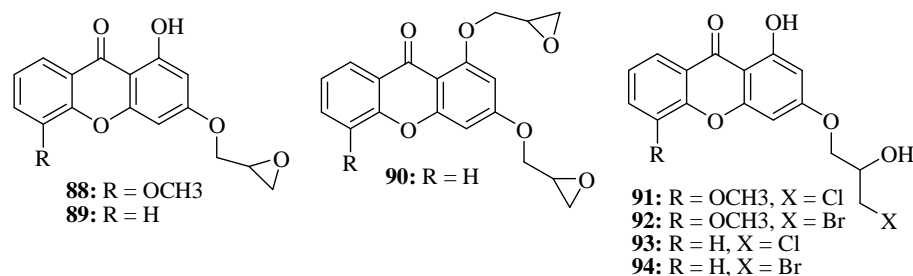


Figure 12. Some 3-(2,3-epoxypropoxy)xanthenes and their epoxide ring opened halohydrin analogues

Table 6. Cytotoxicities of compounds 88-90 against various human cancer cells

Cells (origin)/compound	IC ₅₀ ^a (μ M)							Adriamycin
	88	89	91	92	93	94	90	
LnCap (prostate)	>100	93.1 \pm 16.9	>100	>100	>100	64.4 \pm 3.1	9.0 \pm 0.2	4.6 \pm 0.6
MCF-7 (breast)	>100	68.4 \pm 4.8	>100	97.8 \pm 0.2	>100	53.5 \pm 5.4	3.2 \pm 0.8	4.5 \pm 0.3
HCT 116 (colon)	>100	80.8 \pm 3.1	31.4 \pm 3.0	>100	>100	16.9 \pm 0.5	10.2 \pm 0.7	7.7 \pm 0.2
MDA-MB231 (breast)	>100	>100	81.4 \pm 3.5	99.8 \pm 11.1	>100	76.3 \pm 5.0	12.8 \pm 0.9	17.6 \pm 0.3
Hela (cervix)	>100	68.7 \pm 8.7	60.3 \pm 3.3	>100	>100	98.1 \pm 6.3	23.3 \pm 1.7	3.3 \pm 0.4

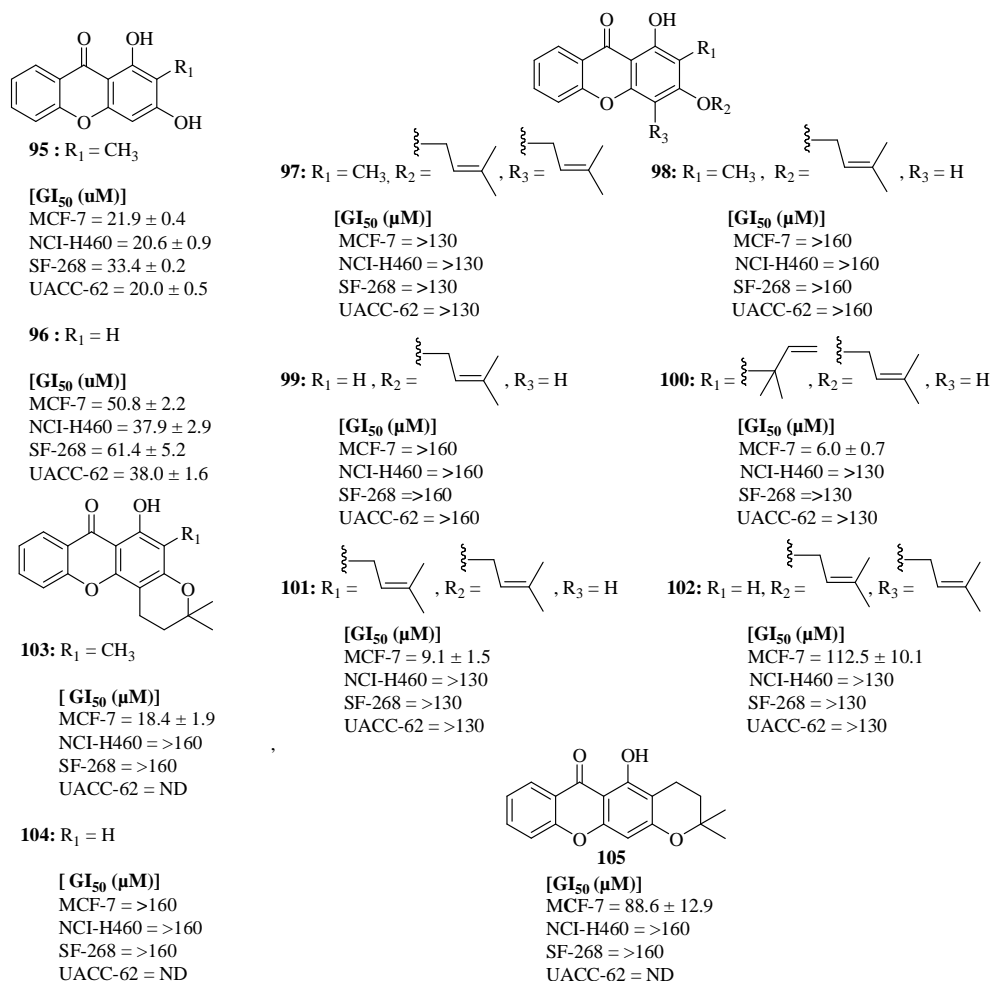
^a Each value is the average of four experiments.

Figure 13. Xanthenes with their anti-tumor activity against different cell lines

In 2007, Raquel A.P. Castanheiro *et al.* synthesized 11 xanthenes **95-105** (Figure 13). Structure elucidation, and antitumor activity of these xanthenes are reported, being the compounds **97**, **98**, **100-102** and **103** described for the first time. Xanthenes **95** and **96** were used as building blocks to obtain the prenylated derivatives **97-102**.

Prenylation was carried out using prenyl bromide in alkaline medium. Dihydropyranoxanthenes **103–105** were obtained from compounds **98** and **99** by an oxidative ring closure. The structure of the compounds was established by IR, UV, MS, and NMR (^1H , ^{13}C , COSY, HSQC, and HMBC) techniques and for compounds **98**, **100**, and **105** the structure was confirmed by X-ray crystallographic analysis. The effect of the 11 xanthenes on the *in vitro* growth of four human tumor cell lines, MCF-7 (breast adenocarcinoma), NCI-H460 (non small cell lung cancer), SF-268 (central nervous system cancer), and UACC-62 (melanoma) is also described (Figure 13) [38].

In 2008, Martine Varache-Lembege *et al.* synthesised several arylhydrazonomethyl derivatives of Formula II **106–123** (Table 7) in order to explore the antiproliferative effect associated with the xanthone framework, from various isomeric 1,3-dihydroxyxanthone carbaldehydes. Variation in the position of the aldehydic function led to three sets of compounds, bearing the hydrazonomethyl chain at positions 5, 6 or 7 on the xanthone nucleus, respectively. The anti-proliferative effect of the compounds was evaluated *in vitro* using the MTT colorimetric method against two human cancer cell lines (MCF-7, breast adenocarcinoma, and KB 3.1, squamous cell oral carcinoma) for two time periods (24 h and 72 h) (Table 7). Among the series, four compounds exhibited interesting growth inhibitory effects against both the cell lines, with IC_{50} values in the micromolar concentration range (Table 8). When compared with doxorubicin, the xanthone derivatives showed moderate cytotoxic effects. Surprisingly, unlike doxorubicin, these compounds displayed no significant time-dependent change in the concentration causing 50% inhibitory effect in proliferation. This unusual cytotoxicity profile led to the hypothesis that these molecules could be endowed with a mechanism of action distinct to that of doxorubicin [39].

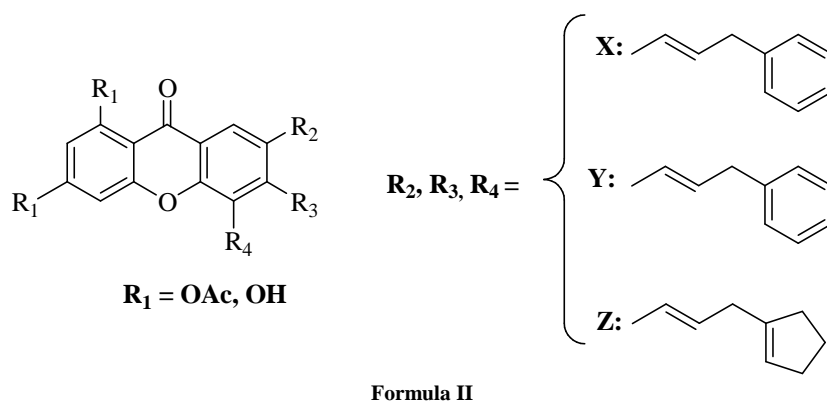


Table 7. Effects of studied xanthenes of Formula II on the viability of MCF-7 and KB 3.1 cells

Compound	R ₁	R ₂	R ₃	R ₄	MCF-7		KB 3.1	
					10 μM	1 μM	10 μM	1 μM
106	OAc	X	H	H	100	100	100	100
107	OH	X	H	H	72	100	82	100
108	OA	H	X	H	100	100	100	100
109	OH	H	X	H	100	100	61	100
110	OAc	H	H	X	100	100	82	100
111	OH	H	H	X	100	100	96	100
112	OAc	Y	H	H	70	85	60	98
113	OH	Y	H	H	41	58	90	95
114	OAc	H	Y	H	100	100	87	100
115	OH	H	Y	H	3	100	2	77
116	OAc	H	H	Y	79	80	90	95
117	OH	H	H	Y	12	86	3	96
118	OAc	Z	H	H	14	64	14	100
119	OH	Z	H	H	64	90	92	99
120	OAc	H	Z	H	13	35	13	85
121	OH	H	Z	H	70	73	80	93
122	OAc	H	H	Z	48	80	66	95
123	OH	H	H	Z	82	97	75	90

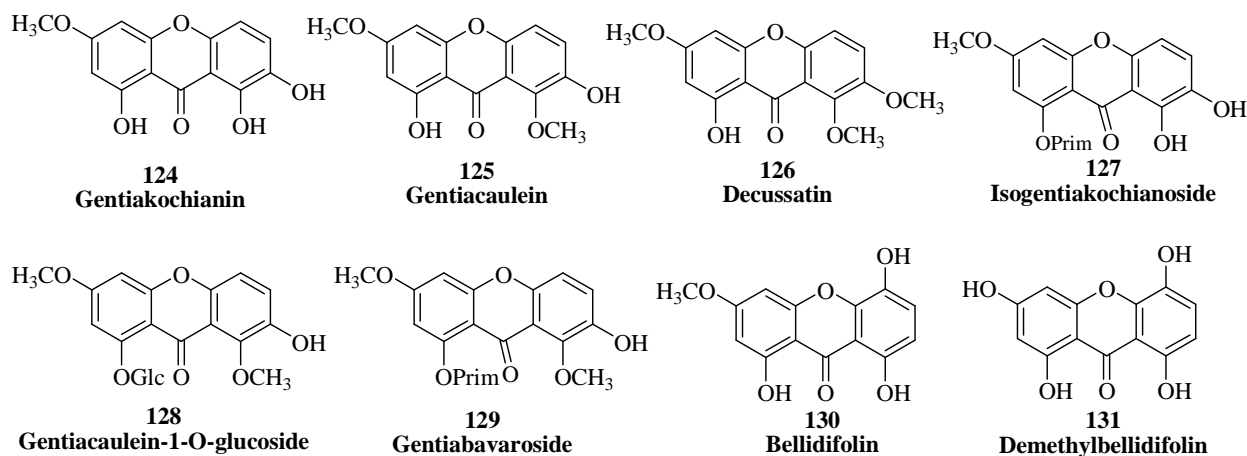
Viability was estimated as the percentage of living cells after incubation of the cells for 24 h with two concentrations (1 μM and 10 μM) of the molecules tested (100 indicates no activity; 0 indicates complete cell death) with final DMSO concentration of 0.1%.

Table 8. Effect of time of incubation on anti-proliferative activity against KB 3.1 and MCF-7 cells (IC₅₀, μM)

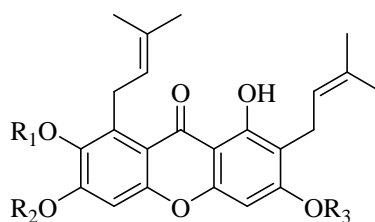
	KB 3.1			MCF-7		
	24 h	72 h	R _(24/72)	24 h	72 h	R _(24/72)
119	11.3 ± 1.1	4.7 ± 0.9	2.4	9.3 ± 1.3	7.0 ± 1.0	1.3
120	1.6 ± 0.3	1.8 ± 0.4	0.9	1.9 ± 0.4	2.4 ± 0.2	0.8
122	6.8 ± 0.6	6.5 ± 0.3	1.05	5.1 ± 0.6	5.6 ± 0.5	0.9
Doxorubicin	0.010 ± 0.003	0.0004 ± 0.0001	25.0	0.018 ± 0.004	0.0007 ± 0.0001	25.7

Cell viability after a further 96-h period in fresh culture medium was estimated as the compound concentration required for 50% growth inhibition. For each drug, a R_(24/72) value was calculated and represents the ratio of the IC₅₀s (μM) obtained after 24-h and 72-h treatment, respectively. Data represent mean values (±S.D.) for three independent experiments.

In 2008, Aleksandra Isakovic *et al.* studied that xanthenes gentiakochianin and gentiacaulein derivatives **124-131** (Figure 14) as the active principles responsible for the in vitro anti-glioma action of ether and methanolic extracts of the plant *Gentiana kochiana*. Gentiakochianin and gentiacaulein induced cell cycle arrest in G₂/M and G₀/G₁ phases, respectively, in both C6 rat glioma and U251 human glioma cell lines. The more efficient anti-proliferative action of gentiakochianin was associated with its ability to induce microtubule stabilization in a cell-free assay. Both the xanthenes reduced mitochondrial membrane potential and increased the production of reactive oxygen species in glioma cells, but only the effects of gentiakochianin were pronounced enough to cause caspase activation and subsequent apoptotic cell death. The assessment of structure-activity relationship in a series of structurally related xanthenes from *G. kochiana* and *Gentianella austriaca* revealed dihydroxylation at positions 7, 8 of the xanthonic nucleus as the key structural feature responsible for the ability of gentiakochianin to induce microtubule-associated G₂/M cell block and apoptotic cell death in glioma cells [40].

**Figure 14. Xanthenes gentiakochianin and gentiacaulein derivatives**

In 2008, Tomohiro Itoh *et al.* indicated the anticancer activity induced by xanthenes such as α-mangostin **132**, β-mangostin **133** and γ-mangostin **134** (Figure 15) which were major constituents of the pericarp of mangostin fruits. They examined the effect of xanthenes on cell degranulation in rat basophilic leukemia RBL-2H3 cells. Antigen (Ag)-mediated stimulation of high affinity IgE receptor (FcεRI) activates intracellular signal transductions resulting in the release of biologically active mediators such as histamine. The release of histamine and other inflammatory mediators from mast cell or basophils is the primary event in several allergic responses. These xanthenes suppressed the release of histamine from IgE-sensitized RBL-2H3 cells. In order to reveal the inhibitory mechanism of degranulation by xanthenes, they examined the activation of intracellular signaling molecules such as Lyn, Syk, and PLCγs. All the xanthenes tested significantly suppressed the signaling involving Syk and PLCγs. In Ag-mediated activation of FcεRI on mast cells, three major subfamilies of mitogen-activated protein kinases were activated. The xanthenes decreased the level of phospho-ERKs. Furthermore, the levels of phospho-ERKs were observed to be regulated by Syk/LAT/Ras/ERK pathway rather than PKC/Raf/ERK pathway, suggesting that the inhibitory mechanism of xanthenes was mainly due to suppression of the Syk/ PLCγs /PKC pathway. Although intracellular free Ca²⁺ concentration ([Ca²⁺]_i) was elevated by FcεRI activation, it was found that α- or γ-mangostin treatment was reduced the [Ca²⁺]_i elevation by suppressed Ca²⁺ influx [41].



132: a-Mangostin: $R_1=CH_3$, $R_2=R_3=H$

133: b-Mangostin: $R_1=R_3=CH_3$, $R_2=H$

134: g-Mangostin: $R_1=R_2=R_3=H$

Figure 15. Xanthenes: α -mangostin, β -mangostin and γ -mangostin

In 2009, Emilia Sousa *et al.* synthesised bis-intercalators, a bisxanthone and a minor product, 1-(6-bromohexyloxy)-xanthone. The synthesized compounds bis-alkoxyxanthone **135**, bromoalkoxyxanthone **136**, dihydroxyxanthone **137**, hydroxybromoalkoxyxanthone **138** and bis-bromoalkoxyxanthone **139** (Figure 16) showed no capacity to inhibit the growth of human tumor cell lines was observed for the bisxanthone, the bromoalkoxyxanthone revealed this biological activity. In light of these results bromoalkylation of 3,4-dihydroxyxanthone furnished two bromohexyloxyxanthenes that were investigated for their effect on the *in vitro* growth of human tumor cell lines MCF-7 (ER+, breast), MDA-MB-231 (ER-, breast), NCI-H460 (non-small lung), and SF-268 (central nervous system) (Table 9). The X-ray structure of 1-(6-bromohexyloxy)-xanthone revealed that the xanthone skeleton remains essentially planar forming a dihedral angle of $61.3(2)^\circ$ with the 6-bromohexyl side chain. These results revealed bromoalkoxyxanthenes as interesting scaffolds to look for potential anticancer drugs [42].

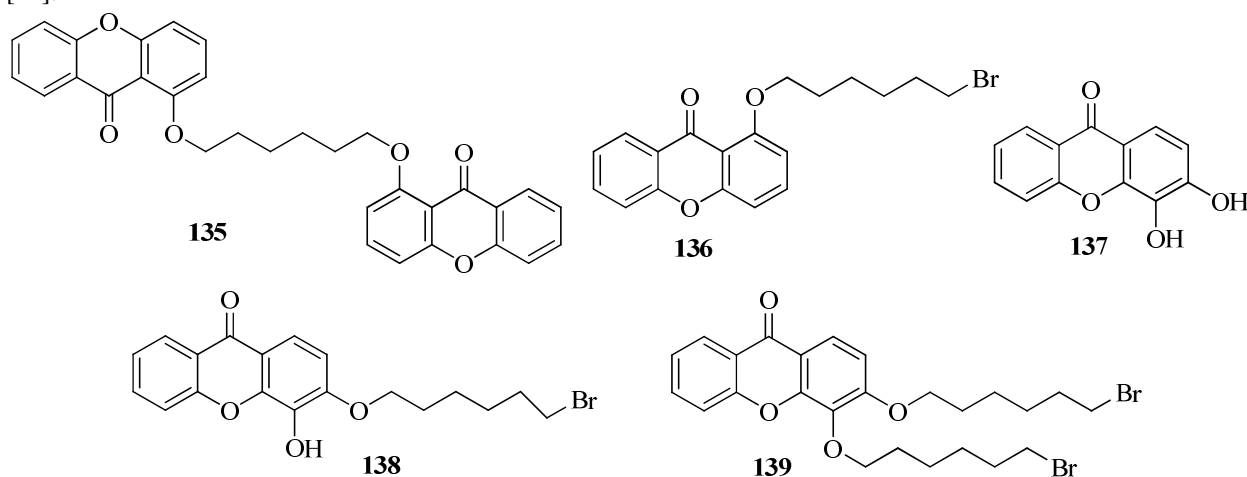


Figure 16. Bis intercalators xanthone derivatives

Table 9. Effect of compounds on the growth of human tumor cell lines

Compounds	GI ₅₀ (μ M)			
	SF-268	NCI-H460	MCF-7	MDA-MB-231
135	>100	>100	>100	>100
136	30.2 \pm 3.6	30.7 \pm 3.2	22.7 \pm 1.3	>100
137	22.6	11.4	52.4 \pm 6.3	22.8 \pm 4.8
138	>100	>100	>100	>100
139	>100	>100	20.5 \pm 1.9	56.8 \pm 11.2

Results are given in concentrations that were able to cause 50% of cell growth inhibition (GI₅₀) after a continuous exposure of 48 h and represent means \pm SEM of 3–5 independent experiments performed in duplicate and carried out independently.

Doxorubicin was used as positive control, GI₅₀: MCF-7 = 42.8 \pm 8.2 nM; MDA-MB-231 = 10.86 \pm 1.28 nM; SF-268 = 94.0 \pm 7.0 nM; NCI-H460 = 94.0 \pm 8.7 nM. ND = not determinate.

In 2009, Hui-Fang Wang *et al.* synthesized and characterized two new complexes ZnL₂.2H₂O **140** and CuL₂.2H₂O **141** (HL = 1-hydroxy 6-(2-(1-piperidinyloxy)ethoxy)xanthone) (Figure.17). Their interactions with calf thymus DNA (ct DNA) were investigated by absorption spectroscopy, fluorescence spectroscopy, ethidium bromide (EB) displacement experiments, circular dichroism spectroscopy and viscosity measurements. Experimental results

suggested that there were intercalative interactions of the complexes with DNA. The binding affinity of complex **141** was higher than that of **140**. In addition, the cytotoxic effects of both complexes were evaluated with lung adenocarcinoma (GLC-82), esophagus squamous cancer (ECA109) and human gastric cancer (SGC7901) cells using MTT assay (Table 10). Both were potent exhibiting significant cytotoxicity in vitro [43].

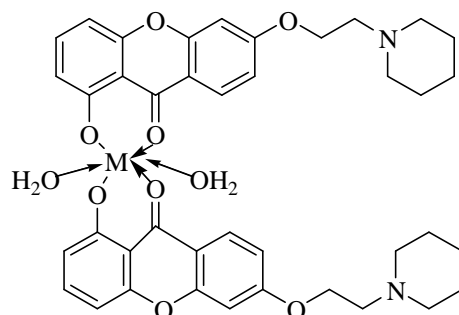
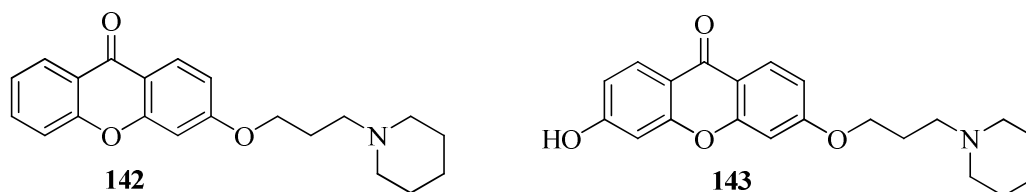


Figure 17. Metal complex of xanthone

Table 10. IC₅₀ values for the cell growth inhibition

Compound	IC ₅₀ value (μM)		
	GLC-82	ECA109	SGC7901
140	22.08	>50	19.98
141	16.20	21.04	15.40

In 2011, Jen-Hao Cheng *et al.* prepared xanthenes to develop novel antioxidant as anticancer agents. In vitro screening, the synthetic xanthenes revealed significant inhibitory effects on xanthine oxidase and ABTS radical-cation scavenging activity. The selective compounds **142** and **143** (Figure 18) induced an accumulation of NTUB1 cells in the G₁ phase arrest and cellular apoptosis by the increase of ROS level. The combination of cisplatin and **141** significantly enhanced the cell death in NTUB1 cells. Compounds **142** and **143** did not show cytotoxic activity in selected concentrations against SV-HUC1 cells. The present results suggested that antioxidants **142** and **143** may be used as anticancer agent for enhancing the therapeutic efficacy of anticancer agents and to reduce their side effect [44].



Xanthine oxidase inhibitory activity of 136:

IC₅₀ (μM) : 37.8 ± 3.9

Free radical scavenging activity of 1 of ABTS:

IC₅₀ (μM) : 90.0 ± 4.9

Xanthine oxidase inhibitory activity of 137:

IC₅₀ (μM) : 82.3 ± 2.8

Free radical scavenging activity of 2 of ABTS:

IC₅₀ (μM) : 69.3 ± 2.6

Figure 18. Novel xanthenes antioxidant as anticancer agents

In 2011, Kyu-Yeon Jun *et al.* synthesized Epoxide ring-opened xanthone derivatives **144**, **145**, **146**, **147** (Figure 19) and tested for their topoisomerase inhibitory activity and cytotoxicity. These compounds showed no activity against human topo I at the same concentration, where camptothecin inhibited 69% human topo I mediated relaxation of supercoiled pBR322 (Table 11). Most of the compounds showed topo II α specific inhibitory activity. To clarify the mechanism of action of these compounds, the most potent compound (compound **145**) of the synthesized analogues was further studied by testing its ATPase inhibitory activity and through molecular docking experiments. The results showed that the topo II α inhibitory activity of compound **145** was inversely proportional to ATP concentration. In the ATPase inhibitory test, ATP hydrolysis was reduced less efficiently by compound **145** (28.5 ± 4.6%) than novobiocin (60.4 ± 8.1%). Molecular docking study revealed compound **145** to have a stable binding pattern to the ATP-binding domain of human topo II [45].

The cytotoxicity assay for compounds was accomplished with a range of human tumor cell lines. The inhibitory

activities (IC_{50}) are presented as the micromolar concentrations of the compounds, as listed in (Table 12).

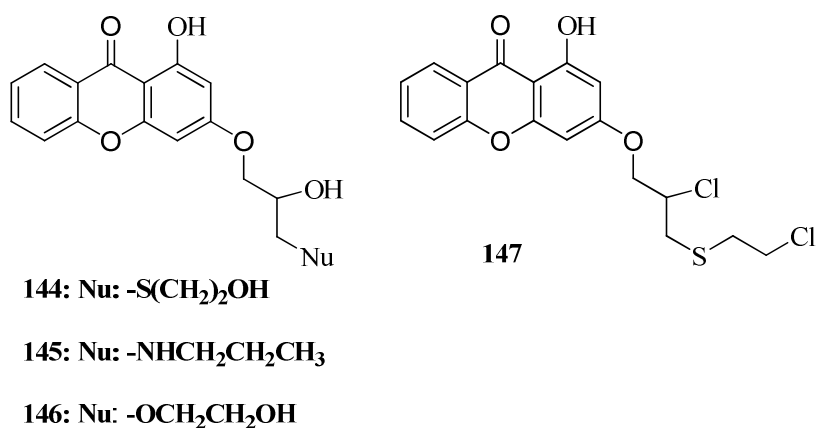


Figure 19. Epoxide ring-opened xanthone derivatives

Table 11. Topo I and II inhibitory activities of compounds

Compounds	Topo I (% inhibition)		Topo II (% inhibition)	
	20 μM	10 μM	20 μM	100 μM
Camptothecin	69.15			
Etoposide		26.04	39.11	77.07
144	0.00	26.32	49.09	63.75
145	0.00	41.23	70.01	100.00
146	0.00	23.43	43.68	89.25
147	0.00	15.80	22.24	45.33

Table 12. Cytotoxicities of compounds against the five cancer cell lines

Compd/cells	IC_{50}^a (μM)				
	HeLa	HCT116	DU145	MDA-MB231	HL60
Adriamycin	1.32 ± 0.15	6.81 ± 1.43	2.47 ± 1.03	0.84 ± 0.08	0.32 ± 0.07
Etoposide	2.36 ± 0.47	9.50 ± 1.35	2.19 ± 0.79	1.23 ± 0.38	1.28 ± 0.07
Camptothecin	1.08 ± 0.07	3.97 ± 0.76	0.31 ± 0.03	0.97 ± 0.07	0.065 ± 0.004
144	9.15 ± 2.69	23.94 ± 4.58	3.47 ± 1.80	5.13 ± 1.65	19.86 ± 2.48
145	11.62 ± 0.11	23.71 ± 1.77	0.76 ± 0.39	4.11 ± 0.57	4.15 ± 2.09
146	15.38 ± 1.04	46.70 ± 5.98	15.55 ± 2.15	10.41 ± 2.59	16.58 ± 0.64
147	4.64 ± 2.03	14.80 ± 0.26	0.004 ± 0.001	1.32 ± 0.07	3.41 ± 1.30

^a Each data point represents the mean \pm SD of three different experiments performed in triplicate. The cell lines used were HeLa, human cervix tumor cell line; HCT116, human colorectal carcinoma cell line; DU145, human prostate tumor cell line; MDA-MB231, human breast adenocarcinoma cell line; HL60, human myelogenous leukemia cell line.

In 2012, Chiao-Ting Yen *et al.* synthesized a series of prenyl- and pyrano-xanthones **148**, **149**, **150** (Figure 20) derived from 1,3,6-trihydroxy-9H-xanthen-9-one, a basic backbone of gambogic acid (GA) and evaluated for in vitro cytotoxic effects against four human cancer cell lines (KB, KBvin, A549, and DU-145) and anti-inflammatory activity toward superoxide anion generation and elastase release by human neutrophils in response to fMLP/CB. Among them, prenylxanthones were generally less active than pyranoxanthones in both anticancer and anti-inflammatory assays. Two angular 3,3-dimethylpyranoxanthones (**148** and **150**) showed the greatest and selective activity against the KBv in multidrug resistant (MDR) cell line with IC_{50} values of 0.9 and 0.8 $\mu g/mL$, respectively. An angular 3-methyl-3-prenylpyranoxanthone (**149**) selectively inhibited elastase release with 200 times more potency than phenylmethylsulfonyl fluoride (PMSF), the positive control. The inhibitory effect of the test drugs on cell viability was measured by the MTT colorimetric method [46].

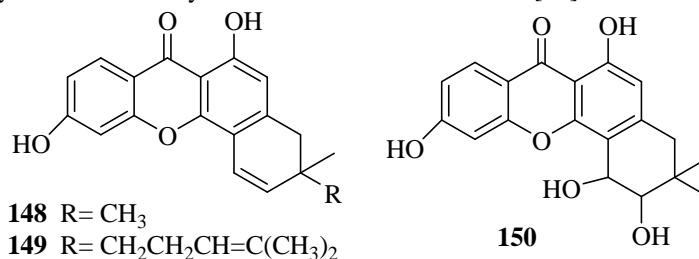


Figure 20. Prenyl- and pyrano-xanthones

In 2013, Dya Fita Dibwe *et al.* found that the $CHCl_3$ extract of the roots of *Securidaca longe pedunculata*

(Polygalaceae), collected at Democratic Republic of Congo, killed PANC-1 human pancreatic cancer cells preferentially in nutrient-deprived medium (NDM). Phytochemical investigation on the CHCl₃ extract led to the isolation of compounds including five new polymethoxylated xanthenes [1,6,8-trihydroxy-2,3,4,5-tetramethoxyxanthone (**151**), 1,6-dihydroxy-2,3,4,5,8-pentamethoxyxanthone (**152**), 8-hydroxy-1,4,5,6-tetramethoxy-2,3-methylenedioxyxanthone (**153**), 4,6,8-trihydroxy-1,2,3,5-tetramethoxyxanthone (**154**), 4,8-dihydroxy-1,2,3,5,6-pentamethoxyxanthone (**155**)] and a new benzyl benzoate [benzyl 3-hydroxy-2-methoxybenzoate (**156**)] (Figure 21). Among them, 1,6,8-trihydroxy-2,3,4,5-tetramethoxyxanthone (**151**) and 1,6-dihydroxy-2,3,4,5,8-pentamethoxyxanthone (**152**) displayed the potent preferential cytotoxicity with PC₅₀ of 22.8 and 17.4 μM, respectively (Table 13). They triggered apoptosis-like PANC-1 cell death in NDM with a glucose-sensitive mode [47].

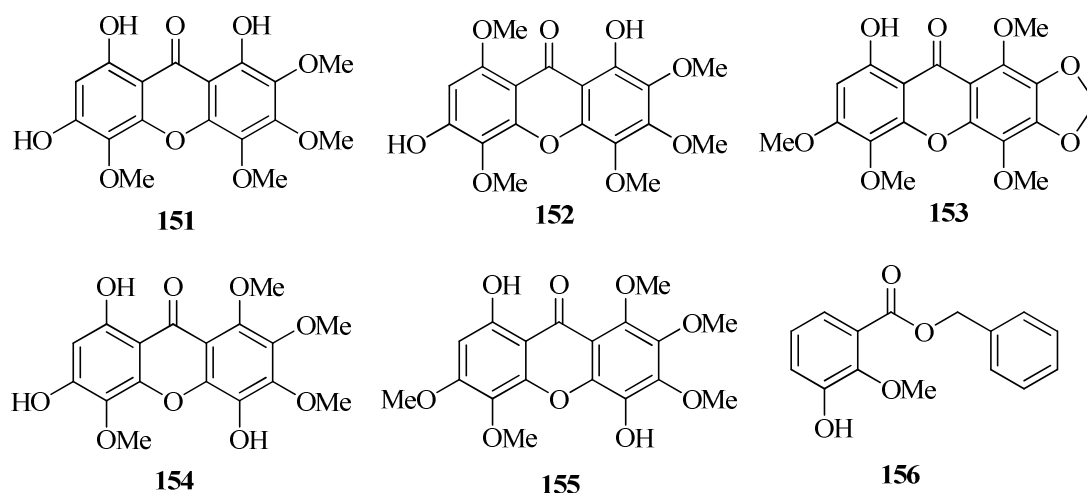


Figure 21. Polymethoxylated xanthenes

Table 13. Preferential cytotoxicity of compounds on human pancreatic cancer PANC-1 cells in NDM

Compound	PC ₅₀ (μM)
151	22.7
152	17.4
Others	>100
Arctigenin ^a	0.5
Taxol ^b	>100

^{a,b} Positive and negative controls, respectively.

In 2013, Carlos M. G. Azevedo *et al.* optimized antitumor xanthone derivatives with their GI₅₀ values **157-165** (Figure 22) following a multidimensional approach that involved the synthesis of analogues, the study of their lipophilicity and solubility, and the evaluation of their growth inhibitory activity on four human tumor cell lines. A new synthetic route for the hit xanthone derivative was also developed and applied for the synthesis of its analogues. Among the used cell lines, the HL-60 showed to be in general more sensitive to the compounds tested, with the most potent compound **157** having a GI₅₀ of 5.1 μM, lower than the hit compound. Lipophilicity was evaluated by the partition coefficient (K_p) of a solute between buffer and two membrane models, namely liposomes and micelles. The Partition coefficients in liposomes-buffer and micelle-buffer for synthesized compounds are also shown (Table 14) [48].

Table 14. Partition coefficients in liposomes-buffer and micelle-buffer for compounds synthesized

Compounds	LogK _p liposomes	LogK _p micelles
157	3.35 ± 0.02	3.28 ± 0.02
158	3.25 ± 0.08	3.35 ± 0.04
159	3.86 ± 0.08	3.92 ± 0.01
160	3.53 ± 0.04	3.58 ± 0.01
161	3.32 ± 0.10	3.76 ± 0.0
162	4.02 ± 0.03	4.01 ± 0.06
163	—	3.90 ± 0.06
165	4.62 ± 0.02	4.70 ± 0.04

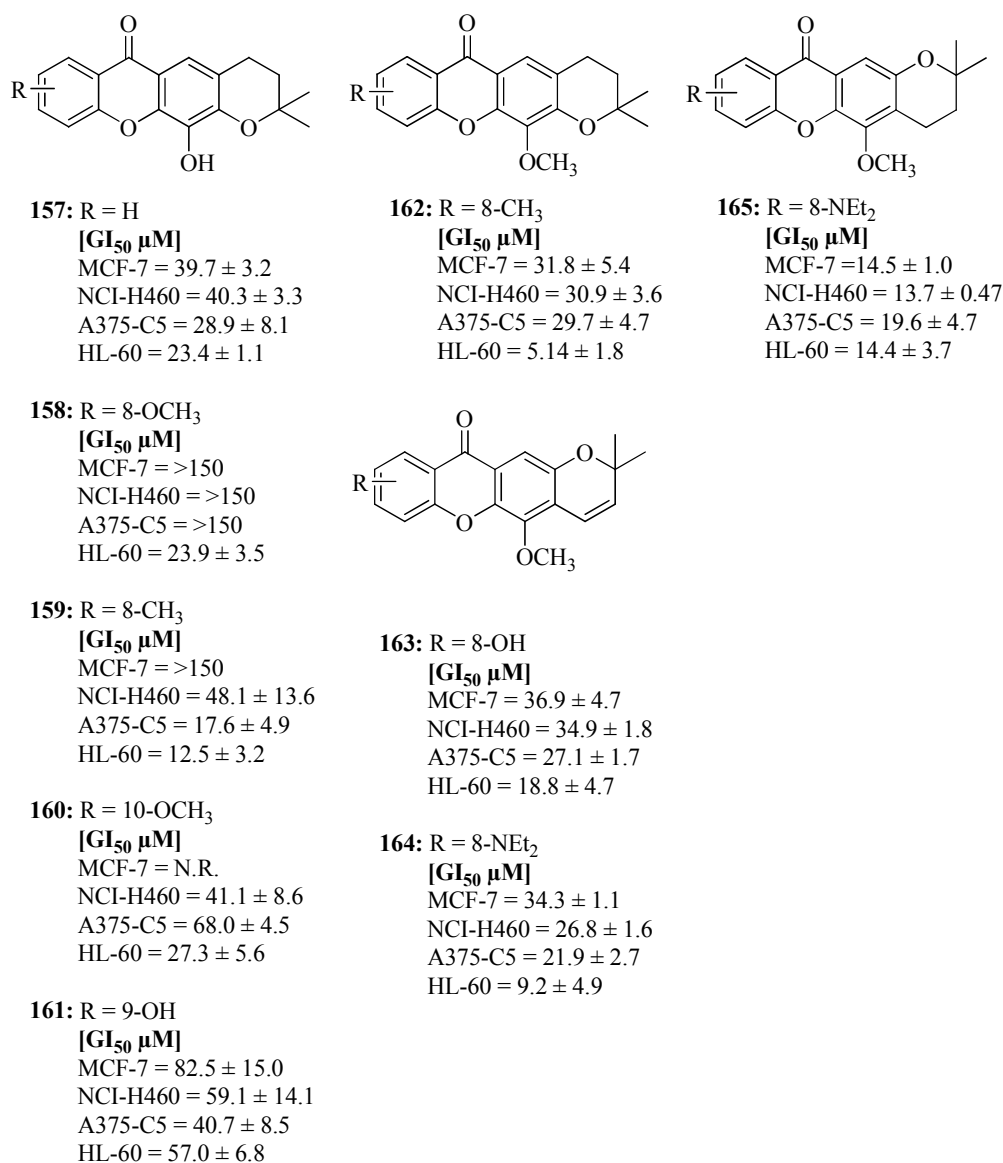


Figure 22. Antitumor xanthone derivatives

In 2013, Carlos M.G. Azevedo *et al.* synthesized new pyranoxanthenes **165-176** (Figure 23). The benzopyran and dihydrobenzopyran moieties can be considered as “privileged motifs” in drug discovery being good platforms for the search of new bioactive compounds. Accordingly, with the aim of rationalizing the importance of the fused ring orientation and oxygenation pattern in pyranoxanthenes, this study describes the synthesis of new pyranoxanthenes and evaluation of their cell growth inhibitory activity in four human tumor cell lines as well as their lipophilicity (Table 15 and Table 16) [49].

Table 15. Cell growth inhibitory activity in four human tumor cell lines

Compound	GI ₅₀ (μM)			
	MCF-7	NCI-H460	A375-C5	HL-60
166	13.3 ± 1.3	32.9 ± 7.1	6.2 ± 0.6	3.2 ± 0.7
168	39.6 ± 0.6	31.7 ± 2.6	29.6 ± 4.7	38.9 ± 9.8
169	45.1 ± 3.3	47.3 ± 6.0	42.5 ± 5.5	31.8 ± 6.1
170	88.6 ± 12.9	>160	N.D.	N.D.
171	50.9 ± 3.5	44.5 ± 1.4	37.9 ± 6.5	36.7 ± 3.3
172	>150	>150	>150	8.8 ± 5.9
173	107.9 ± 13.9	>150	>150	>70
174	N.R.	N.R.	69.5 ± 5.9	9.6 ± 1.7
175	39.7 ± 3.2	40.3 ± 3.3	28.9 ± 8.1	23.4 ± 1.1
176	N.R.	42.9 ± 16.1	47.4 ± 4.1	9.6 ± 3.2

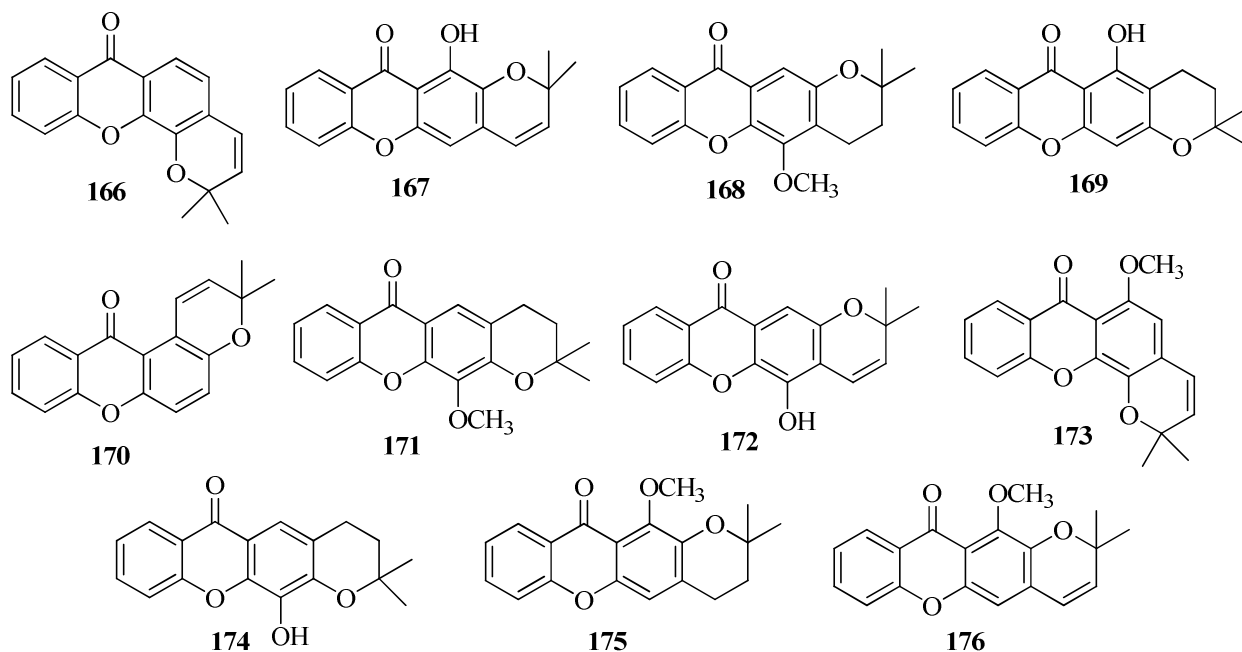


Figure 23. Pyranoxanthenes

Table 16. Partition coefficients in liposomes-buffer and micelle-buffer for a chemical library of Pyranoxanthenes

Compound	Log K_p liposomes	Log K_p micelles
166	3.42 ± 0.02	3.50 ± 0.12
167	4.17 ± 0.06	4.15 ± 0.08
168	3.92 ± 0.04	3.88 ± 0.02
169	-	4.32 ± 0.04
170	4.14 ± 0.08	4.10 ± 0.04
171	3.60 ± 0.08	3.59 ± 0.06
172	3.06 ± 0.16	3.29 ± 0.06
173	3.32 ± 0.12	3.33 ± 0.02
174	3.35 ± 0.02	3.28 ± 0.02
175	3.09 ± 0.18	3.58 ± 0.08
176	3.54 ± 0.01	3.76 ± 0.03

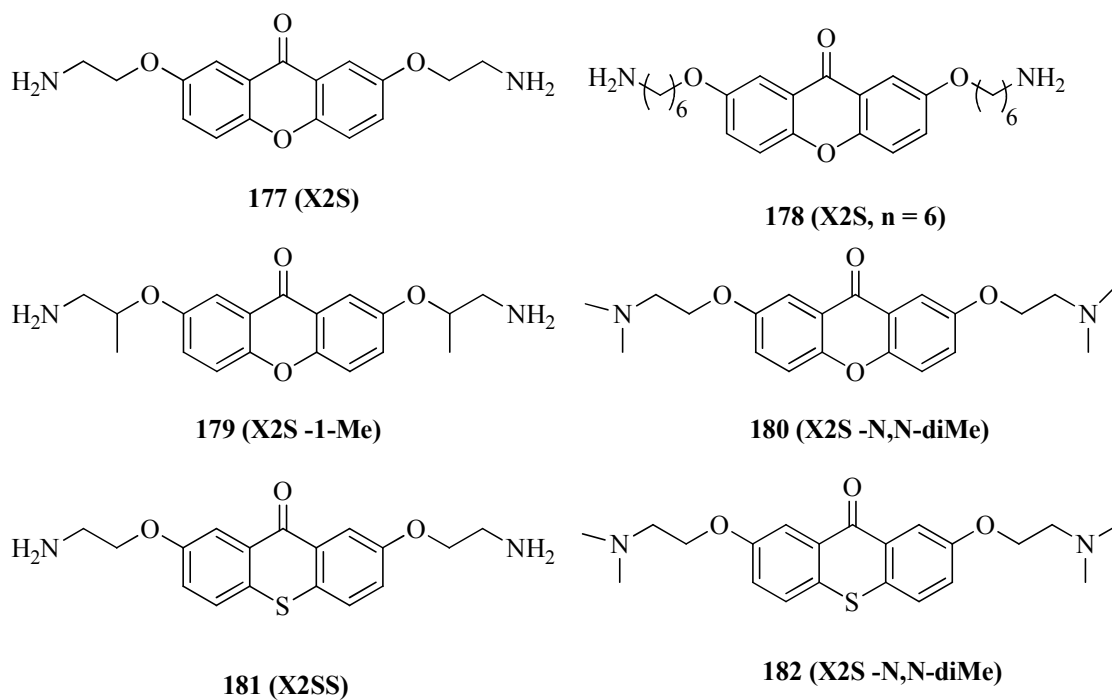


Figure 24. Aminoalkoxy-substituted thioxanthone derivatives

In 2013, Asako Murata *et al.* demonstrated that an aminoalkoxy-substituted thioxanthone derivatives **177-182** (Figure 24) interferes Dicer-mediated processing of pre-miRNA. Various biological processes have been found to be regulated by miRNA-mediated gene silencing. A small molecule that modulates the miRNA pathway will provide the biological tool for elucidating mechanisms of miRNA-mediated gene regulation, and can be the drug lead for miRNA related diseases [50].

In 2013, So-Eun Park *et al.* prepared several alkylamine ($n = 3-6$) **183-192** (Figure 25) and evaluated for the pharmacological activity and mode of action. In the topoisomerase II α (topo II α) inhibition test, compound **186** showed strongest inhibitory activity among the compounds at 10 μM . Inhibitory activities (topo I and topo II) of the compounds are in the order of **186** ($n = 4$) > **177** ($n = 3$) >> **187** ($n = 5$) \approx **188** ($n = 6$); **190** ($n = 4$) >> **189** ($n = 3$) \approx **191** ($n = 5$) \approx **192** ($n = 6$) where n is the number of carbon in the aliphatic side chain in ring C (Table 17) and compounds **189-192** have additional methoxy group in ring A compared to compounds **185, 186-188**. Compound **186** showed efficient cytotoxicities against T47D (IC_{50} : $0.93 \pm 0.04 \mu\text{M}$) and HCT15 (IC_{50} : $0.78 \pm 0.01 \mu\text{M}$) cells, which are higher than etoposide (Table 18). Compound **186** was also an ATP-competitive human topo II α catalytic inhibitor with partially blocking human topo II α -catalyzed ATP hydrolysis and intercalating into DNA. Compound **186** induced much less DNA damage than etoposide in HCT15 human colorectal carcinoma cells. Overall, compound **186** can be a potential anticancer agent acting as topo II α catalytic inhibitor with low DNA damage [51].

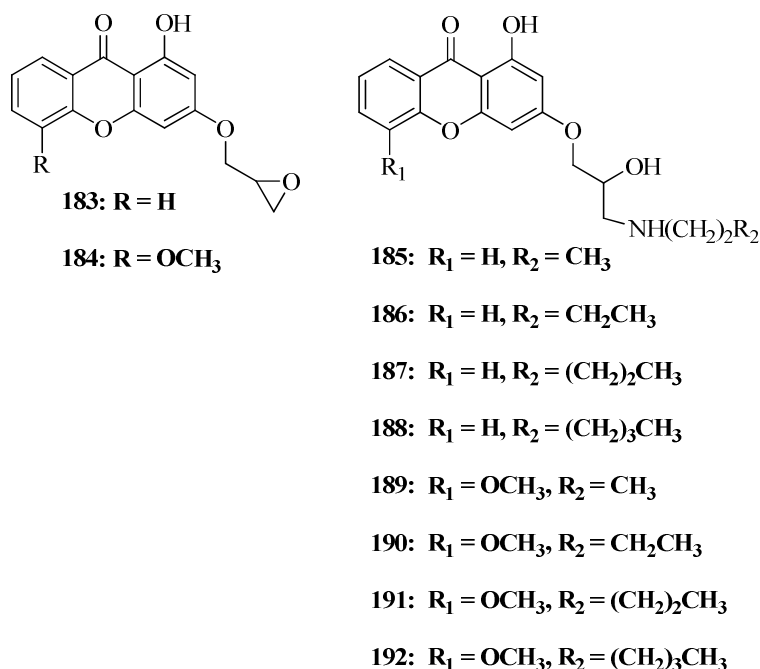


Figure 25. Alkylamine xanthone derivatives

Table 17. Topo I and IIa inhibitory activities of compounds

Compounds	Topo I(% inhibition)		Topo II (% inhibition)		
	20 μM	10 μM	20 μM	100 μM	IC ₅₀ (μM)
Concentration					
Camptothecin	26.1	--	--	--	--
Etoposide	-	18.0	30.2	82.1	28.2 \pm 0.47
185	0.0	50.2	60.2	93.8	10.4 \pm 0.15
186	0.0	64.0	67.7	95.1	9.0 \pm 0.08
187	3.0	0.7	52.1	92.9	16.4 \pm 4.81
188	0.0	0.0	43.6	80.7	19.7 \pm 1.22
189	0.0	6.0	64.4	100.0	12.0 \pm 0.09
190	0.0	24.2	68.1	100.0	11.2 \pm 0.97
191	0.0	2.0	62.6	100.0	13.8 \pm 2.15
192	0.0	0.0	61.2	100.0	13.8 \pm 2.15

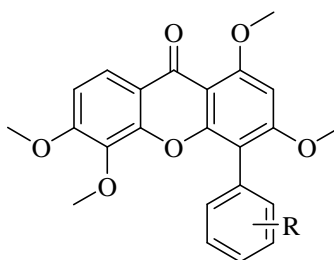
Table 18. Cytotoxicities of compounds 1, 4-10 against cancer cell lines

Compd/cells	IC ₅₀ ^a (μM)			
	T47D	HCT15	DU145	HEK293
Adriamycin	0.41 ± 0.09	1.38 ± 0.39	2.68 ± 0.51	3.07 ± 1.67
Etoposide	3.42 ± 2.26	5.12 ± 3.64	9.29 ± 0.71	0.72 ± 0.11
Camptothecin	0.3 ± 0.09	0.42 ± 0.10	0.39 ± 0.34	0.78 ± 0.87
185	6.49 ± 0.09	5.49 ± 0.13	1.98 ± 0.12	4.28 ± 0.03
186	0.93 ± 0.04	0.78 ± 0.01	1.98 ± 0.01	3.44 ± 0.08
187	1.62 ± 0.02	0.71 ± 0.004	1.13 ± 0.11	2.65 ± 0.04
188	1.28 ± 0.03	1.53 ± 0.11	1.15 ± 0.02	1.45 ± 0.01
189	3.33 ± 0.14	5.39 ± 0.08	1.48 ± 0.08	3.62 ± 0.66
190	2.97 ± 0.04	9.11 ± 0.9	3.31 ± 0.06	1.74 ± 0.03
191	9.80 ± 0.07	1.00 ± 0.004	0.91 ± 0.02	7.22 ± 0.97
192	6.17 ± 0.02	6.32 ± 0.03	1.79 ± 0.11	4.53 ± 0.87

^a Each data point represents the mean ± SD of three different experiments performed in triplicate.

The cell lines used were T47D, human ductal breast epithelial tumor cell line; HCT15, human colorectal carcinoma cell line; DU145, human prostate tumor cell line; HEK293, human embryonic kidney 293 cell line.

In 2013, Ming Dai *et al.* synthesized a series of novel derivatives of phenyl substituted tetramethoxy xanthone based on Formula III **193-196** and evaluated for their *in vitro* cytotoxicity against human hepatocellular carcinoma (HCC) and non-tumor hepatic cells (Table 19). Among these derivatives, compound **193** was more potent than positive control 5-fluorouracil (5-Fu) on QGY-7703 and SMMC-7721 cells with IC₅₀ values of 6.27 μM, 7.50 μM and 15.56 μM, 14.55 μM, respectively (Table 20). Furthermore, compounds **193**, **194**, **195**, and **196** exhibited much better selectivity toward the normal hepatic cell line QSG-7701 than 5-Fu. Additionally, compound **193** significantly induced cell apoptosis in QGY-7703 cells [52].



Formula III

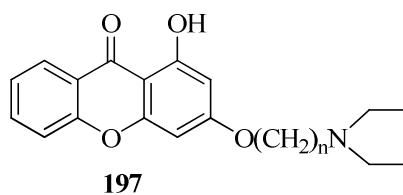
Table 19. Inhibition rates of compounds of Formula III against the QGY-7703 cell line at 10 μM

Compound	R	Yield	Inhibitory ratio (%)
193	H	91%	66.45
194	4'-CH ₃ (CH) ₃	88%	52.67
195	4'-C(CH ₃) ₃	88%	56.31
196	3'-CH ₃	82%	51.36

Table 20. Effects of the target compounds on proliferation of human HCC cells and normal hepatic cells

Compd	IC ₅₀ (μM)			
	QGY-7703	HepG-2	SMMC-7721	QSG-7701
193	6.27	19.18	7.50	>100
194	26.14	32.46	20.11	>100
195	33.13	39.21	18.15	>100
196	13.26	5.00	14.82	>100
5-Fu	15.66	12.48	14.55	0.60

In 2014, Zheng-Min Yang *et al.* synthesized a series of novel 1-hydroxyl-3-aminoalkoxy xanthone derivatives and evaluated for *in-vitro* anticancer activity against four selected human cancer cell lines (nasopharyngeal neoplasm CNE, liver cancer BEL-7402, gastric cancer MGC-803, lung adenocarcinoma A549). Compound **197** (Figure 26) shows excellent broad spectrum anticancer activity with IC₅₀ values ranging from 3.57 to 20.07 μM. The *in vitro* anticancer activity effect and action mechanism of compound **197** on human gastric carcinoma MGC-803 cell were further investigated. Morphological features of apoptosis and necrosis were examined after MGC-803 cells were exposed to 3g for 24 h. The results showed that compound **197** exhibits dose- and time-dependent anticancer effects on MGC-803 cells through apoptosis, which might be associated with its decreasing intracellular calcium and the mitochondrial membrane potential [53].



[IC₅₀ μM]

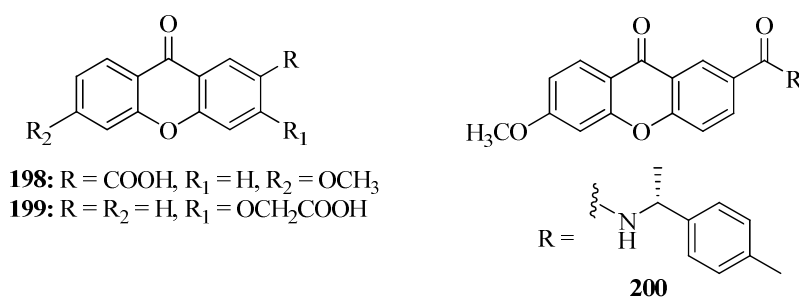
CNE = 3.63

BEL-7402 = 20.07

MGC-803 = 3.57

A549 = 7.5

Figure 26. 1-hydroxyl-3-aminoalkoxy xanthone derivative and anticancer activity in-vitro



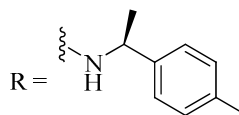
Yield % = 98

GI₅₀ (μM)

A375-C5 (melanoma) = >150

MCF-7 (breast adenocarcinoma) = >150

NCI-H460 (non-small cell lung cancer) = 85.88 ± 5.30



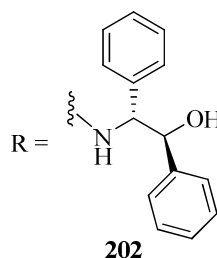
Yield % = 97

GI₅₀ (μM)

A375-C5 (melanoma) = >150

MCF-7 (breast adenocarcinoma) = 91.91 ± 6.27

NCI-H460 (non-small cell lung cancer) = 42.62 ± 1.77



Yield % = 94

GI₅₀ (μM)

A375-C5 (melanoma) = 32.15 ± 2.03

MCF-7 (breast adenocarcinoma) = 22.55 ± 1.99

NCI-H460 (non-small cell lung cancer) = 14.05 ± 1.82

Figure 27. Chiral derivatives of xanthones

In 2014, Carla Fernandes *et al.* developed a highly efficient and practical methodology for synthesis of new chiral derivatives of xanthenes (CDXs) **198-202** (Figure 27) in enantiomerically pure form. According to this approach, CDXs were synthesized by coupling a carboxyxanthone **198** and a carboxymethoxyxanthone **199** with both enantiomers of commercially available chiral building blocks, namely six amino alcohols, one amine and one amino ester. The synthesized CDXs were evaluated for their effect on the *in vitro* growth of three human tumor cell lines, namely A375-C5 (melanoma), MCF-7 (breast adenocarcinoma), and NCI-H460 (non-small cell lung cancer). The most active compound was CDX **5** being active in all human tumor cell lines. The growth inhibitory effects, in some cases, demonstrated to be depending on the stereo chemistry of the CDXs. An interesting example was observed with the enantiomers **200** and **201**, which demonstrated high enantioselectivity for MCF-7 and NCI-H460 cell lines [54].

In 2014, Xiang Fei *et al.* synthesized novel xanthone derivatives **204-208** based on α -mangostin **203** and evaluated as anti-cancer agents by cytotoxicity activity screening using 5 human cancer cell lines (Figure 28). A xanthone-derived natural product, α -mangostin is isolated from various parts of the mangostin, *Garcinia mangostana* L. (Clusiaceae), a well-known tropical fruit. The structure-activity relationship studies revealed that phenol groups on C₃ and C₆ are critical to anti-proliferative activity and C₄ modification is capable to improve both anti-cancer activity and drug-like properties [55].

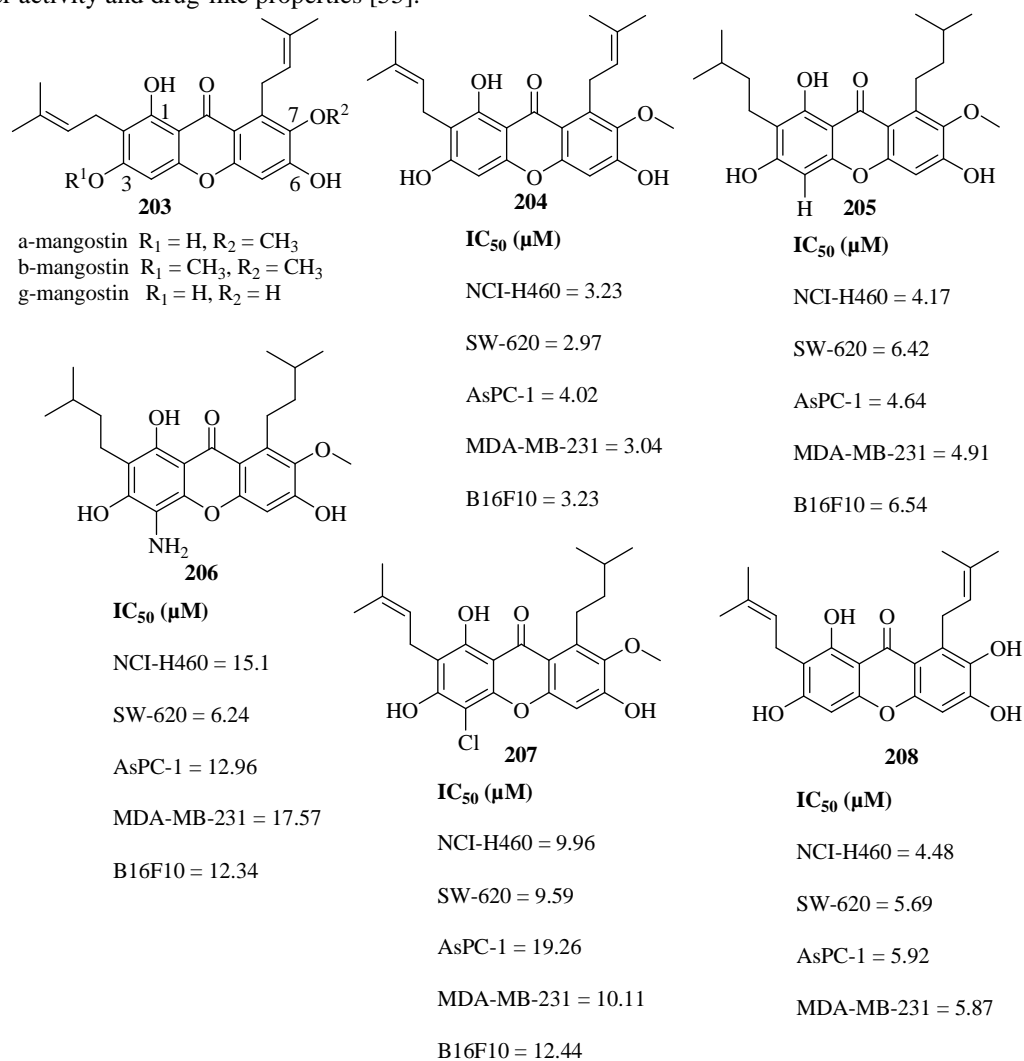


Figure 28. Xanthone derivatives based on α -mangostin

In 2014, Tsung-Chih Chen *et al.* synthesized a series of tetracyclic heterocyclic azathioxanthenes **209-213** and evaluated for cell proliferations, topoisomerase inhibitions, and NCI-60 cell panel assay, respectively. The IC₅₀ value of each target compound was measured by MTT assay against PC-3 and DU-145 cells, respectively. The values of IC₅₀ for five compounds **209**, **210**, **211**, **212**, and **213** were less than 10 μM against PC-3 and/or DU-145 cells, respectively (Figure 29).

Camptothecin, Etoposide and Doxorubicin were used as standard derivatives for MTT assay.

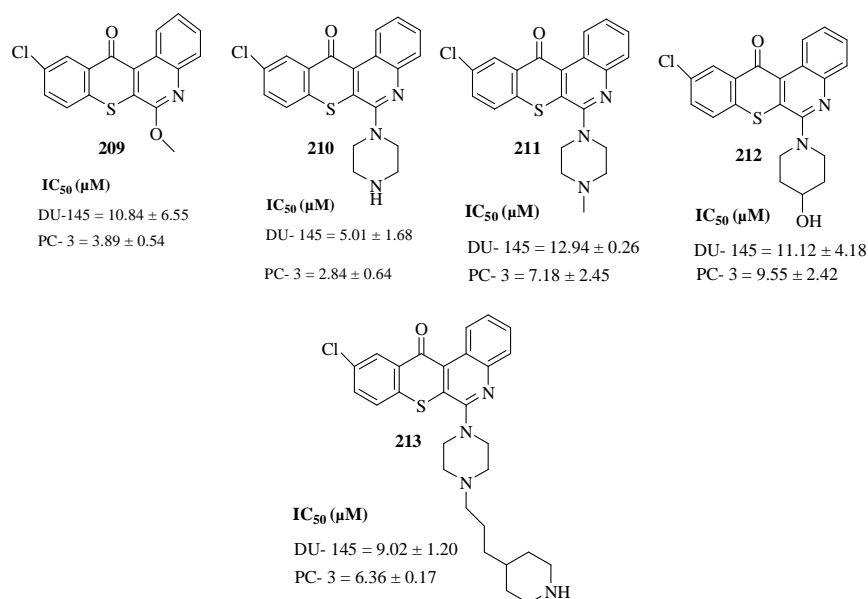


Figure 29. Tetracyclic heterocyclic azathioxanthenes

Compounds **209**, **210**, **211**, **212** and **213** were selected for primary topo I and II activity assays at 25 and/or 50 μM , respectively. Compounds **210**, **212**, and **213** showed various inhibitory effect against topo I at 50 μM . Compounds **209** and **210** exerted slight inhibitory effect against topo II at 50 μM . Compound **210** was chosen for further testing against topo I and II in a concentration-dependent manner doses at 1, 5, 10, 25, 50 μM . Compound **210** not only exhibited more potent inhibitory activity than compound **209**, **212**, **213** and **CPT**, but also completely blocked topoisomerase-mediated DNA relaxation at 25 μM . Compound **210**-treated PC-3 cells were examined to see the effect of compound **210** on apoptosis and related protein, PARP, and procaspase-3. Compound **210** induced apoptosis in PC-3 cells followed by increasing the DNA fragmentation via cleavage of PARP and decreasing procaspase-3 [56]. In 2014, Somayeh Motavallizadeh *et al.* prepared several novel N-(9-oxo-9H-xanthen-4-yl)benzenesulfonamide derivatives as anti-proliferative agents. The synthesized compounds were investigated for *in vitro* anti-proliferative activity against a panel of tumor cell lines including breast cancer cell lines (MDA-MB-231, T-47D) and neuroblastoma cell line (SK-N-MC) using MTT colorimetric assay. 4-methoxy-N-(9-oxo-9H-xanthen-4-yl)benzenesulfonamide **214** (Figure 30) showed the highest antiproliferative activity against MDA-MB-231, T-47D, and SK-N-MC cells. Etoposide was used as a positive standard drug.

Substituted benzenesulfonamide derivatives were also evaluated against human leukemia (CCRF-CEM), breast adenocarcinoma (MDA-MB-468), and colorectal carcinoma (HCT-116) cell lines at the concentration of 50 μM . pentafluoro derivatives **215** and **216** (Figure 30) exhibited higher antiproliferative activity than doxorubicin against human leukemia cell line (CCRF-CEM) and breast adenocarcinoma (MDA-MB-468) cells [57].

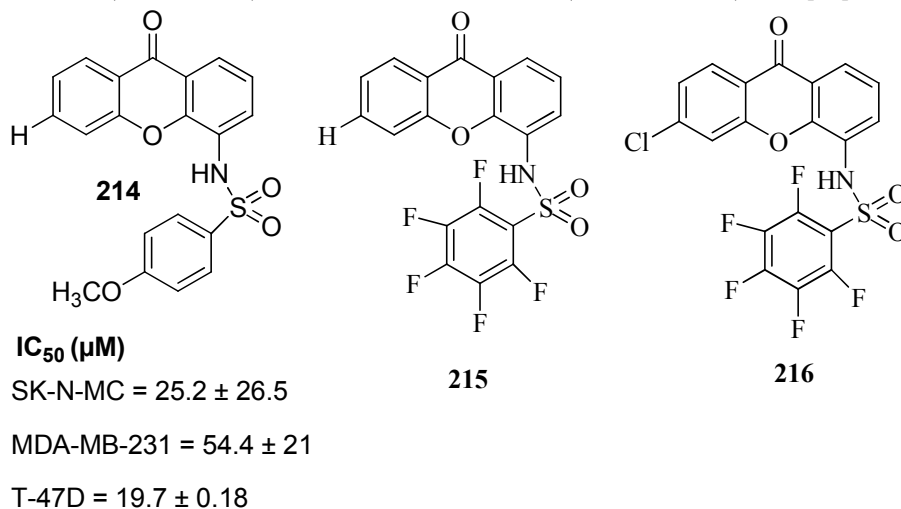


Figure 30. N-(9-oxo-9H-xanthen-4-yl)benzenesulfonamide derivatives

2-3. Anti-convulsant xanthenes

In 2008, Henryk Marona *et al.* prepared a series of appropriate alkanolamine and amide derivatives related to Formula IV **217-240** of xanthone (Table 21) and evaluated for anticonvulsant activity using maximal electroshock (MES) and subcutaneous pentylenetetrazole (scMet) induced seizures, and for neurotoxicity (TOX) using the roto rod test on mice and rats. A modification of the chemical structure of the most active compound, **218** and **219** as well as (R,S)-2-N-(6-chloro-2-xanthonemethyl)- amino-1-propanol **237** by the introduction of a tertiary amine instead of secondary one, and the replacement of the hydroxy group in the relevant compounds mentioned above by a chloride did not increase or eliminate anti-MES activity (compounds **228** and **230** are active at 100 mg/kg; compound **229** is inactive), and greatly increased the neurotoxicity (neurotoxic at 100 mg/kg) (Table 22). The Anti-MES activity determined in rats treated with 30 mg/kg (po) of the compounds under investigation is summarized in (Table 23).

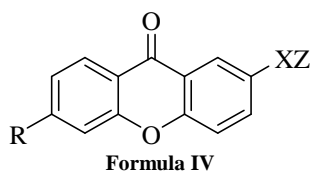
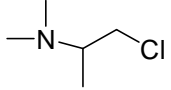
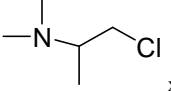
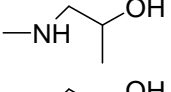
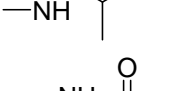
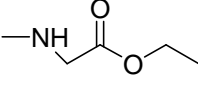
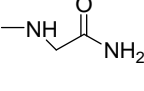
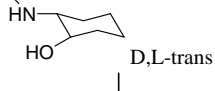
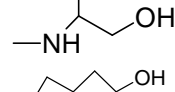
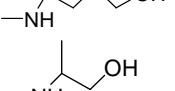
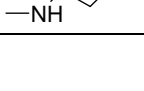


Table 21. Alkanolamine and amide derivatives Formula IV of xanthone

Compounds	R	X	Z
217	Cl	CH ₂	
218	Cl	CH ₂	
219	Cl	CH ₂	
220	Cl	CH ₂	
221	Cl	CH ₂	
222	Cl	CH ₂	
223	Cl	CH ₂	
224	Cl	CH ₂	
225	Cl	CH ₂	
226	Cl	CH ₂	
227	Cl	CH ₂	
228	Cl	CH ₂	
229	Cl	CH ₂	
230	Cl	CH ₂	

231	Cl	CH ₂	
232	Cl	CH ₂	
233	Cl	CH ₂	
234	Cl	CH ₂	
235	H	CO	
236	H	CO	
237	H	CO	
238	H	CO	
239	H	CO	
240	Cl	CO	

^a(R) isomer.
^b(S) isomer

Table 22. Anticonvulsant screening project (ASP), phase I: test results in mice after intraperitoneal injection

Compound	Dose (mg/kg)	Activity										
		MES ^a			ScMet ^b			Tox ^c				
		0.25h	0.5h	1h	4h	0.5h	4h	0.25h	0.5h	1h	4h	
217	3		0/4						0/4			
	10		0/4						0/4			
	30		1/1		0/1	0/1	0/1		2/4			0/2
	100		3/3		3/3	0/1	0/1		6/8			1/4
	300		1/1		1/1	0/1	0/1		4/4			2/2
218	30		0/1		0/1	0/1	0/1		0/4			0/2
	100		2/3		0/3	0/1	0/1		1/8			0/4
	300		1/1		1/1	0/1	0/1		2/4			0/2
219	30		0/1		0/1	0/1	0/1		0/4			0/2
	100		2/3		2/3	2/5	0/1		0/8			0/4
	300		1/1		1/1	0/1	0/1		2/4			0/2
220	30		0/1		0/1	0/1	0/1		0/4			0/2
	100		2/3		0/3	0/1	0/1		5/8			1/4
	300		1/1		1/1	0/1	0/1		4/4			2/2
221	30		0/1		0/1	0/1	0/1		0/4			0/2
	100		3/3		0/3	0/1	0/1		2/8			1/4
	300		1/1		1/1	0/1	0/1		4/4			2/2
222	30		0/1		0/1	0/1	0/1		1/4			0/2
	100		1/3		0/3	0/1	0/1		1/8			0/4
	300		1/1		1/1	0/1	0/1		3/4			0/2
223	30		0/1		0/1	0/1	0/1		0/4			0/2
	100		1/3		0/3	0/1	0/1		6/8			0/4
	300		0/4						4/4			1/1
224	30		1/2		1/3	0/1	0/1		0/4			0/4
	100		1/1		1/1	0/1	0/1		1/8			2/2
	300							4/4				
225	30		0/1		0/1	0/1	0/1		0/4			0/2
	100	1/3	0/3	2/3	0/3	0/1	0/1	2/3	3/8	0/3		0/4
	300		1/1		0/1	0/1	0/1		4/4			2/2
226	30		0/1		0/1	0/1	0/1		1/4			0/2
	100		1/3		0/3	0/1	0/1		1/8			0/4
	300		1/1		1/1	0/1	0/1		4/4			1/2

227	30	0/1	0/1	0/1	0/1	1/4	0/2
	100	2/3	0/3	0/1	0/1	0/8	0/4
	300	1/1	0/1	0/1	0/1	3/4	0/2
228	30	0/1	0/1	0/1	0/1	1/4	1/2
	100	3/3	1/3	0/1	0/1	5/8	0/4
	300	1/1	1/1	0/1	0/1	4/4	2/2
229	30	0/1	0/1	0/1	0/1	0/4	0/2
	100	0/3	0/3	0/1	0/1	1/8	0/4
	300	0/1	0/1	0/1	0/1	1/4	1/2
230	30	0/1	0/1	0/1	0/1	1/4	0/3
	100	2/3	0/3	1/3	0/1	0/1	0/3
	300	1/1	1/1	0/1	0/1	1/4	0/2

^a Number of animals protected/number of animals tested in the MES test.

^b Number of animals protected/number of animals tested in the ScMet test.

^c Number of animals exhibiting toxicity/number of animals tested in the rotorod test.

Table 23. Anticonvulsant screening project; phase VI a: test results in rats (dose 30 mg/kg po)

Compound	Test	Time (h)				
		0.25	0.50	1.00	2.00	4.00
217	MES ^a	1/4	1/4	1/4	2/4	2/4
	TOX ^b	0/4	0/4	0/4	0/4	0/4
218	MES	0/4	0/4	0/4	1/4	1/4
	TOX	0/4	0/4	0/4	0/4	0/4
219	MES	1/4	0/4	0/4	0/4	1/4
	TOX	0/4	0/4	0/4	0/4	0/4
220	MES	0/4	0/4	1/4	0/4	2/4
	TOX	0/4	0/4	0/4	0/4	0/4
221	MES	1/4	0/4	0/4	0/4	0/4
	TOX	0/4	0/4	0/4	0/4	0/4
222	MES	0/4	0/4	0/4	0/4	0/4
	TOX	0/4	0/4	0/4	0/4	0/4
223	MES	0/4	0/4	0/4	0/4	0/4
	TOX	0/4	0/4	0/4	0/4	0/4
224	MES	1/4	0/4	0/4	0/4	3/4
	TOX	0/4	0/4	0/4	0/4	0/4

^a Maximal electroshock test, number of animals protected/number of animals tested.

^b Rotorod test for neurological toxicity, number of animals exhibiting toxicity, number of animals tested

Table 24. Quantitative anticonvulsant activity and neurotoxicity in mice dosed intraperitoneally of 218 and 219 and some prototype AEDS

	TPE ^a (h)	TD ₅₀ [*]	ED ₅₀ ^b	ED ₅₀ ScMet ^c
218	2, 2	482.62 (454.48–526.17) [27.82]	77.44 (62.29–98.53) [6.66] PI 6.23	>500.00 PI < 0.96
219	1/4, 1	<500.00 (0.00) [0.00]	72.97 (52.99–95.26) [5.28] PI < 6.851	>350.00
Phenytoin**	1/2, 2	42.8 (36.4–47.5) [10.2]	6.48 (5.65–7.24) [12.4] PI 6.6	>50 PI < 0.9
Carbamazepine**	1/4, 1/4	47.8 (39.2–59.2) [7.98]	9.85 (8.77–10.7) [20.8] PI 4.9	>50 PI < 1.0
Valproate**	1/4, 1/4	483 (412–571) [12.3]	287 (237–359) [7.31] PI 1.7	290 (176–249) [8.51] PI 2.3

^a Time to peak effect. The first value is for the rotorod test; the second is for the anticonvulsant tests. In the neurotoxicity assay, all doses of 2^a were tested at 1/4th through 24 h; for 2^b were tested at 1/4 h through 8 h. For determination of TPE_{MES}, four mice were used, for TPE_{TOX}—eight mice.

^b Dose (mg/kg) eliciting the MES protection in 50% of animals (32 mice were used to determine of ED₅₀ MES).

^c Dose (mg/kg) eliciting the ScMet protection in 50% animals (16 mice were used to determine of ED₅₀ scMet).

* Doses (mg/kg) eliciting evidence of minimal neurological toxicity in 50% of animals; 95% confidence interval is shown in parentheses; the slope regression line is shown in brackets. PI: neurotoxic dose/median effective dose (TD₅₀/ED₅₀) for anticonvulsant test; (32 mice were used to determine of toxicity (TOX)).

The most promising compounds seem to be the appropriate aminoalkanoic derivatives of 6-chloroxanthone, among which the R(-) and S(+)-2-amino-1-propanol derivatives of 6-chloro-2-methylxanthone (**218** and **219**) displayed anti-MES activity (in mice) with a protective index (TD₅₀/ED₅₀) of 6.23 < 6.85, corresponding to that of phenytoin,

carbamazepine and valproate (Table 24). The most active compound **219**, was determined to have an affinity to the benzodiazepine (BDZ) receptor and voltage-dependent Ca^{2+} channel (VDCC) by using radio ligand binding assays. The enantiomeric purities of 2^a and 2^b were determined using an analytical liquid chromatography–mass spectrometry method [58].

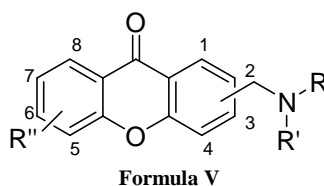


Table 25. Structure of the tested compounds

Compound	Configuration	Position	R''	Position	R'	R
241	R,S	6	OCH ₃	2	H	
242	R					
243	S					
244	R,S	6	OCH ₃	4	H	
245	R,S*HCl	6	CH ₃	4	H	
246	R					
247	S					
248	R,S	6	OCH ₃	4	H	
249	R					
250	S					
251	R,S	6	OCH ₃	4	CH ₃	
252	—	6	OCH ₃	4	H	
253	—	7	Cl	2	CH ₃	
254	—	7	Cl	2	H	
255	R,S	7	Cl	2	H	
256	R					
257	S					

In 2013, Natalia Szkaradek *et al.* synthesized a series of 17 new aminoalkanol derivatives based on Formula V **241-257** of 6-methoxy- or 7-chloro-2-methylxanthone as well as 6-methoxy-4-methylxanthone based on Formula V (Table 25) and evaluated for anticonvulsant activity in mice. All compounds were verified in mice after intraperitoneal (ip) administration in maximal electroshock (MES) and subcutaneous pentetrazole (scMet) induced seizures as well as neurotoxicity assessment. The anticonvulsant screening showed that all evaluated compounds revealed activity in the MES test (Table 26). Eleven of the tested substances showed protection against electrically evoked seizures in the majority of the tested mice at the dose of 100 mg/kg. Additionally, one was effective at the dose of 30 mg/kg. Five substances were active at the dose of 300 mg/kg or at the dose of 100 mg/kg in the minority

of the tested mice. The most promising compound revealed ED₅₀ value of 47.57 mg/kg in MES (mice, ip, 1 h after administration) and at the same time its TD₅₀ was evaluated as above 400 mg/kg and these values gave PI (calculated as TD₅₀/ED₅₀) of more than 8.41 (Table 27). Three other synthesized xanthone derivatives also proved to act as anti-convulsant and showed ED₅₀ values in MES test (mice, ip) ranged 80–110 mg/kg. Results were quite encouraging and suggested that in the group of xanthone derivatives new potential anticonvulsants might be found.

Table 26. The results of anticonvulsant activity evaluation in mice (ip)

Compound	Dose (mg/kg)	MES ^a				ScMet ^a		Neurotoxicity ^b			
		0.25h	0.5h	1.0h	4.0h	0.5h	4.0h	0.25h	0.5h	1.0h	4.0h
241	30	—	0/1	—	0/1	0/1	0/1	—	0/4	—	0/2
	100	—	3/3	—	0/3	0/1	0/1	—	0/8	—	0/4
	300	—	1/1	—	1/1	0/1	0/1	—	3/4	—	1/2
242	30	—	0/1	—	0/1	0/1	0/1	—	0/4	—	0/2
	100	—	3/3	—	1/3	0/1	0/1	—	2/8	—	0/4
	300	—	1/1	—	1/1	0/1	0/1	—	1/4	—	0/2
243	3	—	0/4	—	—	—	—	—	0/4	—	—
	10	—	1/4	—	—	—	—	—	0/4	—	—
	30	—	1/1	—	0/1	0/1	0/1	—	0/1	—	0/2
244	100	—	3/3	—	3/3	0/1	0/1	—	1/8	—	0/4
	300	—	1/1	—	1/1	0/1	0/1	—	3/4	—	2/2
	30	—	0/1	—	0/1	0/1	0/1	—	0/4	—	0/2
245	100	—	3/3	—	2/3	0/1	0/1	—	8/8	—	1/4
	300	—	—	—	—	—	—	—	4/4	—	—
	30	—	0/1	—	0/1	0/1	0/1	—	0/4	—	0/2
246	100	—	2/3	—	0/3	0/1	—	—	6/8	—	3/3
	300	—	—	—	—	—	—	—	4/4	—	—
	30	—	0/1	—	0/1	0/1	0/1	—	0/4	—	0/2
247	100	—	0/3	—	0/3	0/1	0/1	—	2/8	—	0/4
	300	—	1/1	—	1/1	0/1	—	—	4/4	—	2/2
	30	—	0/1	—	0/1	0/1	0/1	—	0/4	—	0/2
248	100	—	1/3	—	0/3	0/1	0/1	—	4/8	—	0/4
	300	—	0/1	—	1/1	0/1	0/1	—	2/4	—	0/2
	30	—	0/1	—	0/1	0/1	0/1	—	0/4	—	0/2
249	100	—	3/3	—	0/3	0/1	0/1	—	8/8	—	0/4
	300	—	1/1	—	—	Death	—	—	4/4	—	1/1
	30	—	0/1	—	0/1	0/1	0/1	—	0/4	—	0/2
250	100	—	2/3	—	0/3	0/1	0/1	—	0/8	—	0/4
	300	—	1/1	—	1/1	0/1	0/1	—	4/4	—	0/2
	30	—	0/1	—	0/1	0/1	0/1	—	2/4	—	0/2
251	100	—	2/3	—	1/3	0/1	0/1	—	4/8	—	1/4
	300	—	1/1	—	1/1	0/1	0/1	—	4/4	—	1/2
	30	—	0/1	—	0/1	0/1	1/5	—	1/4	—	1/2
252	100	0/3	0/2	0/3	0/3	0/1	0/1	0/3	3/8	0/3	0/4
	300	—	1/1	—	1/1	0/1	1/5	—	1/4	—	0/2
	30	—	0/1	—	0/1	0/1	0/1	—	0/4	—	0/2
253	100	—	2/2	—	0/3	0/1	0/1	—	8/8	—	0/4
	300	—	—	—	—	—	—	—	4/4	—	—
	30	—	0/1	—	0/1	0/1	0/1	—	1/4	—	0/2
254	100	—	2/3	—	2/3	0/1	0/1	—	3/8	—	0/4
	300	—	1/1	—	1/1	0/0	0/1	—	3/4	—	0/2
	30	—	0/1	—	0/1	0/1	0/1	—	0/4	—	1/2
255	100	1/3	0/3	0/3	0/3	0/1	0/1	0/3	1/8	1/3	0/4
	300	—	1/1	—	1/1	0/1	0/1	—	2/4	—	0/2
	30	—	0/1	—	0/1	0/1	0/1	—	0/4	—	0/2
256	100	—	0/3	—	2/3	0/1	0/1	—	0/8	—	0/4
	300	—	0/1	—	1/1	0/1	0/1	—	0/4	—	0/2
	30	—	0/1	—	0/1	0/1	0/1	—	0/4	—	0/2
257	100	—	1/3	—	0/3	0/1	0/1	—	0/8	—	0/4
	300	—	1/1	—	1/1	0/1	0/1	—	2/4	—	0/2
	30	—	0/1	—	0/1	0/1	0/1	—	0/4	—	0/2
258	100	—	2/3	—	3/3	0/1	0/1	—	0/8	—	0/4
	300	—	0/1	—	1/1	0/1	0/1	—	0/4	—	0/2

^a Number of animals protected/number of animals tested in the MES and ScMet tests.

^b Number of animals displaying motor impairment/number of animals used in the rotarod test.

Compounds were also examined for their anti-MES activity and neurotoxicity after oral administration (po) in rats at the dose of 30 mg/kg (Table 28). According to the obtained results, compounds **241** and **243** seemed to be the most potent. They exhibited activity after 15 min of administration, which persisted until 4 h of observation with concomitant lack of neurotoxicity [59].

Table 27. The results of anticonvulsant quantification in mice after intraperitoneal Administration

Compound	ED50 MES ¹ (mg/kg)	ED50 ScMet ¹ (mg/kg)	TD50 ² (mg/kg)
241	79.96 ^a (66.65–92.61) PI = 2.66	>500 ^a PI <0.43	212.85 ^b (171.85–275.38)
242	107.26 ^b (68.07–148.03) PI = 2.51	>175 ^b PI <1.54	269.27 ^b (235.76–301.79)
243	47.57 ^b (33.87–60.16) PI >8.41	>200 ^b	>400 ^c
257	17 79.74 ^b (63.71–102.12) PI = 3.93	>375 ^d PI <0.84	313.09 ^d (251.13–382.27)

¹ Dose of the compound which gives protection against seizures in 50% of tested animals; 95% confidence interval is shown in brackets.

² Dose of the compound which produces neurotoxicity in 50% of tested animals;

PI (protection index) = TD₅₀/ED₅₀; results observed after 0.5 h^a; 1.0 h^b; 0.25 h^c;

2.0 h^d of administration of the compound

Table 28. The results of anticonvulsant activity evaluation in rats (po)

Compound	Test	Dose (mg/kg)	Time/results				
			0.25 h	0.5 h	1.0 h	2.0 h	4.0 h
241	MES ^a	30	1/4	3/4	0/4	2/4	2/4
	TOX ^b	30	0/4	0/4	0/4	0/4	0/4
242	MES ^a	30	0/4	0/4	1/4	0/4	1/4
	TOX ^b	30	0/4	0/4	0/4	0/4	0/4
243	MES ^a	30	2/4	1/4	1/4	3/4	1/4
	TOX ^b	30	0/4	0/4	0/4	0/4	0/4
245	MES ^a	30	0/4	2/4	0/4	0/4	1/4
	TOX ^b	30	0/4	0/4	0/4	0/4	0/4
246	MES ^a	30	0/4	1/4	0/4	3/4	0/4
	TOX ^b	30	0/4	1/4	1/4	0/4	1/4
247	MES ^a	30	0/4	0/4	1/4	0/4	0/4
	TOX ^b	30	0/4	0/4	0/4	0/4	0/4
248	MES ^a	30	0/4	0/4	0/4	0/4	0/4
	TOX ^b	30	0/4	0/4	0/4	0/4	0/4
249	MES ^a	30	1/4	0/4	1/4	2/4	1/4
	TOX ^b	30	0/4	0/4	0/4	0/4	0/4
250	MES ^a	30	0/3	1/4	1/4	2/4	0/4
	TOX ^b	30	0/3	0/4	0/4	0/4	0/4
252	MES ^a	30	0/4	1/4	1/4	0/4	1/4
	TOX ^b	30	0/4	0/4	0/4	0/4	0/4
253	MES ^a	30	0/4	0/4	0/4	0/4	0/4
	TOX ^b	30	0/4	0/4	0/4	0/4	0/4
255	MES ^a	30	0/4	0/4	2/4	0/4	1/4
	TOX ^b	30	0/4	0/4	0/4	0/4	0/4
256	MES ^a	30	1/4	0/4	2/4	0/4	1/4
	TOX ^b	30	0/4	0/4	0/4	0/4	0/4

^a Number of animals protected/number of animals tested in the MES test.

^b Number of animals displaying motor impairment/number of animals used in neurotoxicity test.

In 2013, A. M. Waszkielewicz *et al.* synthesized a series of new xanthone derivatives with piperazine moiety. Five of the tested compounds were evaluated for their anticonvulsant properties. In terms of anticonvulsant activity, 6-methoxy-2-([4-(benzyl)piperazin-1-yl]methyl)-9H-xanthen-9-one **258** (Figure 31) proved best properties. Its ED50 determined in maximal electroshock (MES) seizure assay was 105 mg/kg b.w. (rats, p.o.) (Table29) [60].

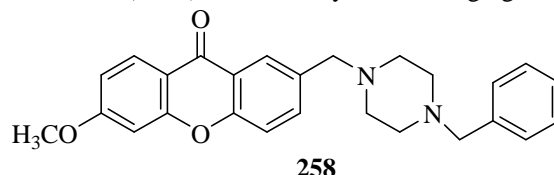


Figure 31. Xanthone derivative with piperazine moiety

Table 29. Result of anticonvulsant quantification of compound 258 (rats, p.o.)

Compound	ED ₅₀ MES ^a [mg/kg]	ED ₅₀ ScMet ^a [mg/kg]	TD ₅₀ ^b [mg/kg]
258	105 ^d (34.01–319.03) PI > 2.86	>250 ^d	>300 ^c

a Dose of the compound which gives protection against seizures in 50% of tested animals; 95% confidence interval is shown in brackets.

b Dose of the compound which produces neurotoxicity in 50% of tested animals; PI = TD₅₀/ED₅₀.

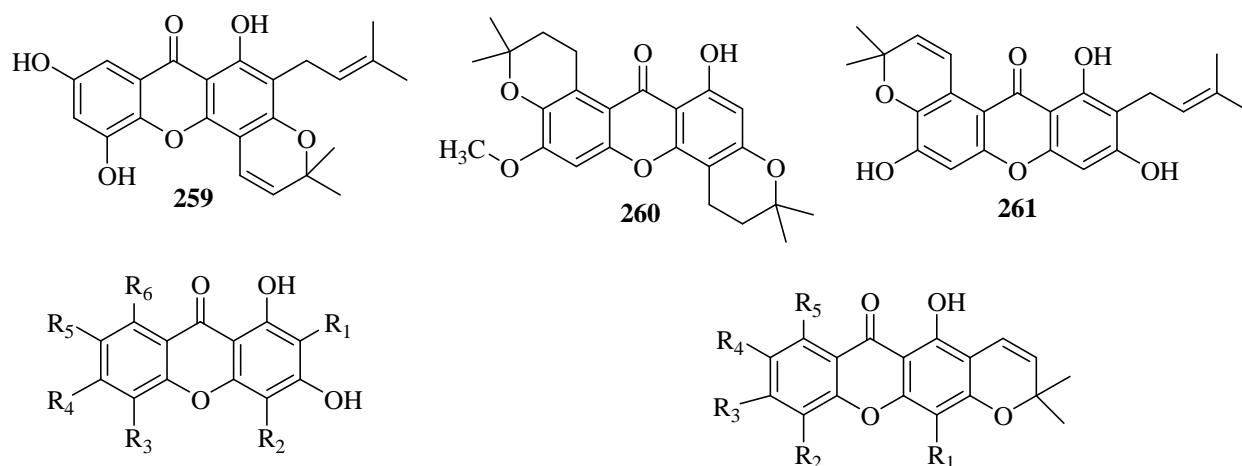
c Results observed after 0.0 h of administration of the compound.

d Results observed after 4.0 h of administration of the compound.

2-4. Anti-microbial xanthenes

2-4-1. Anti-bacterial xanthenes

In 2009, Joseph Ngoupayo *et al.* did phytochemical investigation of the methanol extract of the twigs of *Garcinia staudtii*, yielded four new prenylated xanthenes, staudtiixanthenes A-D **259**, **260**, **262**, **265** and a-mangostin **263**, garcinone B **261**, demethylcalabaxanthone **266**, Gartanin **264** and xanthone V1 **267** (Figure 32). These compounds have been evaluated for antibacterial activity against methicillin-resistant *Staphylococcus aureus* (MRSA). Compounds **259**, **262**, **265** with the 5, 7-dihydroxy groups showed a better activity than the others (Table 30). The new compounds were also screened for phagocyte chemiluminescence, neutrophil chemotaxis, T-cell proliferation, cytokine production from mononuclear cells and cytotoxicity. They were found to exhibit potent immunomodulatory activities [61].



262: R₁ = R₂ = prenyl; R₃ = R₅ = OH; R₄ = R₆ = H

265: R₁ = prenyl; R₂ = R₄ = OH; R₃ = R₅ = H

263: R₁ = R₆ = prenyl; R₂ = R₃ = H; R₄ = OH; R₅ = OCH₃

266: R₁ = R₂ = R₃ = H; R₄ = OH; R₅ = prenyl

264: R₁ = R₂ = prenyl; R₃ = R₆ = OH; R₄ = R₅ = H

267: R₁ = R₄ = R₅ = H; R₂ = R₃ = OH

Figure 32. Prenylated xanthone derivatives

Table 30. MIC value of xanthone derivatives 258-266 against MRSA

Compound	258	259	260	261	262	263	264	265	266
MIC (μg/mL)	128	64	128	16	32	128	32	128	—

In 2010, Hyung Won Ryu *et al.* isolated a series of xanthenes **268-273** (Figure 33) from the seedcases of *Garcinia mangostana* and evaluated for bacteria neuraminidase inhibitory activity. The most potent neuraminidase inhibitor **272** which has an IC₅₀ of 270 nM features a 5,8-diol moiety on the B ring. Interestingly, structure–activity studies reveal that these xanthenes show different kinetic inhibition mechanisms depending upon the arrangement of hydroxyl groups in the B ring. Compound **270** possessing a 6,7-diol motif on the B-ring operated under the enzyme isomerization model ($k_5 = 0.1144 \mu\text{M}^{-1} \text{s}^{-1}$, $k_6 = 0.001105 \text{s}^{-1}$, and $K_i^{\text{app}} = 7.41 \mu\text{M}$), whereas compound **272** possessing a 5,8-diol unit displayed simple reversible slow-binding inhibition ($k_3 = 0.02294 \mu\text{M}^{-1} \text{s}^{-1}$, $k_4 = 0.001025 \text{s}^{-1}$, and $K_i^{\text{app}} = 0.04468 \mu\text{M}$) (Table 31) [62].

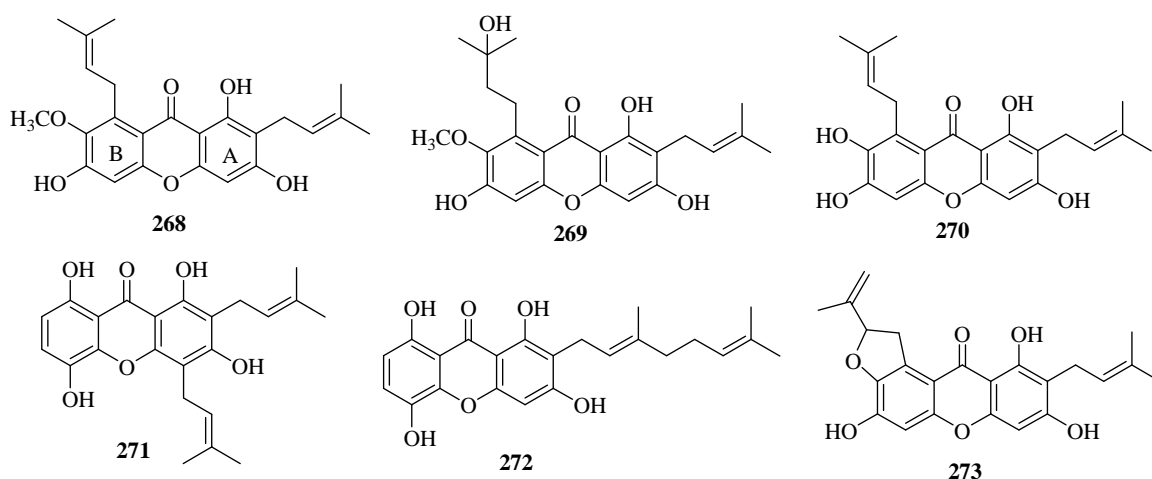
Figure 33. Xanthenes isolated from the seedcases of *Garcinia mangostana*

Table 31. Inhibitory effects of compounds on neuraminidase activities

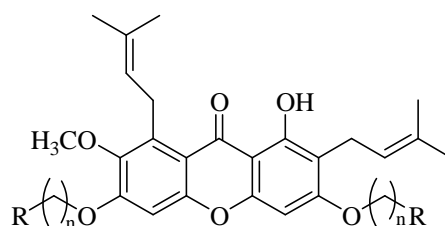
Compound	Neuraminidase	
	IC ₅₀ ^a (μM)	Kinetic mode (K _i , μM) ^b
268	12.2 ± 1.2	Competitive (5.8)
269	5.7 ± 0.8	Competitive (3.3)
270	2.2 ± 0.4	Competitive (0.8)
271	2.9 ± 0.3	Competitive (3.6)
272	0.27 ± 0.05	Competitive (0.15)
273	14.6 ± 0.8	Competitive (6.8)
Quercetin	9.8 ± 0.2	NT ^c

^a All compounds were examined in a set of experiments repeated three times; IC₅₀ values of compounds represent the concentration that caused 50% enzyme activity loss.

^b Values of inhibition constant.

^c Not tested.

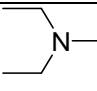
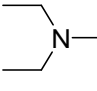
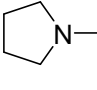
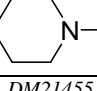
In 2013, Hanxun Zou *et al.* tuned the amphiphilic conformation of α -mangostin, a natural compound that contains a hydrophobic xanthone scaffold Formula VI, to improve its antimicrobial activity and selectivity for Gram-positive bacteria. A series of xanthone derivatives was obtained by cationic modification of the free C3 and C6 hydroxyl groups of α -mangostin with amine groups of different pKa values. Compounds **274–279** exhibited excellent antimicrobial activity against clinical isolates of MRSA and *S. aureus* with minimum inhibitory concentrations (MIC) of 0.39–1.56 μg/mL (Table 32), which were superior or comparable to those of α -mangostin [63].



Formula VI

Table 32. In Vitro Antibacterial Activity (MIC), Hemolytic Properties (HC50) and Selectivity of α -Mangostin Derivatives

Compound	n	R	pKa of conjugated amine, R-H	MIC ₉₉		Selectivity		
				(μg ml ⁻¹) ^a		HC ₅₀ ^b (μg ml ⁻¹)	(HC ₅₀ /MIC ₉₉)	
				MRSA	S.aureus		MRSA	S.aureus
274	3		10.98	0.39	0.78	16.3 ± 2	41.7	20.9
275	4		10.98	0.39	0.39	19.6 ± 3	50.3	50.3

276	5		10.98	0.78	1.56	14.0 ± 2	18.0	9.00
277	6		10.98	1.56	1.56	26.5 ± 2	17.0	17.0
278	4		11.27	1.56	1.56	25.0 ± 3	16.0	16.0
279	4		11.22	1.56	0.78	19.3 ± 3	12.3	24.7

^a MRSA: MRSA DM21455, clinical isolate, source: eye; *S. aureus*: *S. aureus* ATCC29213.

^b The HC50 value was obtained by extrapolating the fitted curve to 50% lysis of red blood cells.

Compound **275** exhibited potent antimicrobial properties against Gram-positive bacteria. Compound **275** also killed bacteria rapidly without inducing drug resistance and was nontoxic when applied topically (Table 33).

Table 33. MIC Values of **275** against Gram-positive Bacteria, including Six Strains of MRSA from Clinical Isolates

Gram-positive strains	MIC	Selectivity
MRSA ATCC 700669	0.095	206.3
MRSA DM09808R; source: eye	1.56	12.6
MRSA DB57964/04	0.78	25.1
MRSA DM21595; source: wound	0.39	50.3
MRSA DR42412; source: sputum	0.39	50.3
MRSA DR68004; source: blood	1.56	12.6
VISA 10:DB6506	0.78	25.1
Staphylococcus aureus ATCC29213	0.39	50.3
Staphylococcus aureus ATCC 6538	1.56	12.6
Staphylococcus aureus ATCC 6538P	0.78	25.1
Staphylococcus aureus ATCC 29737	1.56	12.6
Streptococcus faecium ATCC 10541	0.195	100.5
Streptococcus epidermidis ATCC 12228	0.78	25.1
Enterococcus faecalis ATCC 29212	0.78	25.1

In 2014, Enas E. Eltamany *et al.* isolated microluside A [4 (19-*para*-hydroxy benzoyloxy-O- β -D-cellobiosyl), 5 (30-*para*-hydroxy benzoyloxy-O- β -D-glucopyranosyl)xanthone **280**] (Figure 34) is a unique O-glycosylated disubstituted xanthone isolated from the broth culture of *Micrococcus* sp. EG45 cultivated from the Red Sea sponge *Spheciospongia vagabunda*. The antimicrobial activity evaluation showed that **280** exhibited antibacterial potential against *Enterococcus faecalis* JH212 and *Staphylococcus aureus* NCTC 8325 with MIC values of 10 and 13 μ M, respectively [64].

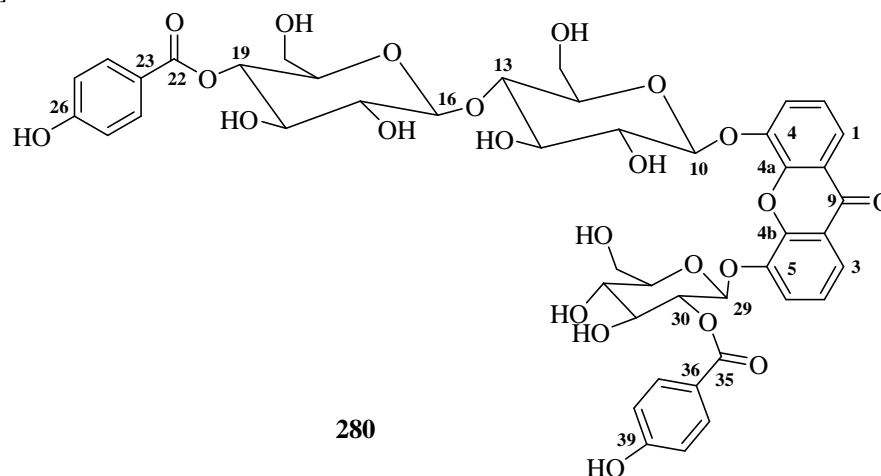


Figure 34. Structure of microluside A

2-4-2. Anti-parasitic xanthenes

In 1993, Keiichi Matsuzaki *et al.* isolated the structure of the anticoccidial antibiotic xanthoquinodin **281** (Figure 35), from *Hwnicolu* sp. FO-888. It contains a new type of xanthone and anthraquinone conjugate system [65].

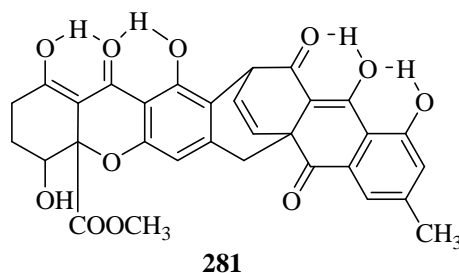


Figure 35. Xanthoquinodin

2-4-3. Anti-fungal xanthenes

In 2002, Stephane Moreau *et al.* synthesized a series of arylhydrazones derivatives of **285-292** (Figure 36) from various 6,8-diacetoxy- or 6,8 dihydroxy-9-oxo-9H-xanthene carboxaldehydes and evaluated for their *in vitro* antifungal properties against two human pathogenic yeasts (*Candida albicans* and *C.krusei*) according to a diffusion method (Table 34). The activity was strongly dependent from the position of the (1-arylhiazinyl-2-ylidene)methyl chain in the xanthone molecular skeleton. Compounds having the nitrogen side chain in the 4-position, with a further halogen substitution on the terminal phenyl ring showed fungistatic effects. Within this series, the 4-fluorophenylhydrazinyl derivative **287g** exhibited the highest activity, particularly against *C. krusei*, with a greater efficacy than that of econazole, used as reference (Table 34) [66].

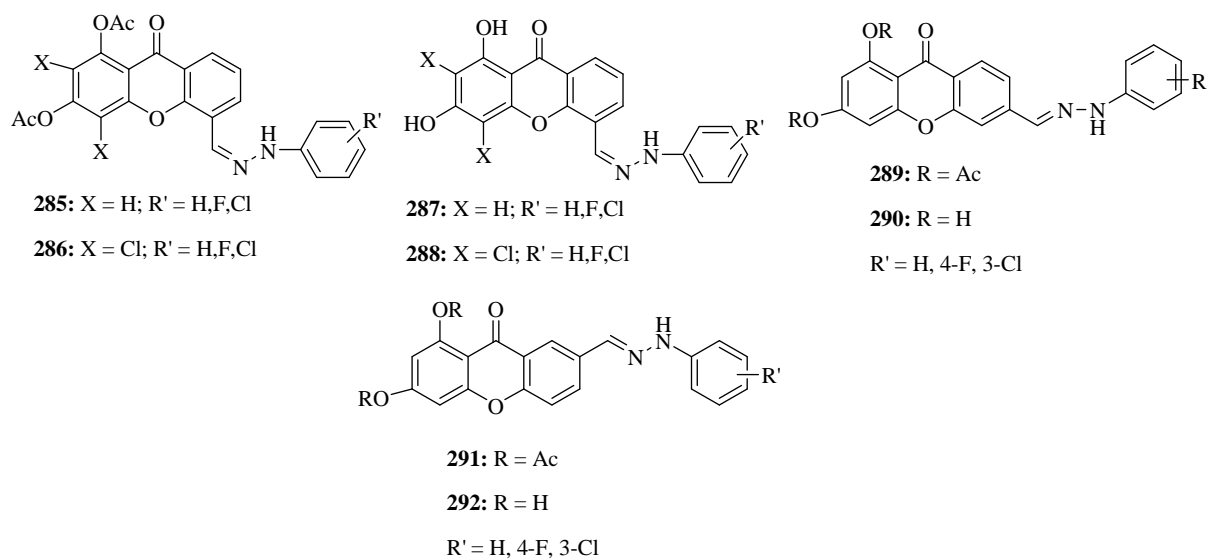


Figure 36. Arylhydrazones derivatives

Table 34. *In vitro* growth inhibitory effects a of 4-, 3- and 2-(2-arylhiazonomethyl)xanthenes against *C. albicans* b and *C. krusei* c (diffusion method: 100 µg substance/test disk)

Compound	Acetylated derivatives				Free hydroxylated derivatives											
	1 series		2series		3series		4series		5series		6series		7series		8series	
R'	CA	CK	CA	CK	CA	CK	CA	CK	CA	CK	CA	CK	CA	CK	CA	CK
a H	-	-	-	-	-	-	-	-	-	-	-	-	-	-	-	-
b 2-Cl	+	++	-	-	-	-	-	+	-	-	-	-	-	-	++	+++
c 3-Cl	+	++++	-	-	-	-	+	++	+	+	-	-	-	-	-	+++
d 4-Cl	-	-	-	-	-	-	-	-	-	+	-	-	-	-	+	+
e 2-F	+	++	-	-	-	-	-	+	++	++++	-	-	-	-	-	+
f 3-F	-	+	-	-	-	-	-	++	+	++++	-	-	-	-	-	+++
g 4-F	++	++++	-	-	-	-	+	++	+++	++++	-	-	-	-	++++	++++
h 2,4-diCl	-	-	-	-	-	-	-	-	+	+	-	-	-	-	+	+
i 2,5-di Cl	-	-	-	-	-	-	-	-	-	-	-	-	-	-	-	-
j 2,4-di F	-	+	-	-	-	-	-	++	-	+	-	-	-	-	-	+++

^a Size of inhibition zones: (-) 6-7 mm, (+) 8-10 mm, (++) 11-14 mm, (+++) 15-19 mm, (++++) 20 mm and more.

^b *C. albicans* = CA.

^c *C. krusei* = CK.

In 2011, Justin J. Omolo *et al.* synthesized xanthenes. Exposure of the phenol, (5-bromo-2-hydroxyphenyl) (2,4,5-trimethoxyphenyl)methanone **295** (Figure 37) to ceric ammonium nitrate (CAN) resulted in the formation of 7-bromo-3,4a-dimethoxy-2H-xanthen-2,9(4aH)-dione **296** (Figure 37) and 5-bromo-2',5'-dimethoxy-3H-spiro [benzofuran-2,1'-cyclohexa[2,5]diene]-3,4'-dione **297** (Figure 37). The brominated spirobenzofuran **297** (Figure 37) was then subjected to Suzuki–Miyaura reactions to give six derivatives **299 (a–f)** (Figure 37). These compounds, related diones and xanthenes displayed mostly noteworthy antimicrobial activity, particularly towards the yeasts *Cryptococcus neoformans* and *Candida albicans* (Table 35). Diones **294** and **298** (Figure 38) displayed significant activity (7.8 µg/mL) against *C. albicans* and *C. neoformans*, respectively. Furthermore, dione **293** (Figure 38) displayed the most significant activity (3.6 µg/mL) against both yeasts (Table 35) [67].

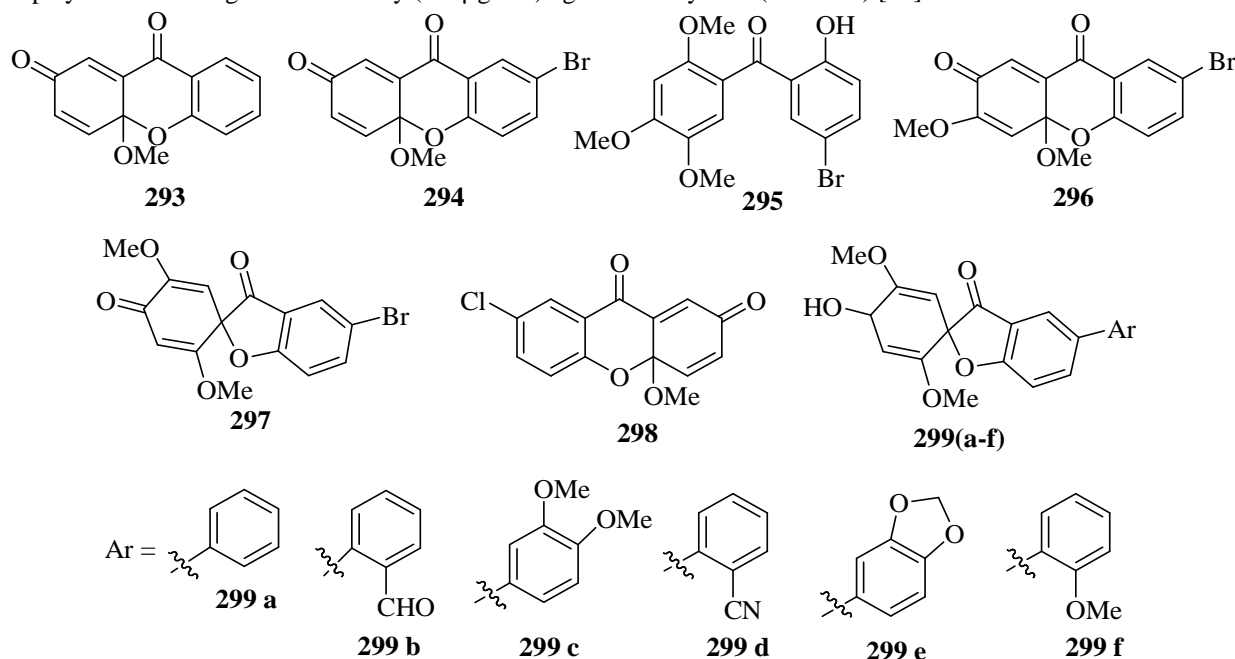


Figure 37. Diones and xanthenes

Table 35. Antimicrobial and antifungal activity of selected compounds

Compound	Bacillus cereus ATCC 11778	Staphylococcus aureus ATCC 2587	Escherichia coli ATCC 8739	Moraxella catarrhalis ATCC 232446	Cryptococcus neoformans ATCC 90112	Candida albicans ATCC 10231
Pathogen (MIC µg/mL)						
293	31.3	93.7	125.0	125.0	3.6	3.6
295	31.3	62.5	62.5	125.0	15.6	7.8
296	31.3	62.5	187.5	125.0	15.6	31.3
297	31.3	62.5	62.5	125.0	15.6	31.3
298	156.2	156.2	312.0	156.2	7.8	156.2
299a	46.9	62.5	125.0	>250	23.4	31.3
299b	15.6	15.6	62.5	125.0	15.6	31.3
299c	31.3	62.5	62.5	125.0	15.6	62.5
299d	31.3	62.5	62.5	125.0	15.6	23.4
299e	31.3	62.5	62.5	125.0	15.6	62.5
299f	31.3	62.5	62.5	125.0	15.6	23.4
Ciprofloxacin	0.08	1.25	0.12	1.25	NA	NA
Amphotericin B	NA	NA	NA	NA	2.5	3.0

NA = Not appropriate control; media control (not presented) demonstrated sterility and solvent control (not presented) had no additional antimicrobial effects.

2-4-4. Anti-viral xanthenes

In 2009, Young Bae Ryu *et al.* derived a series of xanthone derivatives **306–307** (Figure 38) from *Cudrania tricuspidata* which are shown to display nanomolar inhibitor activity against neuraminidase (EC 3.2.1.18) as well as competitive inhibition modes. Compound **307** bearing vicinal dihydroxy group on the A-ring displays nanomolar activity ($IC_{50} = 0.08 \pm 0.01 \mu\text{M}$), a 200-fold increase in activity relative to that of the first reported xanthone derived neuraminidase inhibitor, mangiferin ($IC_{50} = 16.2 \pm 4.2 \mu\text{M}$) (Table 36). The 6,7-vicinal dihydroxy group plays a crucial role for inhibitory activity because compound **303**, which has one of these hydroxyl groups prenylated was inactive (33% at 200 µM), whereas other compounds **300–302** and **305–307** showed nanomolar activity (0.08–0.27 µM) and competitive inhibition modes. Interestingly all inhibitors manifested enzyme isomerization inhibition

against neuraminidase. The most potent inhibitor, compound **307** showed similar interaction with a transition-state analogue of neuraminic acid in active site [68].

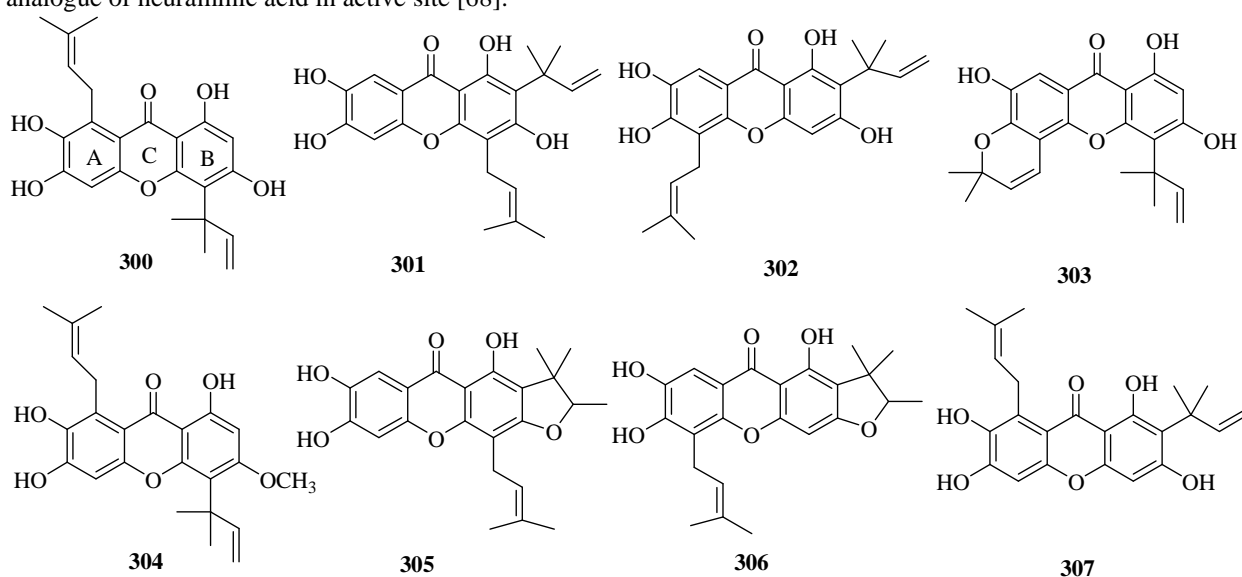


Figure 38. Xanthone derivatives extracted from *Cudrania tricuspidata*

Table 36. Inhibitory effects of isolated compounds 1-8 on neuraminidase activities

Entry	IC ₅₀ ^a (μM)	Inhibition type (K _i , μM)
300	0.245 ± 0.03	Competitive (0.136 ± 0.01)
301	0.186 ± 0.02	Competitive (0.103 ± 0.02)
302	0.228 ± 0.01	Competitive (0.138 ± 0.02)
303	33% at 200 μM	Not tested
304	1.271 ± 0.21	Competitive (0.950 ± 0.02)
305	0.278 ± 0.08	Competitive (0.143 ± 0.02)
306	0.186 ± 0.04	Competitive (0.098 ± 0.01)
307	0.080 ± 0.01	Competitive (0.058 ± 0.01)
Quercetin ^b	2.7 ± 0.5	Not tested
Apigenin ^b	17.4 ± 0.7	Not tested
Mangiferin ^b	16.2 ± 4.24	Not tested

^a All compounds were examined in a set of experiments repeated three times; IC₅₀ values of compounds represent the concentration that caused 50% enzyme activity loss.

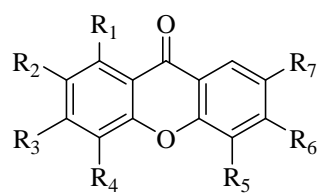
^b These compounds were used as a positive control

In 2012, Trong Tuan Dao *et al.* isolated 10 xanthone products related to Formula VII **308-316** and a derivative **317** (Figure 39), by bioassay-guided fractionation from the EtOAc-soluble extract of *Polygala karensium*, in the course of an anti-influenza screening program for natural products. The emergence of the H1N1 swine flu pandemic has the possibility to develop the occurrence of disaster drug-resistant viruses by additional reassortments in novel influenza A virus. Compounds **308**, **309**, **311**, **313** and **315** with a hydroxy group at C-1 showed strong inhibitory effects on neuraminidases from various influenza viral strains, H1N1, H9N2, novel H1N1 (WT), and oseltamivir-resistant novel H1N1 (H274Y) expressed in 293T cells (Table 37). In addition, these compounds reduced the cytopathic effect of H1N1 swine influenza virus in MDCK cells. Results suggest that xanthones from *P. karensium* may be useful in the prevention and treatment of disease by influenza viruses [69].

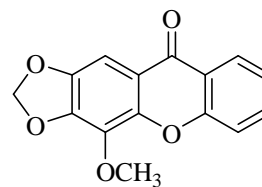
Table 37. Inhibitory effects of compounds 1-10 on the neuraminidase activity

Compound	IC ₅₀ ^a (μg/mL)			
	H1N1	H9N2	H1N1 (WT)	H1N1 (H274Y)
308	23.29 ± 2.08	15.46 ± 1.69	11.15 ± 0.52	7.73 ± 0.85
309	23.54 ± 3.68	22.45 ± 3.45	11.54 ± 0.35	13.01 ± 0.41
310	28.42 ± 1.47	25.59 ± 2.14	9.33 ± 0.6	12.8 ± 1.07
311	26.81 ± 2.18	24.77 ± 2.45	13.41 ± 1.09	9.14 ± 0.39
312	26.87 ± 3.81	19.81 ± 3.34	13.68 ± 0.89	10.80 ± 0.48
Oseltamivir	39.74 ± 1.54 (ng/mL)	4.94 ± 0.56 (ng/mL)	21.09 ± 1.19 (ng/mL)	5.13 ± 0.23

^a All compounds were examined in a set of triplicated experiments



Formula VII

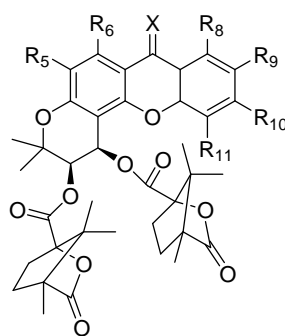


317

	R ₁	R ₂	R ₃	R ₄	R ₅	R ₆	R ₇
308	OH	H	OH	H	H	H	H
309	OH	H	H	H	H	H	OH
310	H	OH	OCH ₃	OCH ₃	H	H	H
311	OH	H	H	OCH ₃	H	H	OH
312	OCH ₃	OCH ₃	OH	H	H	OH	H
313	OH	H	OH	H	H	H	OH
314	OCH ₃	OCH ₃	H	OH	H	H	H
315	OH	OH	OH	H	OH	H	H
316	OCH ₃	H	H	H	H	H	OH

Figure 39. Xanthone derivatives extracted from *Polygala karensium*

In 2012, Ting Zhou *et al.* synthesized 1R,2R-dicamphanoyl-3,3-dimethyl dihydropyrano[2,3-*c*] xanthen-7(1*H*)-one (DCX) derivatives Formula VIII as novel anti-HIV agents against both wild-type and non-nucleoside reverse transcriptase (RT) inhibitor-resistant HIV-1 (RTMDR-1) strains. Twenty-four DCX analogs **318-341** were synthesized and evaluated against the non-drug-resistant HIV-1 NL4-3 strain (Table 38) and selected analogs were also screened for their ability to inhibit the RTMDR-1 strain (Table 39). Compared with the control 2-ethyl-3',4'-di-O-(-)-camphanoyl-2',2'-dimethyldihydropyrano [2,3-*f*]chromone (2-EDCP), one of the best anti-HIV coumarin derivatives in our prior study, three DCX compounds (**319**, **324**, and **334**) showed better activity against both HIV strains with an EC₅₀ range of 0.062-0.081 μM, and five additional compounds (**320**, **323**, **328**, **330** and **333**) exhibited comparable anti-HIV potency. Six DCX analogs (**319**, **323**, **324**, **330** and **333-334**) also showed enhanced selectivity index (SI) values in comparison to the control. Structure-activity relationship (SAR) information suggested that the extended conjugated system of the pyranoxanthone skeleton facilitates the interaction of the small DCX molecule within the viral binding pocket, consequently leading to enhanced anti-HIV activity and selectivity [70].



Formula VIII

Table 38. Anti-HIV activity of DCX analogs (318-341) against HIV-1 NL4-3 strain.^a

Compound	R ₅	R ₆	R ₈	R ₉	R ₁₀	R ₁₁	X	CC ₅₀ ^b (μM)	EC ₅₀ ^c (μM)	SI ^d
318	H	H	H	H	H	H	O	>29.8	0.308	>96.8
319	H	OCH ₃	H	H	H	H	O	>14.3	0.063	>227.0
320	H	OCH ₃	H	H	H	H	NOH	>13.9	0.12	>118.2
321	H	OH	H	H	H	H	O	N/A	N/A	-- ^e
322	H	OCH ₃	H	H	H	CH ₃	O	4.32	1.52	2.84
323	H	OCH ₃	H	H	CH ₃	H	O	>14.0	0.095	>147.4
324	H	OCH ₃	H	CH ₃	H	H	O	11.4	0.065	175.4
325	H	OCH ₃	CH ₃	H	H	H	O	11.6	0.15	77.3
326	H	OCH ₃	H	H	H	OCH ₃	O	N/A	N/A	--
327	H	OCH ₃	H	H	OCH ₃	H	O	>13.7	0.362	>37.8
328	H	OCH ₃	H	OCH ₃	H	H	O	10.8	0.12	88.8
329	H	OCH ₃	OCH ₃	H	H	H	O	11.6	1.70	6.83
330	H	OCH ₃	CH ₃	H	OCH ₃	H	O	>26.8	0.14	>191.5
331	H	OCH ₃	OH	H	H	H	O	8.1	0.33	24.5
332	H	OCH ₃	H	H	H	F	O	7.8	0.23	33.9
333	H	OCH ₃	H	F	H	H	O	26.0	0.10	260
334	H	OCH ₃	F	H	H	H	O	>13.9	0.062	>224.2
335	H	OCH ₃	H	H	Br	H	O	N/A	N/A	--
336	H	OCH ₃	H	Br	H	H	O	9.23	1.47	6.83
337	Br	OCH ₃	H	H	H	H	O	N/A	N/A	--
338	Br	OCH ₃	H	CH ₃	H	H	O	N/A	N/A	--
339	H	OCH ₃	H	CH ₂ Br	H	H	O	>25.2	4.53	>5.55
340	H	OCH ₃	H	H	CN	H	O	9.08	0.20	45.4
341	H	OCH ₃	H	CN	H	H	O	>13.8	0.29	>47.8
EDCP								12.1	0.089	136.0

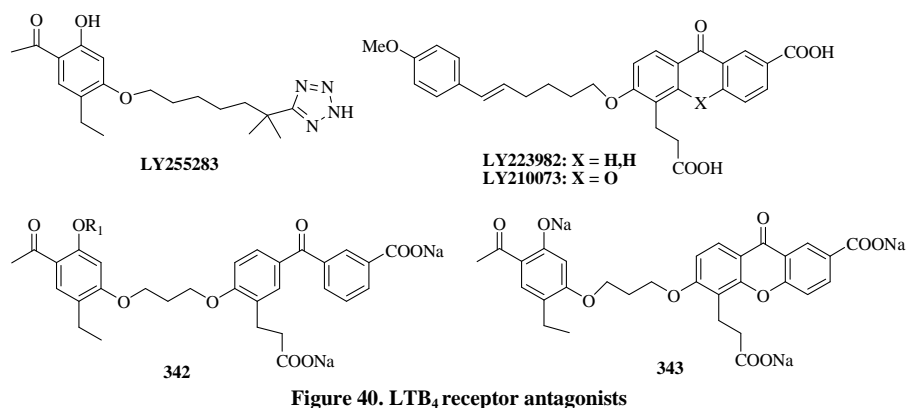
^a All data presented in this table were averaged from at least three independent experiments.^b Cytotoxic activity was determined using a Promega CytoTox-Glo™ assay kit.^c This assay was performed in TZM-bl cell infected with HIV-1 NL4-3 strain.^d Selectivity index = CC₅₀ ÷ EC₅₀.^e No selective anti-HIV activity (CC₅₀ ÷ EC₅₀ < 4).Table 39. Anti-HIV activity of DCX analogs against drug-resistant RTMDR1 HIV strain.^a

Compound	CC ₅₀ (μM)	EC ₅₀ ^b (μM)	SI ^c
318	>29.8	0.546	>54.6
319	>14.3	0.074	>193.2
320	>14.0	0.363	>38.6
324	11.4	0.081	140.7
325	11.6	0.37	31.4
328	10.8	0.42	25.7
333	26.0	0.16	162.5
334	>13.9	0.065	>213.8
EDCP	12.1	0.11	110

^a All data presented in this table were averaged from at least three independent experiments.^b This assay was performed in TZM-bl cell infected with HIV_{RTMDR1} strain.^c Selectivity index = CC₅₀ ÷ EC₅₀.

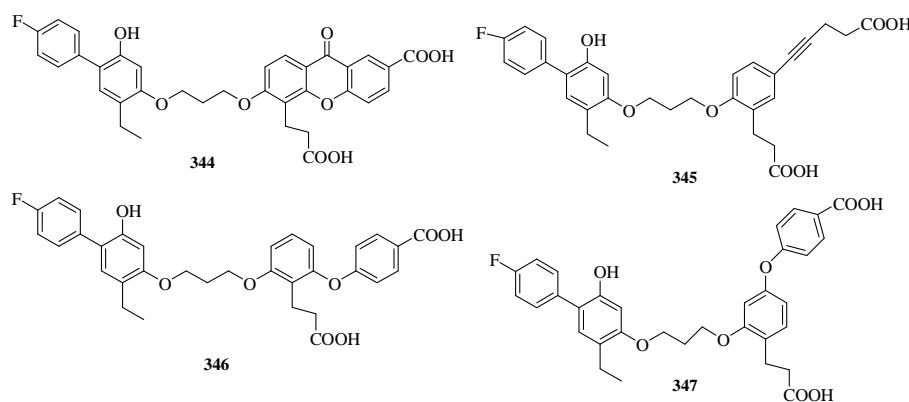
2-5. Anti-asthmatic xanthenes

In 1993, J. Scott Sawyer *et al.* reported the preparation and pharmacologic activity of two new hybrid LTB₄ receptor antagonists, **342** and **343** (Figure 40). Data was obtained on binding to human neutrophils O and guinea-pig lung membranes and inhibition of chemotaxis of human neutrophils (Table 40). Compound **342** was similar in activity to LY223982 in both the neutrophil and guinea-pig lung binding assays, but demonstrated a 10-fold increase in potency relative to LY255283 in the lung binding assay. The xanthone derivative **343** showed better affinity still, with a significant increase in activity in both assays relative to LY255283. Relative to LY210073 (the xanthone derivative of LY223982), compound **343** had similar binding affinity for human neutrophils, but showed a 38-fold increase in affinity for guinea-pig lung membrane receptors. Compounds **342** and **343** inhibited LTB₄-induced chemotaxis of human neutrophils with IC₅₀ values of 16 μM and 0.32 μM, respectively. These compounds are among the most potent in vitro LTB₄ receptor antagonists and add new insight into the critical pharmacophores of the LTB₄ receptor [71].

Figure 40. LTB₄ receptor antagonistsTable 40. Inhibition of Specific Binding of H-LTB₄ and LTB₄-induced chemotaxis

Compound	Human Neutrophils (IC ₅₀ , nM)	Guinea-pig Lung Membranes (K _i , nM)	Human Neutrophil Chemotaxis (IC ₅₀ , μM)
LY255283	85 ± 7.9	77 ± 9.4	7.4
LY223982	13 ± 2.2	7.8 ± 2.0	6.0
LY218873	6.2 ± 0.1	45 ± 7.0	0.90 ± 0.18
342	46	6.8 ± 1.2	16 ± 0.20
343	4.0	1.2 ± 0.11	0.32 ± 0.039
LTB ₄	1.9 ± 0.05	0.12 ± 0.015	--

In 1994, J. Scott Sawyer *et al.* reported the preparation and pharmacologic activity of three spatial analogues **345**, **346** and **347** of LY292728 **344** (Figure 41), a highly potent xanthone dicarboxylic LTB₄ receptor antagonist. Molecular modeling of these compounds has helped to further elucidate the nature of the secondary acid binding site of the LTB₄ receptor. In vitro evaluation of compounds **345** and **346** revealed that both analogues possess extremely potent activity. Compound **347** was found to be 40 to 200 fold less active in inhibiting LTB₄ binding than **345** and **346** (Table 41) [72].

Figure 41. Xanthone dicarboxylic LTB₄ receptor antagonistTable 41. Inhibition of Specific Binding of [³H]LTB₄ and LTB₄-mediated Up-regulation of Human Neutrophil CD11b/CD18

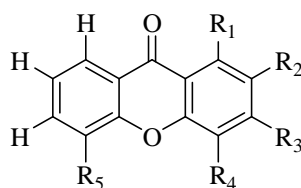
Compound	Human Neutrophil (K _i , nM)	Guinea-pig Lung Membranes (K _i , nM)	Human Neutrophil CD11b/CD18 Up-regulation (IC ₅₀ , nM)
344	0.47	0.040 ± 0.016	1.2 ± 0.10
345 ^a	1.1	0.073 ± 0.021	4.7
346	1.1	0.14 ± 0.012	2.6
347	39	14 ± 0.39	1800
LTB ₄	1.9 ± 0.050	0.12 ± 0.015	—

^aTested as the disodium salt.

2-6. Xanthenes used in diabetic nephropathy

In 2002, Lucilia Saraiva *et al.* evaluated the modulatory activity of a series of 20 simple xanthenes related to Formula IX (**348-367**) (Table 42) on isoforms α, βI, δ, η and ζ of protein kinase C (PKC) using an in vivo yeast phenotypic assay. Hydroxy and/or methoxyxanthenes were synthesised. Compound **354** presented also a comparable high potency on yeast expressing PKC- δ whereas compounds **350** and **364** also presented high potencies on yeast expressing PKC- ζ (see Table 43). Compounds **348** and **358** presented a remarkable potency and

selectivity towards PKC- η (see Table 43). Compounds **351**, **352**, **353** and **357** presented a high selectivity towards PKC- ζ (Table 43). The xanthenes tested differ in their efficacy and potency towards individual PKC isoforms and some showed higher selectivities for PKC- δ , - η or - ζ , suggesting that xanthone derivatives can become valuable research tools to elucidate the physiological roles of these isoforms [73].



Formula IX

Table 42. Chemical structures of xanthone derivatives

Compound	R ₁	R ₂	R ₃	R ₄	R ₅
348	Xanthone	H	H	H	H
349	1-Hydroxyxanthone	OH	H	H	H
350	1-Methoxyxanthone	OCH ₃	H	H	H
351	2-Hydroxyxanthone	H	OH	H	H
352	2-Methoxyxanthone	H	OCH ₃	H	H
353	3-Hydroxyxanthone	H	H	OH	H
354	3-Methoxyxanthone	H	H	OCH ₃	H
355	4-Hydroxyxanthone	H	H	H	OH
356	4-Methoxyxanthone	H	H	H	OCH ₃
357	1,2-Dihydroxyxanthone	OH	OH	H	H
358	1,2-Dimethoxyxanthone	OCH ₃	OCH ₃	H	H
359	2,3-Dihydroxyxanthone	H	OH	OH	H
360	2,3-Dimethoxyxanthone	H	OCH ₃	OCH ₃	H
361	3,4-Dimethoxyxanthone	H	H	OCH ₃	OCH ₃
362	3,5-Dihydroxyxanthone	H	H	OH	OH
363	3,5-Dimethoxyxanthone	H	H	OCH ₃	OCH ₃
364	3-Hydroxy-4-Methoxyxanthone	H	H	OH	OCH ₃
365	3-Hydroxy-5-Methoxyxanthone	H	H	OH	OCH ₃
366	4-Hydroxy-3-Methoxyxanthone	H	H	OCH ₃	OH
367	1,3-Dihydroxy-2-Methylxanthone	OH	CH ₃	OH	H

Table 43. IC₅₀ values of xanthone derivatives at the mammalian PKC- α , - β I, - δ , - η or - ζ

Compound	IC ₅₀ (nM)				
	PKC- α	PKC- β I	PKC- δ	PKC- η	PKC- ζ
348	6300±812**	ND	ND	7±2	ND
349	ND	ND	2510±630	9579±2055*	ND
350	ND	3981±744**	50±18**	2±0.7	13±2**
351	ND	ND	ND	ND	626±73
352	ND	ND	ND	ND	188±41
353	ND	ND	ND	ND	16±4
354	ND	101±12*	19±2	25±8	2000±986*
355	2512±367**	5000±507**	141±14**	9±2	151±21**
356	ND	ND	1032±190 [†]	8700±916 [†]	6±2
357	ND	ND	ND	ND	501±37
358	ND	ND	ND	3±1	2460±690**
359	2500±577**	126±34**	248±27**	1±0.8	79±16**
361	ND	ND	5±2	2876±1143*	2522±1090*
364	ND	9897±3580 [†]	2410±414 [†]	188±62 [†]	4±0.8
366	ND	ND	1021±232**	2±1	21±10
367	5623±681**	3660±352** [†]	1585±127** [†]	16±4	28±10

IC₅₀ values were considered to be the concentration that caused 50% growth inhibition (assuming that 100% growth inhibition was that caused by 10⁻⁵ M PMA for PKC- α , - β I, - δ and - η or by 10⁻⁵ M arachidonic acid for PKC- ζ). Xanthenes were tested in a concentration range of 10⁻¹¹–10⁻⁵ M. Shown are means ± SEM of 20–32 determinations. ND; non-determinable (when the maximal response reached was lower than 50% growth inhibition). Significant differences: relatively to PKC- δ , **p* < 0.05; relatively to PKC- η , ***p* < 0.05; relatively to PKC- ζ , [†]*p* < 0.05 (unpaired Student's *t*-test).

In 2003, Lucilia Saraiva *et al.* evaluated the modulatory activity of two xanthenes (3,4-dihydroxyxanthone **368** and 1-formyl-4-hydroxy-3-methoxyxanthone **369**) (Figure 42) on isoforms α , β I, δ , η and ζ of protein kinase C (PKC) using an in vivo yeast phenotypic assay. In yeast expressing PKC- ζ , arachidonic acid, but not PMA, caused a concentration-dependent growth inhibition of yeast expressing this isoform, with an EC₅₀ of 208.2 ± 30.3 nM (n = 64). Maximal values of growth inhibition caused by 10⁻⁵ M PMA (or arachidonic acid for PKC- ζ), on the PKC isoforms tested are presented on (Table 44). Both xanthenes caused an effect compatible with PKC inhibition,

similar to that elicited by known PKC inhibitors (chelerythrine and NPC 15437) (Table 45). PKC inhibition caused by xanthenes was confirmed using an in vitro kinase assay. The yeast phenotypic assay revealed that xanthenes present differences on their potency towards the distinct PKC isoforms tested. It is concluded that 3,4-dihydroxyxanthone and 1-formyl-4-hydroxy-3-methoxyxanthone may become useful PKC inhibitors and xanthone derivatives can be explored to develop new isoform-selective PKC inhibitors [74].

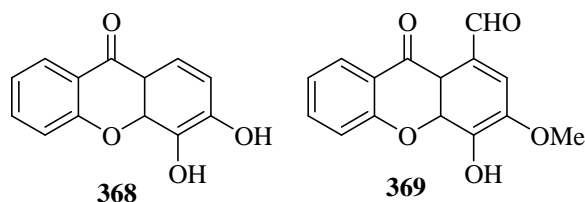


Figure 42. 3,4-Dihydroxyxanthone 367 and 1-formyl-4-hydroxy-3-methoxyxanthone

Table 44. Yeast growth inhibition caused by 10^{-5} M PMA on the PKC isoforms studied

PKC isoforms	Growth inhibition caused by 10^{-5} M PMA
α	40.6 ± 1.9 (n=36)
β I	36.1 ± 1.1 (n=56)
δ	26.6 ± 0.6 (n=52)
η	21.3 ± 0.7 (n=52)
ζ	0.2 ± 1.4 (n=36) ^a

Growth in the presence of solvent was considered to be 0% growth inhibition (100% growth). Each value represents the mean \pm SEM of the indicated n determinations.

PMA (considered a standard activator for the classical and novel PKC isoforms)

^aGrowth inhibition caused by 10^{-5} M arachidonic acid was 23.9 ± 0.7 (n=56).

Table 45. EC_{50} ratios for xanthenes 368 and 369, NPC 15437 and chelerythrine on the individual PKC isoforms tested

Compound	EC_{50} ratio ^a				
	PKC- α	PKC- β I	PKC- δ	PKC- η	PKC- ζ
Xanthone 368	$1.8 \pm 0.2^{*w}$	$0.8 \pm 0.1^{*w}$	$4.5 \pm 0.8^{*w}$	600.0 ± 25.4	40.1 ± 1.8^w
Xanthone 369	79.2 ± 6.9	$28.7 \pm 2.4^{\ddagger}$	$24.0 \pm 1.6^{\ddagger}$	$20.0 \pm 2.8^{\ddagger\ddagger}$	$10.4 \pm 1.1^{\ddagger\ddagger}$
NPC 15437	$5.1 \pm 0.5^{*w}$	$3.7 \pm 0.3^{*w}$	$2.4 \pm 0.1^{*w}$	556.0 ± 44.7	$4.5 \pm 0.1^{\ddagger w}$
Chelerythrine	$1.9 \pm 0.3^{*w}$	$2.9 \pm 0.3^{*w}$	$1.3 \pm 0.1^{*w}$	$63.2 \pm 1.7^{\ddagger}$	$1.4 \pm 0.2^{\ddagger w}$

The EC_{50} values were considered the concentration of PKC activator that caused half of the growth inhibition caused by 10^{-5} M of PMA (arachidonic acid for PKC- ζ). Shown are means \pm SEM of 16–20 determinations. Significant differences: from xanthone 2, * $P < 0.05$; from xanthone 1, $^{\ddagger}P < 0.05$; from PKC- α , $^{\ddagger}P < 0.05$; from PKC- η , $^wP < 0.05$ (one way ANOVA, followed by Tukey's post-hoc test).

^a EC_{50} ratio = EC_{50} (PKC activator + 10^{-5} M compound) / EC_{50} (PKC activator).

2-7. Xanthenes acting on cardio-vascular system

In 2002, Li-Wen Wang *et al.* synthesized a series of xanthenes related to Formula X **370-373** and xanthonoxypropanolamines Formula XI **374** and **375** (Table 46). All the compounds (Tables 46 and 47) were assayed for their ability to lower blood pressure in normotensive Wistar rat. All the compounds tested exhibited effective hypotensive activity in anesthetized rats. An oxypropanolamine side chain substituted at the C-3 position of the xanthone nucleus significantly enhanced the hypotensive activity. In rat thoracic aorta, all the compounds tested significantly depressed the contractions induced by Ca^{2+} (1.9mM) in high K^+ (80mM) medium and the phasic and tonic contractions caused by norepinephrine (3 μ M). In the rat thoracic aorta, the phenylephrine- and high K^+ -induced Ca^{2+} influx were both inhibited by a selective xanthone derivative, **375** (Table 48). In addition to the previously reported result of **375**, evaluated as beta adrenoceptor blocker, the depressor and bradycardia effects of **372** are independent of the parasympathetic passway. These results suggest that **375** showed inhibitory effects on the contractile response caused by high K^+ and norepinephrine in rat thoracic aorta are mainly due to inhibition of Ca^{2+} influx through both voltage-dependent and receptor-operated Ca^{2+} channels. The vasodilating properties of **375** is due to its calcium channel and beta adrenergic blocking effects [75].

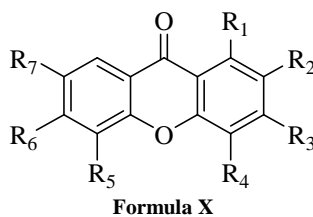
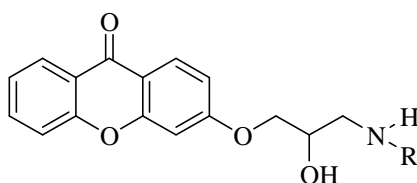


Table 46. Antihypertensive properties of synthetic xanthone derivatives

Compd	R1	R2	R3	R4	R5	R6	R7	Blood pressure (mm Hg) ^a			
								Dose(mg/kg) iv	Before	After	Change (%)
370	H	H	OH	H	OH	H	H	1	118.600±4.632	107.000±4.889	-9.8
								5	114.000±3.531	79.333±7.775**	-30.9
371	H	H	OH	H	H	OH	H	1	107.500±7.500	98.500±8.684	-8.4
								5	105.000±5.244	83.000±4.754*	-21.0
372	OH	H	OH	H	H	OH	OH	1	141.000±4.546	136.667±4.907	-3.1
								5	128.667±2.373	122.567±3.569*	-4.7
								10	124.667±2.722	110.000±7.360*	-11.8
373	H	OH	OH	H	H	OH	OH	1	125.333±2.126	117.000±3.859*	-6.6
								5	147.667±3.538	138.333±5.932*	-6.3
								10	146.667±3.600	134.000±3.742*	-8.6

^aEach value represents the mean ± SEM (n=5); (*p<0.05; **p<0.01)



Formula XI

Table 47. Antihypertensive properties of synthetic xanthone derivatives

Compd	R	Blood pressure (mm Hg) ^a			
		Dose (mg/kg) iv	Before	After	Change (%)
374	-CH ₂ CH ₂ CH ₃	0.1	130.0±8.0	128.0±5.0	-1.6±0.0*
		0.5	119.5±1.8	114.0±2.3	-4.7±0.6*
		1.0	124.8±4.5	101.8±3.7	-18.4±1.8*
		5.0	105.4±3.9	80.3±2.9	-23.71±1.6*
375	-CH-(CH ₃) ₂	0.1	120.0±7.9	111.0±6.7	-7.4±1.1*
		0.5	127.56±6.5	115.7±6.9	-9.3±0.7*
		1.0	127.0±2.6	108.4±3.0	-14.6±1.4*
		5.0	123.6±3.9	84.5±5.5	-32.1±2.8*

^aValue represents the mean ± SEM (n=5) (*p<0.05, **p<0.01)

Table 48. Effect of synthetic xanthone derivatives on high K⁺- and Ca²⁺-induced and norepinephrine induced contraction of rat thoracic aorta^a

Compd (mg/mL) (1m)	K ⁺ (80mM)+Ca ²⁺	Norepinephrine	
		Phasic	Tonic
Control	100.0±4.5	100.0±4.4	100.0±1.2
370 (25)	41.4±1.0**	70.8±14.7*	65.6±5.9*
370 diacetate (100)	43.9±9.4**	62.4±1.7*	50.7±4.6**
371 (100)	4.0±2.8***	7.1±5.1***	0.9±0.7***
374 (100)	38.4±2.5**	9.9±3.1***	8.5±4.4***
375 (100)	3.3±2.4***	21.6±2.4***	15.4±0.5**

^aRat aorta was pre-incubated with various xanthone derivatives or DMSO (0.1%, control) at 37°C for 15 min, then high K⁺ (80mM) and Ca²⁺ (1.9mM) or norepinephrine (3 μM) was added. Percentages of the contraction were calculated and presented as mean ± SEM (n=3); *p<0.05, **p<0.01, ***p<0.001, as compared with the respective control values.

In 2003, De-Jian Jiang *et al.* synthesized 1,3,5,6-tetrahydroxanthone **376** (Figure 43). The relationship between protective effect of xanthone on endothelial cells and endogenous nitric oxide synthase inhibitors was investigated. Endothelial cells were treated with ox-LDL (100 μg/mL) for 48 h. Adhesion of monocytes to endothelial cells and release of lactate dehydrogenase (LDH) was determined. Levels of tumor necrosis factor-α (TNF-α), monocyte chemo attractant protein-1 (MCP-1), nitric oxide (NO) and asymmetric dimethylarginine (ADMA, an endogenous inhibitor of nitric oxide synthase) in conditioned medium and activity of dimethylarginine dimethylaminohydrolase (DDAH) in endothelial cells were measured. Incubation of endothelial cells with ox-LDL (100 μg/mL) for 48 h markedly enhanced the adhesion of monocytes to endothelial cells, increased the release of LDH, the levels of TNF-α, MCP-1 and ADMA, and decreased the content of NO and the activity of DDAH. Xanthone (1,3,5,6-tetrahydroxanthone) (1, 3 or 10 μmol/L) significantly inhibited the increased adhesion of monocytes to endothelial cells and attenuated the increased levels of LDH, MCP-1 and ADMA induced by ox-LDL. Xanthone (1,3,5,6-tetrahydroxanthone) (3 or 10 μmol/L) significantly attenuated the increased level of TNF-α and decreased level of NO and activity of DDAH by ox-LDL. The present results suggest that xanthone (1,3,5,6-tetrahydroxanthone) preserves endothelial cells and inhibits the increased adhesion of monocytes to endothelial cells induced by ox-LDL, and that the protective effect of xanthone (1,3,5,6-tetrahydroxanthone) on

endothelial cells is related to reduction of ADMA concentration via increase of DDAH activity [76].

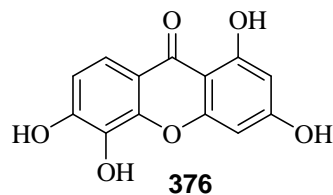


Figure 43. 1,3,5,6-tetrahydroxyxanthone

In 2010, Honggang Hu *et al.* reported xanthone sulfonamides as novel class small molecule inhibitors of ACAT. Inhibitors of acyl-CoA: cholesterol acyltransferase (ACAT) would be useful anti-atherogenic agents, since an absence of ACAT affects the absorption and transformation of cholesterol, indirectly resulting in the reduction of cholesteryl ester accumulation in blood vessels. A series of xanthone sulfonamides were synthesized and evaluated to result in the identification of several potent ACAT inhibitors, among which **377** (Figure 44) proved to be more potent than the positive control Sandoz 58-35 (an inhibitor towards ACAT) (Table 49) [77].

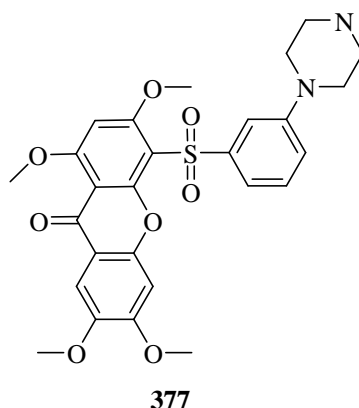


Figure 44. Xanthone sulfonamide

Table 49. Structure and ACAT inhibition rate at 10 µg/mL concentration

Sample	% Inhibition
Sandoz 58-35 ^a	55.00
377	64.80

2-8. Anti-malarial xanthenes

In 2008, Rozalia A. Dodean *et al.* investigated the effect of fluorine upon the heme-binding ability of the xanthone nucleus for 3,6-bis-(ω -*N,N*-diethylaminoxy)-4,5-difluoroxanthone **378** (Figure 45). 2-Fluoro-1,3-dimethoxybenzene was prepared by a new, improved method and used to build up the xanthone nucleus. The interaction of F2C5 with heme was investigated by UV-vis, ¹H NMR, and ¹⁹F NMR spectroscopy. The binding affinity of F2C5 was compared to those of the structurally similar C₅ and other known antimalarial compounds (Table 50). For the first time, NMR studies for the heme–drug interactions are carried out at pH 5.0, physiological for the acidic food vacuole of the malaria parasite. The IC₅₀ values for F2C5 against the multidrug-resistant strains W2 and D6 of *P. falciparum* were compared to those of other known antimalarials (Table 51) [78].

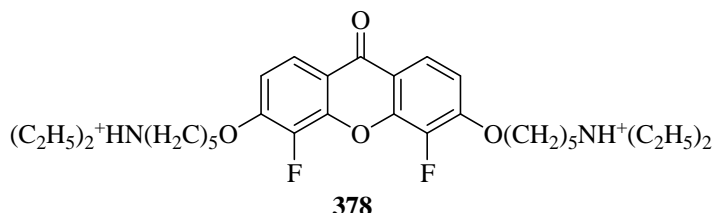


Figure 45. 3,6-bis-(ω -*N,N*-diethylaminoxy)-4,5-difluoroxanthone

Table 50. Binding affinity (K_a) of selected compounds for heme in aqueous solution

Compound	K_a ($10^3 M^{-1}$)
Chloroquine	4.0
Quinine	0.2
Mefloquine	0
378	0.6

Table 51. In vitro antimalarial activity against D6 and W2 strains of *Plasmodium falciparum*

Compound	IC ₅₀ , nM, D6	IC ₅₀ , nM, W2
Quinine	1.1×10^1	6.0×10^1
Chloroquine	7.8×10^0	2.9×10^2
Mefloquine	5.9×10^0	0.7×10^0
378	9.3×10^1	1.5×10^2

In 2009, Masahiko Isaka *et al.* isolated Acremoxanthones A **379** and B **380** (Figure 46), novel anthraquinone-xanthone heterodimers with a unique linkage pattern, together with two known compounds, acremonidins A **381** and C **382** (Figure 46), from the fungus *Acremonium* sp. BCC31806. The structures of the acremoxanthones were determined by analysis of 2D NMR and mass spectrometric data. Acremoxanthones and acremonidins exhibited antibacterial, antifungal, anti-plasmodial and cytotoxic activities. Compounds **379-382** were subjected to in vitro biological assays: antibacterial (*Staphylococcus aureus*, *Bacillus cereus*, *Pseudomonas aeruginosa*, and *Escherichia coli*), antifungal (*Candida albicans*, *Magnaporthe grisea*), antimycobacterial (*Mycobacterium tuberculosis* H37Ra), and antiplasmodial (*Plasmodium falciparum* K1) activities, and cytotoxicity to three cancer cell-lines (KB, BC, and NCI-H187) and non-cancerous Vero cells (Table 52). The Compounds showed significant activity as anti-malarial agents [79].

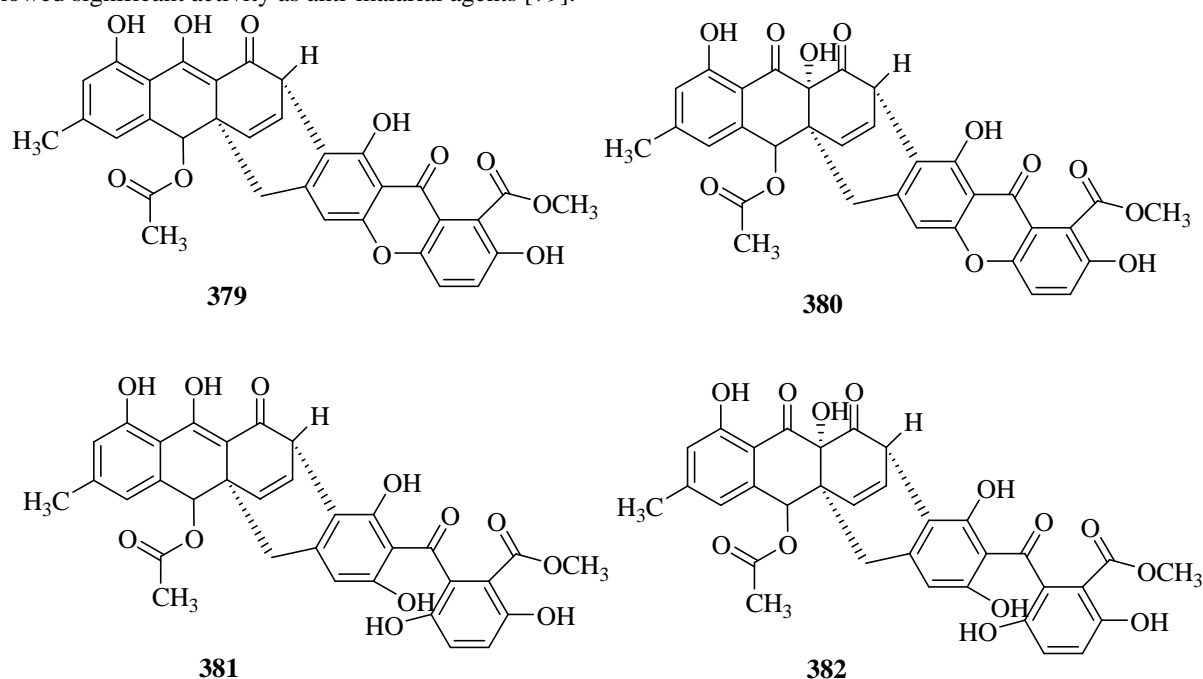


Figure 46. Acremoxanthones and acremonidins

Table 52. Biological activities of compounds

Compd.	<i>S. aureus</i> ^a (MIC, $\mu\text{g/mL}$)	<i>B. cereus</i> ^a (MIC, $\mu\text{g/mL}$)	<i>C. albicans</i> ^b (MIC, $\mu\text{g/mL}$)	<i>P. falciparum</i> ^c (MIC, $\mu\text{g/mL}$)	Cytotoxicity (IC ₅₀ , $\mu\text{g/mL}$) ^d			
					KB	BC	NCI-H187	Vero
379	12.5	>100	1.7	>10	3.3	1.1	0.87	1.2
380	6.25	6.25	>50	3.0	18	9.4	14	12
381	3.13	1.56	>50	5.4	13	5.0	4.5	6.6
382	3.13	3.13	>50	>10	>20	9.3	16	23

^a Antibacterial activity against *Staphylococcus aureus* and *Bacillus cereus* was evaluated using the resazurin microplate assay (REMA). MIC values of a standard antibacterial vancomycin for *S. aureus* and *B. cereus* were 1.0 and 4.0 $\mu\text{g/mL}$, respectively.

^b Antifungal activity against *Candida albicans*. Standard compound, amphotericin B, showed an IC₅₀ value of 0.047 $\mu\text{g/mL}$.

^c Antimalarial activity against *Plasmodium falciparum* K1. Standard antimalarial drug, dihydroartemisinin, showed an IC₅₀ value of 0.0011 $\mu\text{g/mL}$.

^d The IC₅₀ values of a standard compound, ellipticine, against KB, BC, NCI-H187 and Vero cells were 0.27, 0.21, 0.15 and 0.60 $\mu\text{g/mL}$, respectively.

In 2013, Jittra Kornsakulkarn *et al.* isolated three new mycotoxins **383-385** (Figure 47), together from the scale insect fungus *Aschersonia marginata* BCC 28721. Compounds **383** and **385** exhibited moderate cytotoxic activity (Table 53) [80].

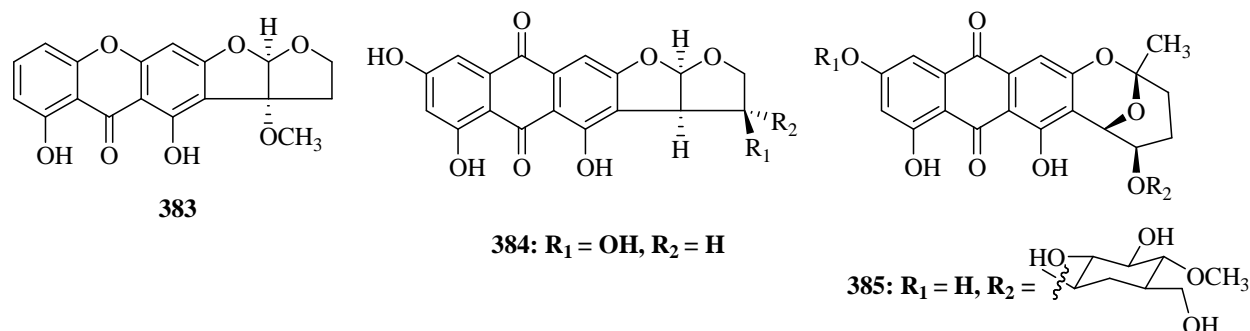


Figure 47. Xanthenes derived from fungus *Aschersonia marginata*

Table 53. Biological activities of compounds

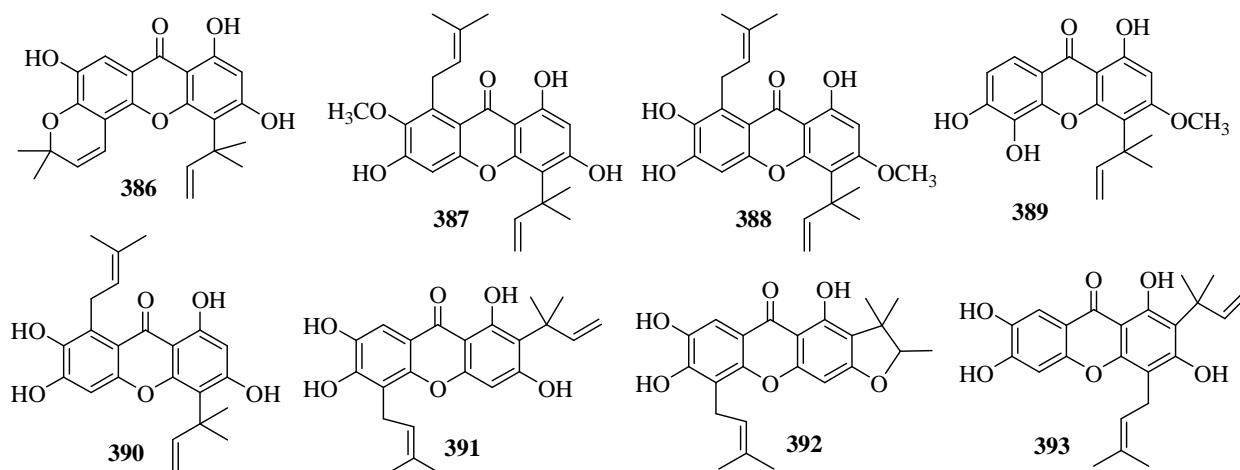
Compounds	Antimalaria, IC ₅₀ (μg/mL)	Cytotoxicity, IC ₅₀ (μg/mL)			
		KB cells	MCF-7 cells	NCIH187 cells	Vero cells
383	>10	21.57	>50	>50	20.11
384	>10	22.94	>50	5.28	8.20
385	>10	>50	>50	>50	>50
Doxorubicin ^a	—	0.71	6.05	0.08	—
Ellipticine ^a	—	1.57	—	0.50	1.71
Dihydroartemisinin ^b	0.0005	—	—	—	—

^a Cytotoxicity controls.

^b Antimalarial control.

2-9. Anti-oxidant xanthenes

In 2005, Byong Won Lee *et al.* isolated new catecholic xanthone, 1,3,7-trihydroxy-4-(1,1-dimethyl-2-propenyl)-5,6-(2,2-dimethylchromeno)-xanthone **386** (Figure 48), from the root bark of *Cudrania tricuspidata* together with seven known xanthenes **387-393** (Figure 48). The structures were fully characterized by analysis of physical and spectral (UV, IR, mass, and NMR) data. Relationships between the structural characteristics of xanthenes and their antioxidant activities (DPPH, superoxide, and hydroxyl radical) were studied. Among the range of catecholic xanthenes, 6,7-dihydroxyl xanthenes (**388-393**) exhibited a strong scavenging effect on the DPPH radical (Table 54). When one of the catecholhydroxyl groups was protected as in compounds **386** and **387**, DPPH radical scavenging activity was markedly decreased (IC₅₀> 200 μM). DPPH activities were consistent with electrochemical response by cyclic voltammetry. Interestingly, compounds (**386, 387**) which had the weak activities on DPPH, exhibited both potent superoxide and hydroxyl radical scavenging activities. The strong activity on the hydroxyl radical of compounds (**386, 387**) could be rationalized by their chelating effect with iron (Fe²⁺) due to a redshift of its complex. The catecholic xanthenes (**388-393**), being able to convert quinone methide intermediate, showed potent cytotoxicities against human cancer cell lines (HT-29, HL-60, SK-OV3, AGS, and A549). In particular, compounds **388, 391, and 392** had strong cytotoxic activities against AGS (LD₅₀< 5 μM) (Table 55). DNA fragmentation patterns induced by catecholic xanthenes revealed that tumor cell death was due to apoptosis [81].

Figure 48. Xanthones extracted from *Cudrania tricuspidata*Table 54. Radical scavenging activities of compounds 386-393 from *Cudrania tricuspidata*^a

Compound	DPPH	O ₂ ⁻	·OH
386	200>	64.5	55.5
387	200>	85.1	24.3
388	17.4	92.8	25.2
389	31.8	29.5	100.7
390	21.3	51.0	21.2
391	13.7	23.6	50.3
392	10.4	26.0	42.6
393	15.4	47.8	74.1
Trolox	10.6	33.6	48.2

^a Results are expressed as IC₅₀ values (μM) by ESR signal intensity.Table 55. In vitro cytotoxicity of prenylated xanthones and adriamycin against human cancer cell lines^a

Compound	HT-29	HL-60	SK-OV3	AGS	A549
386	46.3	35.9	70.4	44.7	61.9
387	50.7	40.8	73.5	49.5	61.7
388	20.7	6.2	23.8	4.7	16.3
389	65.0	45.2	71.3	43.9	57.8
390	41.4	32.8	43.2	32.8	45.8
391	11.4	8.6	38.0	3.9	33.5
392	12.1	8.2	14.6	4.1	11.8
393	28.0	29.5	23.1	15.2	25.8
Adriamycin	1.8	1.1	14.2	1.2	1.3

^a Results are expressed as LD₅₀ values (μM).

In 2006, Ki Hun Park *et al.* isolated the catecholic xanthones and flavonoids **394–406** (Figure 49) from the root bark of *Cudrania tricuspidata*. Compounds **394** and **396–401** exhibited significant antioxidant activity against low-density lipoprotein (LDL) oxidation in the thiobarbituric acid-reactive substance (TBARS) assay (Table 56). Among them, prenylated flavonoids **403–405** showed an inhibitory effect on the NO production and iNOS expression in RAW 264.7 cells. Also, compounds **394**, **395**, **398**, **400**, **402** and **404** preferentially inhibited hACAT-2 than hACAT-1, where as compounds **396**, **397**, **399** and **401** showed a similar specificity against hACAT-1 and -2. However, flavonoids **403**, **405** and **406** dominantly inhibited hACAT-2, not hACAT-1 [82].

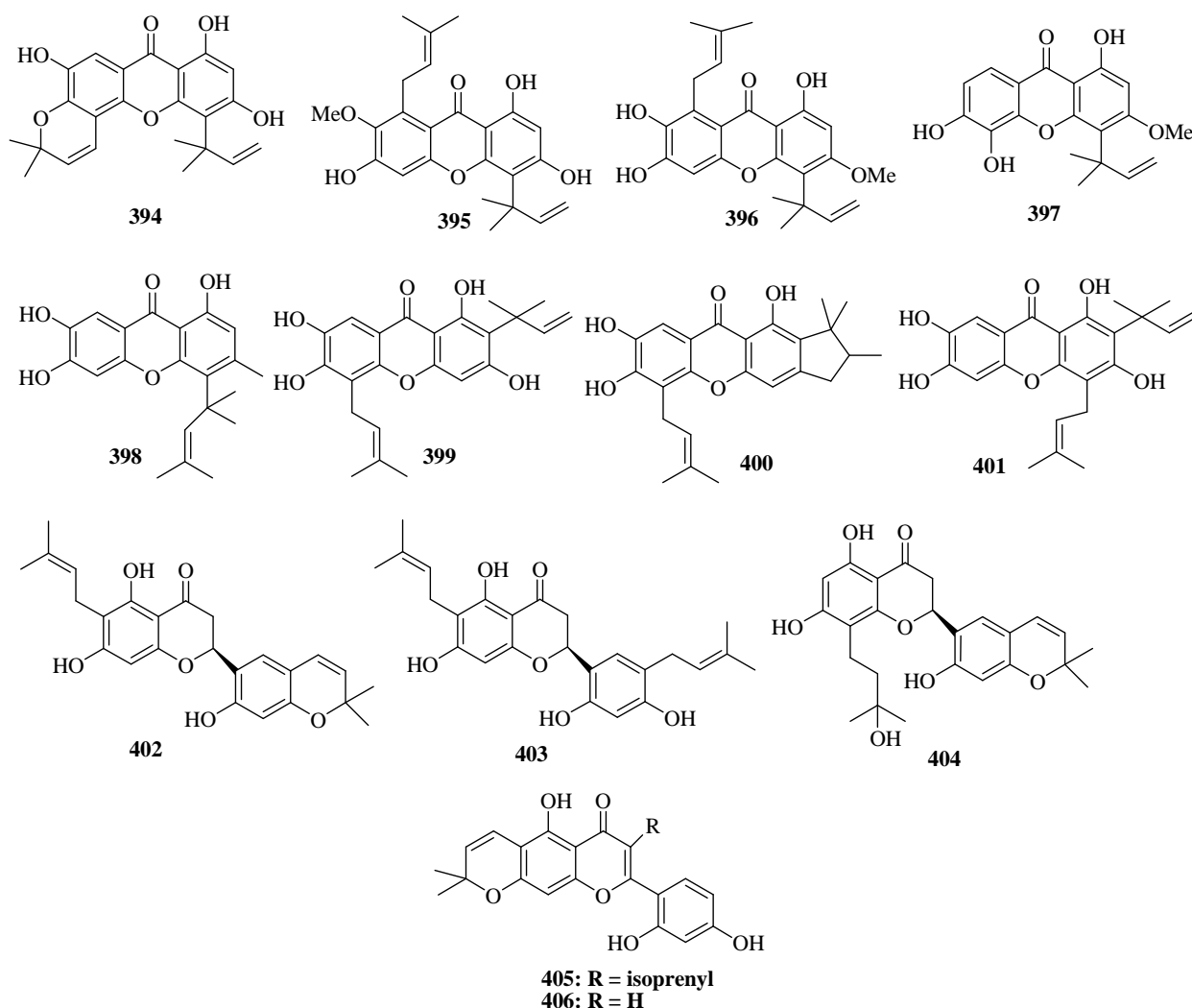


Figure 49. Catecholic xanthenes and flavonoids

Table 56. Antioxidant activity against LDL oxidation and ACAT inhibitory activities of compounds

Compound	LDL (IC ₅₀ , μM) ^a	hACAT-1 (IC ₅₀ , μM) ^b	hACAT-2 (IC ₅₀ , μM) ^b
394	12.6	40	28.8
395	NA	20	19.2
396	6.2	57.6	75.2
397	0.8	148	132.8
398	2.6	89.6	41.6
399	3.8	68.0	74.4
400	2.2	56.8	23.2
401	4.5	96.0	112.0
402	43.2	82.4	24.8
403	65.6	NA	89.6
404	27.2	59.2	44.8
405	46.4	NA	41.6
406	62.4	NA	77.6
Probulcol ^c	3.6		
Oleic acid anilide ^d		0.14	0.17

^a *In vitro* antioxidant activity was measured using human plasma LDL (120 μg/mL). Data are shown as mean values of two independent experiments performed in duplicate.

^b *In vitro* ACAT inhibitory activity was measured using the expressed hACAT-1 or hACAT-2. Data are shown as mean values of two independent experiments performed in duplicate.

^c Probulcol was used as a positive control.

^d Oleic acid anilide was used as a positive control.

In 2010, Clementina M. M. Santos *et al.* evaluated the scavenging activity of the new 2,3-diarylxanthenes relevant to Formula XII **407-409**, Formula XIII **410-412** and Formula XIV **413-415** (Figure 50) for ROS (reactive oxygen species), including superoxide radical (O₂^{•-}), hydrogen peroxide (H₂O₂), singlet oxygen (¹O₂), peroxy radical (ROO[•]) and hypochlorous acid (HOCl), and RNS (reactive nitrogen species) (Table 57), including nitric oxide (NO)

and peroxyxynitrite anion (ONOO⁻) (Table 58), considering the interesting and promising antioxidant activities present in xanthone core. The natural derivatives can present different substitutions in the xanthone core that include hydroxyl, methoxyl, prenyl and glycosyl groups. The obtained results revealed that the 2,3-diarylxanthones are endowed with outstanding ROS and RNS scavenging properties, considering the nanomolar to micromolar range of the IC₅₀ values found. The xanthones with two catechol rings were the most potent scavengers of all tested ROS and RNS. In conclusion, the new 2,3-diarylxanthones are promising molecules to be used for their potential antioxidant properties [83].

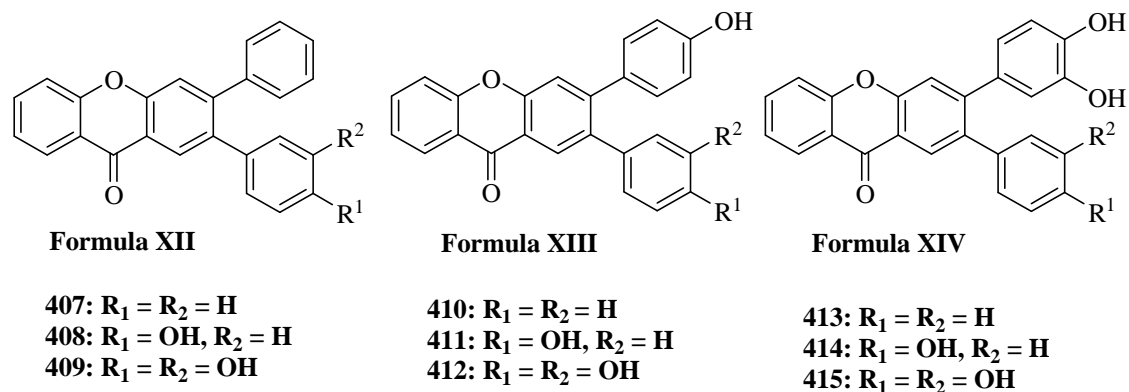


Figure 50. 2,3-diarylxanthone derivatives

Table 57. O₂⁻, H₂O₂, ¹O₂ and HOCl scavenging activity (IC₅₀, mean ± SEM) and ROO[•] scavenging activity (concentration range 0.125–1.0 μM) expressed as ORAC values (mean ± SEM) of the tested 2,3-diarylxanthones and positive controls

Compd	IC ₅₀ (μM)				ORAC _{ROO[•]} ± SEM (μM trolox equiv/ μM compound)
	O ₂ ⁻	H ₂ O ₂	HOCl	¹ O ₂	
<i>2,3-Diarylxanthones</i>					
407	NA ²⁵ μM	NA ¹²⁵ μM	155 ± 25	27% ^{*100} μM	NA ¹ μM
408	NA ²⁰⁰ μM	NA ¹²⁵ μM	72.1 ± 8.6	80 ± 11	1.05 ± 0.09
409	28.1 ± 2.3	9% ^{*125} μM	15.7 ± 1.1	6.0 ± 1.0	0.76 ± 0.01
410	NA ²⁰⁰ μM	NA ¹²⁵ μM	53.8 ± 7.8	68.8 ± 6.2	2.08 ± 0.16
410	166 ± 16	NA ¹²⁵ μM	22.4 ± 2.5	58.4 ± 4.9	2.88 ± 0.09
412	20.3 ± 2.5	14% ^{*250} μM	14.7 ± 1.3	3.3 ± 0.7	0.88 ± 0.12
413	76 ± 11	9% ^{*125} μM	10.8 ± 0.4	4.5 ± 0.6	0.84 ± 0.01
414	31.3 ± 3.2	12% ^{*250} μM	7.5 ± 0.7	6.8 ± 0.5	0.83 ± 0.03
415	10.4 ± 0.8	17% ^{*250} μM	1.2 ± 0.02	2.5 ± 0.2	0.28 ± 0.03
<i>Positive controls</i>					
Tiron	273 ± 32	—	—	—	—
Ascorbic acid	—	602 ± 80	—	—	0.22 ± 0.03
Dihydrolipoic acid	—	—	2.3 ± 0.3	—	—
Quercetin	—	—	—	1.8 ± 0.1	—

NA: no activity was found up to the highest tested concentration (in superscript).

* Scavenging effect (mean%) at the highest tested concentration (in superscript).

Table 58. [•]NO and ONOO⁻ (with and without 25 mM NaHCO₃) scavenging effects (IC₅₀, mean ± SEM) of the tested 2,3-diarylxanthones and positive controls

Compd	[•] NO	IC ₅₀ (μM)	
		ONOO ⁻ without NaHCO ₃	ONOO ⁻ with NaHCO ₃
<i>2,3-Diarylxanthones</i>			
407	39% ^{*200} μM	29% ^{*50} μM	48% ^{*50} μM
408	175 ± 36	1.55 ± 0.14	1.80 ± 0.39
409	1.88 ± 0.18	0.40 ± 0.03	0.54 ± 0.08
410	41% ^{*200} μM	2.66 ± 0.29	2.00 ± 0.15
411	108 ± 18	1.72 ± 0.21	0.97 ± 0.25
412	0.42 ± 0.05	0.26 ± 0.05	0.78 ± 0.26
413	1.22 ± 0.21	0.37 ± 0.09	0.67 ± 0.09
414	0.62 ± 0.10	0.22 ± 0.03	0.89 ± 0.18
415	0.39 ± 0.05	0.17 ± 0.01	0.33 ± 0.06
<i>Positive controls</i>			
Rutin	2.53 ± 0.37	—	—
Ebselen	—	0.50 ± 0.03	2.01 ± 0.22

* Scavenging effect (mean%) at the highest tested concentration (in superscript).

In 2015, Evgeny V. Buravlev *et al.* synthesized a series of new C-4 derivatives of α -mangostin using Mannich reaction and alkylation with 4-bromomethyl-2,6-dialkylphenols. The synthesized compounds **416**, **417**, **418**, **419** and **420** (Figure 51) have been evaluated for their cytotoxic, anti-oxidant and membrane protective properties.

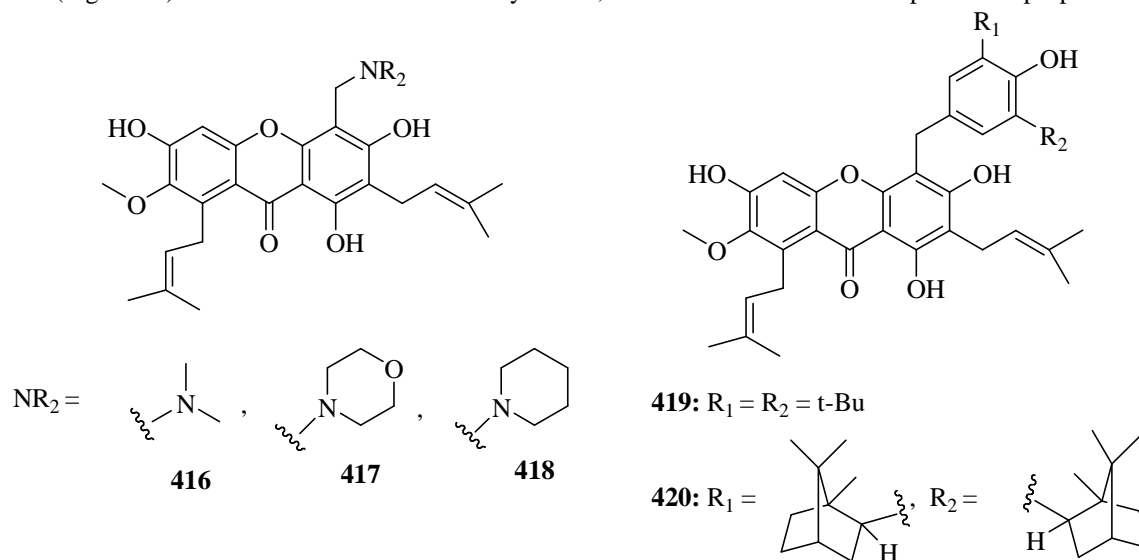


Figure 51. C-4 derivatives of α -mangostin

The dimethylaminomethyl derivative **416** showed significant increase in toxicity with the concentration growth up to 30 μ M, only caused a high level of protective activity of this compound at concentration of 10 μ M. The Mannich bases containing morpholinomethyl **417** and piperidinomethyl **418** fragments were found to be most effective under acute oxidative stress conditions at medium (10 μ M) and high concentrations (30 μ M). The derivative **419** at high concentrations only (30 μ M), which is explained both by low toxicity of these compounds and increase in antioxidant activity with concentration growth. Moderate membrane-protective activity of the derivative **420** was only observed when it was used at low concentrations (1.1M) [84].

2-10. Xanthenes acting on central nervous system

In 2005, Eric Vieira *et al.* designed and synthesized small molecule mGluR1 enhancers based on the lead compound (9*H*-xanthene-9-carbonyl)-carbamic acid butyl ester derived from random screening hit diphenylacetyl-carbamic acid ethyl ester as useful pharmacological tools for the study of the physiological roles mediated by mGlu1 receptors. The corresponding ester bioisosteres 1,2,4-oxadiazoles derivatives related to Formula XV **421-426** and tetrazoles related to Formula XVI **427-431** have been prepared (Table 59). The synthesis and the structure activity relationship of this new class of positive allosteric modulators of mGlu1 receptors discussed in detail (Table 59). In the pharmacokinetic studies, both the methyl-substituted 1,2,4-oxadiazole **421** and the ethyl-substituted tetrazole **428** have an intermediate to high plasma clearance (Cl) and an intermediate volume of distribution (V_{ss}) (Table 60) [85].

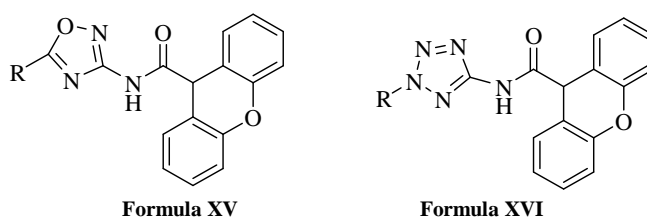


Table 59. Structure–activity relationship of oxadiazoles 421-426 and tetrazoles 427-431

R	mGluR1 EC ₅₀ (nM)	Agonist effect (%) ^a	In vitro metabolism (rat microsomes) (μ l/min/mg protein)	In vitro metabolism category	Solubility (pH 6.5) (μ g/ml)
421 Me	52	100	42	Intermediate	12
422 Et	6	57	78	Intermediate	0.056
423 <i>n</i> -Pr	25	90	97	High	<1
424 <i>i</i> -Pr	22	80	130	High	4
425 Cyprop	23	80	227	High	<1
426 <i>i</i> -Bu	10	54	17	Low	7
427 Me	180	65	16	Low	35
428 Et	65	80	41	Intermediate	21
429 <i>n</i> -Pr	29	80	92	High	4
430 <i>i</i> -Pr	45	70	63	Intermediate	4
431 <i>i</i> -Bu	34	28	229	High	n.m.

n.m. indicates not measured.

Table 60. Pharmacokinetics of selected compounds 421 and 428 (data are mean values, n = 2)

Dose route of Administration	DMPK parameters	421	428
10 (mg/kg) iv bolus	Half-life (h)	0.32	0.49
	Cl (ml/min/kg)	60.0	49.2
	V _{ss} (L/kg)	1.82	2.09
10 (mg/kg) po bolus	C _{max} (ng/ml)	1174	1130
	T _{max} (h)	1.5	1.5
	Brain/plasma	1.5	
15 mg/kg/h iv infusion	CSF/plasma	0.08	
	Brain/plasma		0.16
	CSF/plasma		0.06

In 2012, Carla Fernandes *et al.* reported the synthesis and structure elucidation of three new chiral xanthone (*9H*-xanthon-9-one) derivatives of formula XVII **433-435** (Figure 52). The coupling reactions of the synthesized building block 6-methoxy-9-oxo-9*H*xanthen-2-carboxylic acid **432** (Figure 52) with two enantiomerically pure amino alcohols ((*S*)-(+)-valinol and (*S*)-(+)-leucinol) and one amine ((*S*)-(-)- α -4-dimethylbenzylamine), were carried out using the coupling reagent O-(benzotriazol-1-yl)-*N,N,N',N'*-tetramethyluronium tetrafluoroborate (TBTU). The coupling reactions were performed with yields higher than 97% and enantiomeric excess higher than 99%. Taking into account that these new chiral xanthone derivatives have molecular moieties structurally very similar to local anaesthetics, the ability to block compound action potentials (CAP) at the isolated rat sciatic nerve was also investigated. Nerve conduction blockade might result from a selective interference with Na⁺ ionic currents or from a non-selective modification of membrane stabilizing properties. Thus, the mechanism, by which the three chiral xanthone derivatives cause conduction blockade in the rat sciatic nerve and their ability to prevent hypotonic haemolysis, given that erythrocytes are non-excitable cells devoid of voltage-gated Na⁺ channels, are also described. Data suggest that nerve conduction blockade caused by newly-synthesized xanthone derivatives might result predominantly from an action on Na⁺ ionic currents. This effect can be dissociated from their ability to stabilize cell membranes, which became apparent only upon increasing the concentration of compounds **433-435** to the higher micromolar range [86].

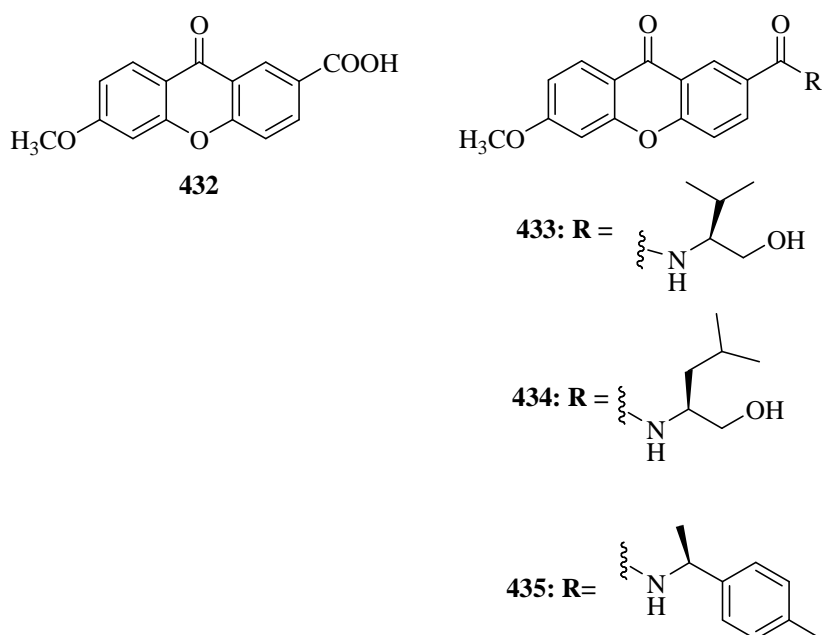


Figure 52. Chiral xanthone derivatives

2-11. Miscellaneous

2-11-1. Xanthenes as xanthine oxidase inhibitors

In 2011, Lina Hu *et al.* synthesised a series of xanthone derivatives of formula XVII **436-445** (Table 61) and a new class of xanthine oxidase inhibitor. Compounds **436**, **438**, **444**, **442** and **445** showed good inhibition against xanthine oxidase (Table 61). The presence of a cyano group at the para position of benzyl moiety turned out to be the preferred substitution pattern [87].

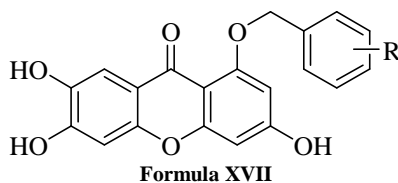


Table 61. In vitro xanthine oxidase inhibitory activity of xanthone derivatives

Compounds	R	IC ₅₀ ^{a,b} (μM)
436	2-CH ₃	7.08 ± 0.65
437	3-CH ₃	13.56 ± 0.28
438	4-CH ₃	5.73 ± 0.10
439	2-F	n.a ^c
440	3-F	n.a
441	4-F	n.a
442	2-Cl	6.41 ± 0.15
443	3-Cl	n.a
444	4-Cl	4.70 ± 0.12
445	4-CN	4.67 ± 0.35

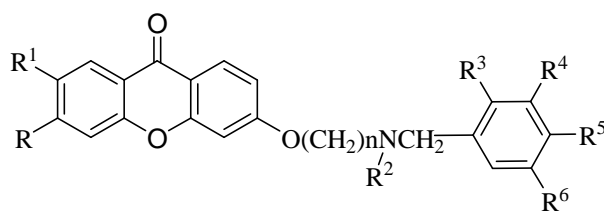
^a IC₅₀ values: the concentration of the inhibitor required to produce 50% inhibition of xanthine oxidase.

^b Each results was performed in triplicate. Allopurinol was used as positive control (IC₅₀ = 24.40 ± 0.50 μM).

^c n.a.: not active (less than 60% inhibition at 10 μg/mL).

2-11-2. Xanthenes as acetylcholinesterase inhibitors

In 2007, Lorna Piazzi *et al.* investigated a previously introduced class of cholinesterase inhibitors. Some new 3-[ω-(benzylmethylamino)alkoxy]xanthen-9-one analogs related to Formula XVIII **446-453** (Table 62) were designed, synthesized, and evaluated for their inhibitory activity against both acetylcholinesterase (AChE) and butyrylcholinesterase (BuChE). From the IC₅₀ values, it clearly appears that the carbamic residue is crucial to obtain highly potent AChE inhibitors. On the other hand, peculiarity of these compounds is the high selectivity toward BuChE with respect to AChE, being compound **451** the most selective one (6000-fold) (Table 63). The development of selective BuChE inhibitors may be of great interest to clarify the physiological role of this enzyme and to provide novel therapeutics for various diseases [88].



Formula XVIII

Table 62. Physicochemical and analytical data of the compounds studied

Compound	n	R	R ¹	R ²	R ³	R ⁴	R ⁵	R ⁶
446	7	H	H	Me	H	H	H	H
447	8	H	H	Me	H	H	H	H
448	9	H	H	Me	H	H	H	H
449	10	H	H	Me	H	H	H	H
450	11	H	H	Me	H	H	H	H
451	12	H	H	Me	H	H	H	H
452	7	OCH ₃	H	Me	H	H	H	H
453	7	OCH ₃	OCH ₃	Me	H	H	H	H

Table 63. Inhibitory activity on isolated AChE and BuChE and IC₅₀ ratio of the compounds studied

Compound	IC ₅₀ (μM)	IC ₅₀ (μM)	Ratio IC ₅₀	Ratio IC ₅₀
	AchE	BuChE	BuChE/AchE	AChE/BuChE
446	2.82 ± 0.61	0.80 ± 0.04	0.28	3.52
447	10.3 ± 6.50	0.08 ± 0.01	0.008	129
448	152	0.10 ± 0.02	6.6	1520
449	388	0.10 ± 0.01	2.6	3880
450	626	0.12 ± 0.01	1.92	5217
451	908	0.15 ± 0.02	1.65	6053
452	7.84 ± 0.51	46.1 ± 3.90	5.9	0.17
453	2.32 ± 0.13	3.08 ± 0.35	1.33	0.75

2-11-3. Xanthenes as *p*-glycoprotein inhibitors

In 2000, M.G. Dijoux-Franc *et al.* prepared Dimethylallyl (DMA) derivatives **455-464** (Figure 53) of a naturally occurring xanthone (decussatin **454**). Their activity as potential P-glycoprotein inhibitors was monitored by affinity of direct binding and compared to that of corresponding DMA-flavones (Table 64). Both classes of compounds exhibited the same structure-activity relationships. Decreasing polarity enhanced the binding affinity for the P-glycoprotein C-terminal cytosolic domain since DMA derivatives were more active, but unsubstituted hydroxyl group close to the carbonyl was required for efficient activity [89].

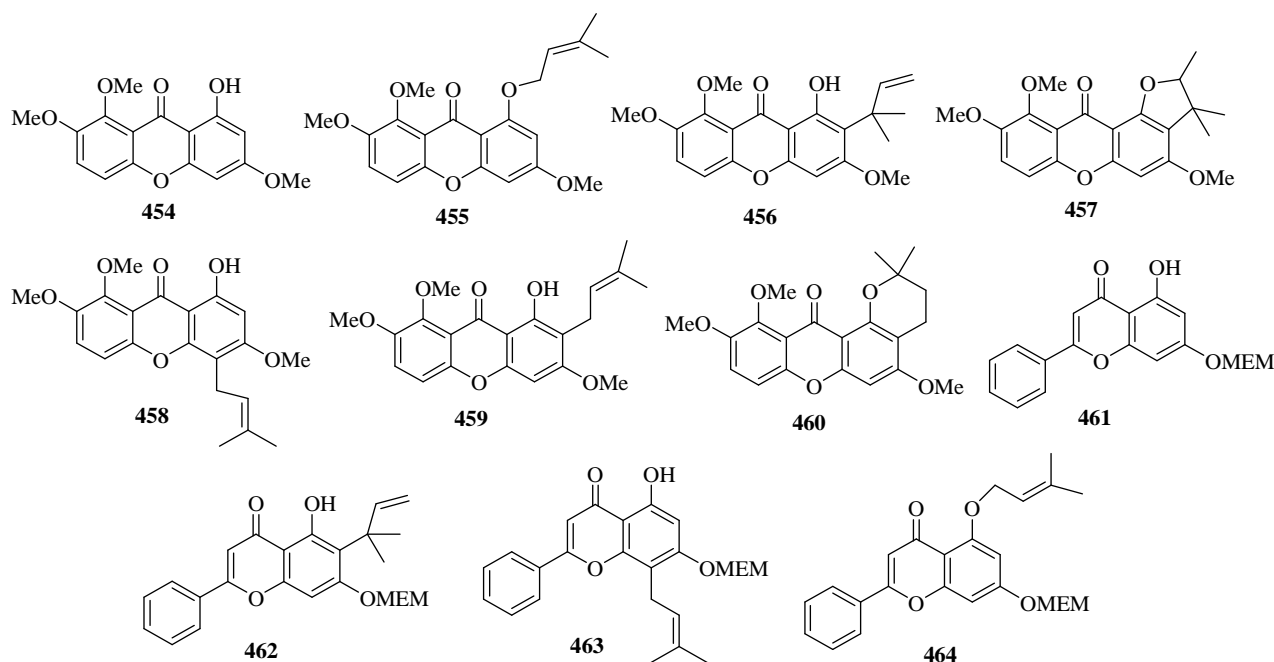


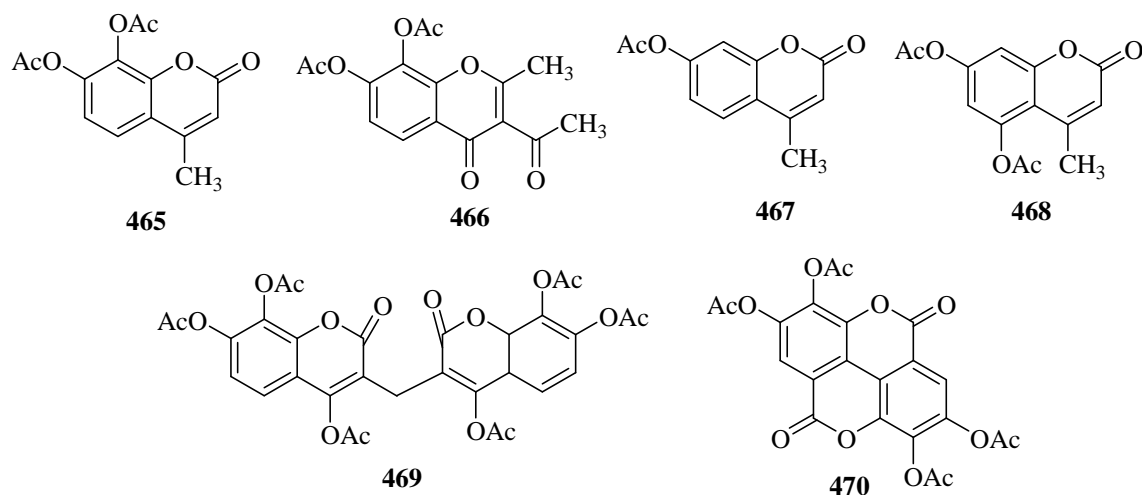
Figure 53. Dimethylallyl (DMA) derivatives of xanthone (decussatin)

Table 64. Differential affinity of binding to P-glycoprotein recombinant domain of prenylated xanthenes; comparison to 7-MEM-chrysin derivatives

Xanthone derivative	Apparent K_d (μ M)	Δ Fmax (%)	Flavone	Apparent K_d (μ M)	Δ Fmax (%)	derivative	K_d (μ M)
455	28.8 \pm 3.4	89.2 \pm 5.7	461	8.05 \pm 0.63	73.1 \pm 2.3		
456	13.9 \pm 0.88	81.8 \pm 1.9	462	0.10 \pm 0.04	42.3 \pm 2.0		
457	0.25 \pm 0.05	45.8 \pm 1.3	463	0.10 \pm 0.01	48.8 \pm 0.6		
458	24.8 \pm 1.4	87.8 \pm 1.8	464	6.10 \pm 0.34	81.8 \pm 1.9		
459	0.59 \pm 0.05	81.9 \pm 1.9					
460	0.39 \pm 0.22	35.0 \pm 4.					

2-11-4. Xanthenes as protein transacetylase inhibitors

In 2007, Hanumantharao G. Raj *et al.* reported the comparison of the specificities of acetoxy derivatives **465-470** (Figure 54) of coumarin, biscoumarins, chromones, flavones, isoflavones and xanthenes with special reference to the phenyl moiety/bulky group on the pyran ring of PA. The earlier work carried out in laboratory led to the identification of a novel rat liver microsomal enzyme termed as acetoxy drug: protein transacetylase (TAase), catalyzing the transfer of acetyl group from polyphenolic acetates (PA) to functional proteins (Table 65). The results clearly indicated that compounds having phenyl moieties, when used as the substrates, resulted in a significant reduction of TAase catalyzed activity. The alteration in TAase catalyzed activation of NADPH cytochrome c reductase and inhibition of benzene-induced micronuclei in bone marrow cells by PA were in tune with their specificities to TAase [90].

**Figure 54. Acetoxy derivatives of coumarin, biscoumarins, chromones, flavones, isoflavones and xanthenes****Table 65. Modulation of micronuclei induction in benzene-treated bone marrow cells of rats by acetylated polyphenols**

Group ^a	Treatment	Mean	Micronuclei/1000 cells
1	Control	1.25	0.6289-1.8711
2	Benzene	7.60	5.8894-8.7106
3	Benzene + 465 ^b	2.66(65) ^c	1.8101-3.5232
1	Control	1.50	0.4243-2.5757
2	Benzene	7.83	6.8016-8.5650
3	Benzene + 467 ^b	4.33(44.6) ^c	3.4765-5.1919
1	Control	1.75	1.1289-2.3711
2	Benzene	7.50	6.0531-8.9464
3	Benzene + 469 ^b	4.66(37.86) ^c	3.8099-5.5235
1	Control	1.75	1.1199-2.3612
2	Benzene	8.00	6.5160-9.4840
3	Benzene + 470 ^b	4.83(39.62) ^c	3.6066-6.060

Group 1. Control Group: Animals received DMSO 0.1 ml i.p. After 1 h, again DMSO 0.1 ml was given i.p.

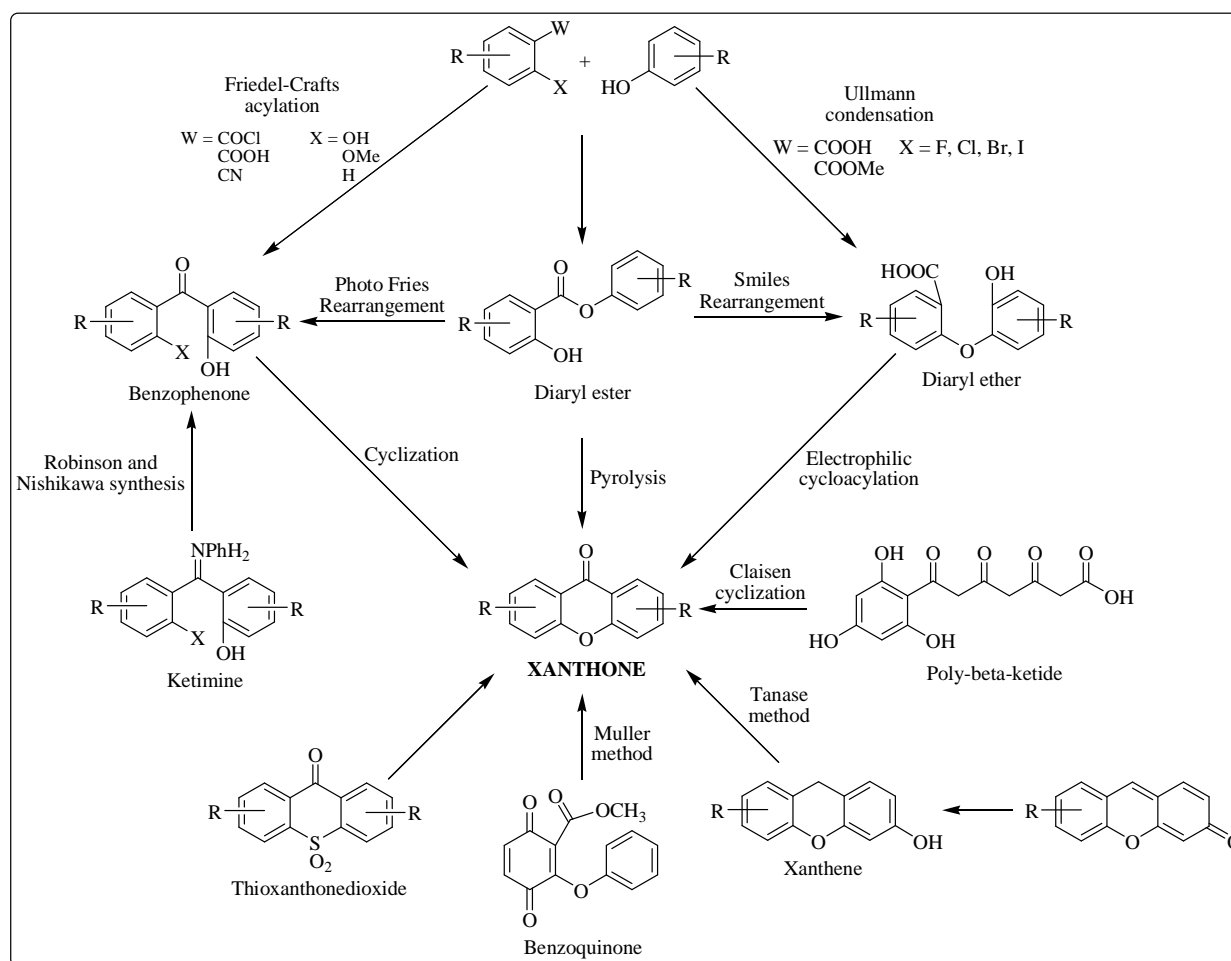
Group 2. Benzene Group: DMSO 0.1 ml was given i.p. After 1 h, benzene 0.03 ml/kg BW in 0.1 ml DMSO was given i.p.

Group 3. Benzene + Test compound: Test compound 300 mg/kg BW in 0.1 ml DMSO was given i.p. After 1 h, was again test compound 300 mg/kg BW in 0.1 ml DMSO along with benzene 0.03 ml/kg BW 0.1 ml DMSO given i.p.

^a Four male rats weighing approximately 100 gm were taken in each case. All animals were sacrificed after 26 h and bone marrow cells were harvested and stained micronuclei were scored as described earlier.

^b These numbers denote the test compound number.

^c Numbers in parenthesis denote the percentage of inhibition of formation of micronuclei in benzene-treated bone marrow cells due to test compound.

3. POPULAR METHODOLOGIES FOR THE SYNTHESIS OF XANTHONIC TRICYCLIC SYSTEM [91].**Figure 55. Methods for synthesis of xanthenes****CONCLUSION**

In brief, we emphasized on different researches related to xanthenes in which we summarized the synthetically obtained xanthone derivatives, arranged in a manner depending upon the biological properties exhibited by them. The recent studies evinced that the use of different substituted xanthone derivatives have left a leading light in the field of search for new agents acquiring different biological activities. The reports revealed that different substitutions on the basic xanthone skeleton bestow it with a wide range of biological attributes. Also some of the xanthone derivatives showed very good results as anticancer agents, for instance compound **84** possesses IC_{50} value as low as $0.65 \mu M$ against PC-3 human cancer cell line. Some compounds such as **225** exhibited potent anticonvulsant activity, as well. Beside this many derivatives showed significant activity against microorganisms (bacteria, virus, fungal etc.). On the other side xanthone derivatives also constitute antiasthmatic and xanthine oxidase inhibition potential (Figure 56).

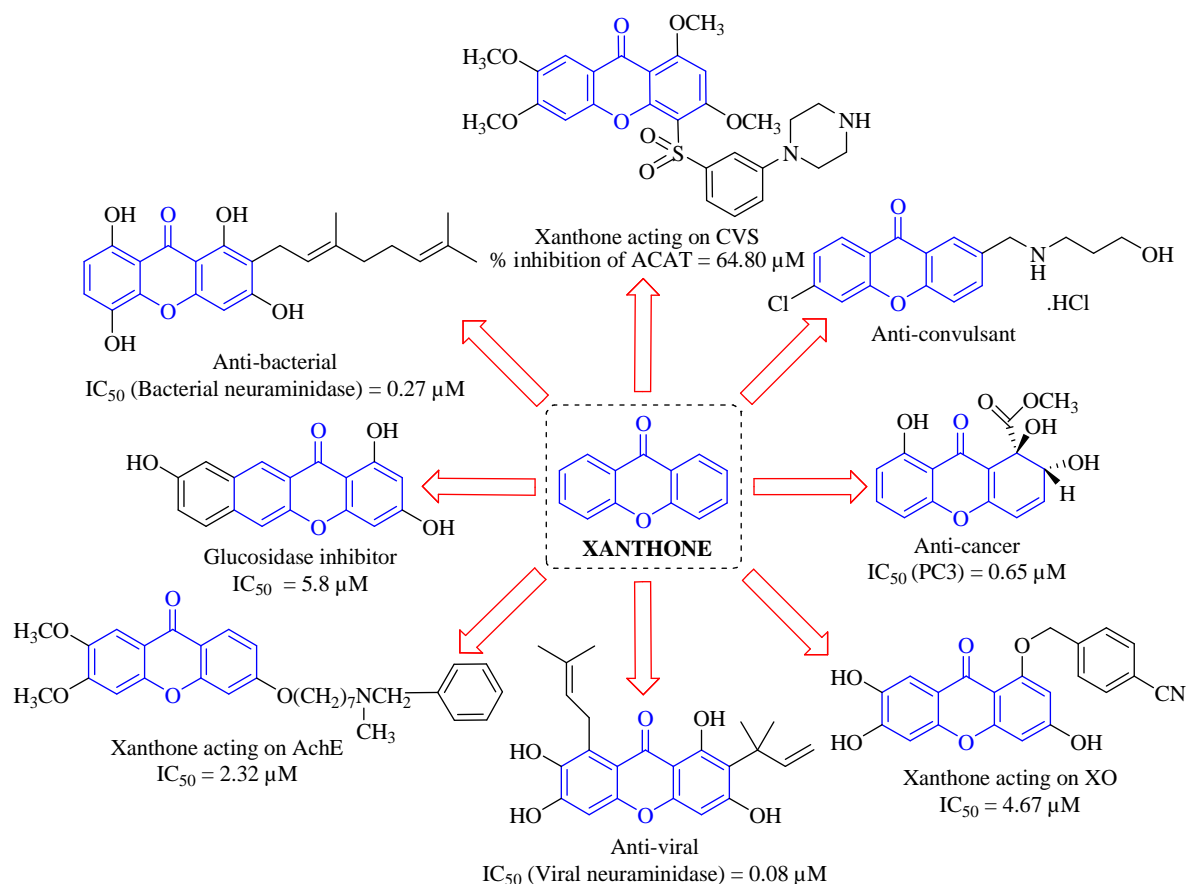


Figure 56. Recently reported xanthone derivatives with diverse biological attributes

Therefore, the review describe xanthenes as one of the widely adopted O-heterocyclic system as a very efficient moiety possessing numerous biological activities. Its potential has been supported by the reports summarized in this review. In future xanthenes would be of great importance for the development of different biologically active entities which could help to eradicate various diseases. Researchers must aim at the development of some new xanthone derivatives with effective and efficient substitutions, thus exploring this central and fundamental nucleus to a large extent.

REFERENCES

- [1] https://en.wikipedia.org/wiki/Heterocyclic_compound. Retrieved on 22 September 2015.
- [2] <http://goldbook.iupac.org/H02798.html>. Retrieved on 22 September 2015.
- [3] TP Selvam; CR James; PV Dniandev and S. K. Valzita, *Res. Pharm.*, **2012**, 2(4), 01-09.
- [4] H Singh, H Singh, S Sharma; PMS Bedi. *Heterocycles*, **2015**, 91(11), 2043-2085.
- [5] <http://www.rxlist.com/clarinex-drug.htm> Retrieved on 24 September 2015.
- [6] JM Nelson; TM Chiller; JH Powers; FJ Angulo. *Clin. Infect. Dis.*, **2007**, 44(7), 977-980.
- [7] <http://www.medicinenet.com>. Retrieved on September 2015.
- [8] <http://www.drugbank.ca>. Retrieved on 24 September 2015.
- [9] <http://www.rxlist.com>. Retrieved on 24 September 2015.
- [10] <http://www.sigmaaldrich.com>. Retrieved on 24 September 2015.
- [11] <http://www.rxlist.com/cerubidine-drug.htm>. Retrieved on 24 September 2015.
- [12] <http://www.webmd.com/drugs/2/drug-5574/carvedilol-oral/details>. Retrieved on 24 September 2015.
- [13] <https://www.google.co.in> Retrieved on 24 September 2015.
- [14] <http://chemocare.com/chemotherapy/drug-info/idamycin.aspx>. Retrieved on 24 September 2015.
- [15] SM Kupchan; DR Streelman; AT Sneden. *J. Nat. Pro.*, **1980**, 43(2), 296-301.
- [16] DK Winter; DL Sloman; JA Porco. *J. Nat. Pro. Rep.*, **2013**, 30(3), 382-391.
- [17] CN Lin; SJ Liou; TH Lee; YC Chuang; S Won. *J. Pharm. P.cology.*, **1996**, 48(5), 539-544.
- [18] CA Chen; RH Yeh; DS Lawrence. *J. Am. Chem. Soc.*, **2002**, 124(15), 3840-3841.

- [19] LF Steiner; SA Summerland. *J. Eco. Ento.*, **1943**, 36, 435-439.
- [20] JH Cheng; AM Huang; TC Hour; SC Yang; YS Pu; CN Lin. *Eur. J. Med. Chem.*, **2011**, 46(4), 1222-1231.
- [21] Angiosperm Phylogeny Group, *Bot. J. Lin. Soc.*, **2003**, 141, 399-436.
- [22] <http://health-gokilfree.blogspot.in/p/ingredients-and-benefits-xanthone-plus.html>. Retrieved 27 Sept 2015.
- [23] <http://www.fit-leader.com/eng/xanthones.shtml>. Retrieved 24 Sept **2015**.
- [24] <http://www.mx3.ph/products/food-supplements/mx3-500mg-capsule/>. Retrieved 24 Sept **2015**.
- [25] Y Liu; L Zou; L Ma; WH Chen; B Wang; ZL Xu. *Bioorg. Med. Chem.*, **2006**, 14(16), 5683-5690.
- [26] EJ Seo; MJ Curtis-Long; BW Lee; HY Kim; YB Ryu; TS Jeong; WS Lee; KH Park. *Bioorg. Med. Chem. Lett.*, **2007**, 17(23), 6421-6424.
- [27] Y Liu; L Ma; WH Chen; B Wang; ZL Xu. *Bioorg. Med. Chem.*, **2007**, 15(8), 2810-2814.
- [28] Y Liu; Z Ke; J Cui; WH Chen; L Ma; B Wang. *Bioorg. Med. Chem.*, **2008**, 16(15), 7185-7192.
- [29] GL Li; JY He; A Zhang; Y Wan; B Wang; WH Chen. *Eur. J. Med. Chem.*, **2011**, 46(9), 4050-4055.
- [30] M Aoki; Y Itezono; H Shirai; N Nakayama; A Sakai; Y Tanaka; A Yamaguchi; N Shimma; K Yokose. *Tetrahedron Lett.*, **1991**, 32(36), 4737-4740.
- [31] YJ Xu; SG Coa; XH Wu; YH Lai; BHK Tan; JT Pereira; SH Goh; G Venkatraman; LJ Harrison; K. Y. Sin. *Tetrahedron Lett.*, **1998**, 39(49), 9103-9106.
- [32] M Pedro; F Cerqueira; ME Sousa; MSJ Nascimento; M Pinto. *Bioorg. Med. Chem.*, **2002**, 10(12), 3725-3730.
- [33] B Madan; I Singh; A Kumar; AK Prasad; HG Raj; VS Parmar; B Ghosh. *Bioorg. Med. Chem.*, **2002**, 10(11), 3431-3435.
- [34] YS Zou; AJ Hou; GF Zhu; YF Chen; HD Sun; QS Zhao. *Bioorg. Med. Chem.*, **2004**, 12(8), 1947-1953.
- [35] K Matsumoto; Y Akao; K Ohguchi; T Ito; T Tanaka; M Iinuma; Y Nozawa. *Bioorg. Med. Chem.*, **2005**, 13(21), 6064-6069.
- [36] EMK Wijeratne; TJ Turbyville; A Fritz; L Whitesell; AAL Gunatilaka. *Bioorg. Med. Chem.*, **2006**, 14(23), 7917-7923.
- [37] S. Woo, J. Jung, C. Lee, Y. Kwon; Y Na. *Bioorg. Med. Chem. Lett.*, **2007**, 17(5), 1163-1166.
- [38] RAP Castanheiro; MMM Pinto; AMS Silva; SMM Cravo; L Gales; AM Damas; N Nazareth; MSJ Nascimento; G. Eaton. *Bioorg. Med. Chem.*, **2007**, 15(18), 6080-6088.
- [39] M Varache-Lembege; S Moreau; S Larrouture; D Montaudon; J Robert; A Nuhlich. *Eur. J. Med. Chem.*, **2008**, 43(6), 1336-1343.
- [40] Isakovic; T Jankovic; L Harhaji; S Kostic-Rajacic; Z Nikolic; V Vajs; V Trajkovic. *Bioorg. Med. Chem.*, **2008**, 16(10), 5683-5694.
- [41] T Itoh; K Ohguchi; M Iinuma; Y Nozawa; Y Akao. *Bioorg. Med. Chem.*, **2008**, 16(8), 4500-4508.
- [42] E Sousa; A Paiva; N Nazareth; L Gales; AM Damas; MSJ Nascimento; M Pinto. *Eur. J. Med. Chem.*, **2009**, 44(9), 3830-3835.
- [43] HF Wang; R Shen; N Tang. *Eur. J. Med. Chem.*, **2009**, 44(11), 4509-4515.
- [44] JH Cheng; AM Huang; TC Hour; SC Yang; YS Pu; CN Lin. *Eur. J. Med. Chem.*, **2011**, 46(4), 1222-1231.
- [45] KY Jun; EY Lee; MJ Jung; OH Lee; ES Lee; HYP Choo; Y Na; Y Kwon. *Eur. J. Med. Chem.*, **2011**, 46(6), 1964-1971.
- [46] CT Yen; K Nakagawa-Goto; TL Hwang; S Morris-Natschke; K Bastow; YC Wu. *Bioorg Med Chem Lett.*, **2012**, 22(12), 4018-4022.
- [47] DF Dibwe; S Awale; S Kadota; H Morita; Y Tezuka. *Bioorg. Med. Chem.*, **2013**, 21(24), 7663-7668.
- [48] CMG Azevedo; CMM Afonso; D Sousa; RT Lima; MH Vasconcelos; M Pedro; J Barbosa; AG Corrêa; S Reis; MMM Pinto. *Bioorg. Med. Chem.*, **2013**, 21(11), 2941-2959.
- [49] CMG Azevedo; CMM Afonso; JX Soares; S Reis; D Sousa; RT Lima; MH Vasconcelos; M Pedro; J Barbosa; L Gales; MMM Pinto. *Eur. J. Med. Chem.*, **2013**, 69, 798-816.
- [50] Murata; T Fukuzumi; S Umemoto; K Nakatani. *Bioorg. Med. Chem. Lett.*, **2013**, 23(1), 252-255.
- [51] SE Park; IH Chang; KY Jun; E Lee; ES Lee; Y Na; Y Kwon. *Eur. J. Med. Chem.*, **2013**, 69, 139-145.
- [52] M Dai; X Yuan; J Kang; ZJ Zhu; RC Yue; H Yuan; BY Chen; WD Zhang; RH Liu; QY Sun. *Eur. J. Med. Chem.*, **2013**, 69, 159-166.
- [53] ZM Yang; J Huang; JK Qin; ZK Dai; WL Lan; GF Su; H Tang; F Yang. *Eur. J. Med. Chem.*, **2014**, 85, 487-497.
- [54] C Fernandes; K Masawang; ME Tiritan; E Sousa; V Lima; C Afonso; H Bousbaa; W Sudprasert; M Pedro; MM Pinto. *Bioorg. Med. Chem.*, **2014**, 22(3), 1049-1062.
- [55] X Fei; M Jo; B Lee; SB Han; K Lee; JK Jung; SY Seo; YS Kwak. *Bioorg. Med. Chem. Lett.*, **2014**, 24(9), 2062-2065.
- [56] TC Chen; CL Wu; CC Lee; CL Chen; DS Yu; HS Huang. *Eur. J. Med. Chem.*, **2014**, 103, 615-627.
- [57] S Motavallizadeh; A Fallah-Tafti; S Maleki; AN Shirazi; M Pordeli; M Safavi; SK Ardestani; S Asd; R Tiwari; D Oh; A Shafiee; A Foroumadi; K Parang; T Akbarzadeh. *Tetrahedron Lett.*, **2014**, 55(2), 373-375.
- [58] H Marona; E Pekala; L Antkiewicz-Michalu; M Walczak; E Szneler. *Bioorg. Med. Chem.*, **2014**, 16(15), 7234-7244.

- [59] N Szkaradek; A Gunia; AM Waszkielewicz; L Antkiewicz-Michaluk; M Cegła; E Szneler; H Marona. *Bioorg. Med. Chem.*, **2013**, 21(5), 1190-1198.
- [60] M Waszkielewicz; A Gunia; N Szkaradek; K Pytka; A Siwek; G Satała; AJ Bojarski; E Szneler; H Marona. *Bioorg. Med. Chem. Lett.*, **2013**, 23(15), 4419-4423.
- [61] J Ngoupayo; T K Tabopda; MS Ali. *Bioorg. Med. Chem.*, **2009**, 17(15), 5688-5695.
- [62] HW Ryu; MJC Long; S Jung; YM Jin; JK Cho; YB Ryu; WS Lee; KH Park. *Bioorg. Med. Chem.*, **2010**, 18(17), 6258-6264.
- [63] H Zou; JJ Koh; J Li; S Qiu; TT Aung; H Lin; R Lakshminarayanan; X Dai; C Tang; FH Lim; L Zhou. *J. Med. Chem.*, **2013**, 56(6), 2359-2373.
- [64] EE Eltamany; UR Abdelmohsen; AK Ibrahim; HA Hassanean; U Hentschel; SA Ahmed. *Bioorg. Med. Chem. Lett.*, **2014**, 24(21), 4939-4942.
- [65] K Matsuzaki; N Tabata; H Tomoda; Y Iwai; H Tanaka; S Oamura. *Tetrahedron Lett.*, **1993**, 34(51), 8251-8254.
- [66] S Moreau; M Varache-Lembege; S Larrouture; D Fall; A Neveu; G Deffieux; J Vercauteren; A Nuhrich. *Eur. J. Med. Chem.*, **2002**, 37(3), 237-253.
- [67] JJ Omolo; MM Johnson; SF Vuuren; CB Koning. *Bioorg. Med. Chem. Lett.*, **2011**, 21(23), 7085-7088.
- [68] YB Ryu; MJ Curtis-Long; JW Lee; JH Kim; JY Kim; KY Kang; WS Lee; KH Park. *Bioorg. Med. Chem.*, **2009**, 17(7), 2744-2750.
- [69] TT Dao; TT Dang; PH Nguye; E Kim; PT Thuong; WK Oh. *Bioorg. Med. Chem. Lett.*, **2012**, 22(11), 3688-3692.
- [70] T Zhou; Q Shi; CH Chen; L Huang; P Ho; SL Morris-Natschke; KH Lee. *Eur. J. Med. Chem.*, **2012**, 47(1), 86-96.
- [71] JS Sawyer; RF Baldwin; LL Froelich; DL Saussy; WT Jackson. *Bioorg. Med. Chem. Lett.*, **1993**, 3(10), 1981-1984.
- [72] JS Sawyer; EA Schmittling; NJ Bach; SR Baker; LL Froelich; DL Saussy; P Marder; WT Jackson. *Bioorg. Med. Chem. Lett.*, **1994**, 4(17), 2077-2082.
- [73] L Saraiva; P Fresco; E Pinto; E Sousa; M Pinto; J Goncalves. *Bioorg. Med. Chem.*, **2002**, 10(10), 3219-3227.
- [74] L Saraiva; P Fresco; E Pinto; E Sousa; M Pinto; J Goncalves. *Bioorg. Med. Chem.*, **2003**, 11(7), 1215-1225.
- [75] LW Wang; JJ Kang; IJ Chen; CM Teng; CN Lin. *Bioorg. Med. Chem.*, **2002**, 10(3), 567-572.
- [76] DJ Jiang; GY Hu; JL Jiang; HL Xiang; HW Deng; YJ Li. *Bioorg. Med. Chem.*, **2003**, 11(23), 5171-5177.
- [77] H Hu; H Liao; J Zhang; W Wu; J Yan; Y Yan; Q Zhao; Y Zou; X Chai; S Yu; Q Wu. *Bioorg. Med. Chem. Lett.*, **2010**, 20(10), 3094-3097.
- [78] RA Dodean; JX Kelly; D Peyton; GL Gard; MK Riscoe; RW Winter. *Bioorg. Med. Chem.*, **2008**, 16(3), 1174-1183.
- [79] M Isaka; S Palasarn; P Auncharoen; S Komwijit; EBG Jones. *Tetrahedron Lett.*, **2009**, 50(3), 284-287.
- [80] J Kornsakulkarn; S Saepua; P Laksanacharoen; P Rachtawee; C Thongpanchang. *Tetrahedron Lett.*, **2013**, 54(29), 3813-3815.
- [81] BW Lee; JH Lee; ST Lee; HS Lee; WS Lee; TS Jeong; KH Park. *Bioorg. Med. Chem. Lett.*, **2005**, 15(24), 5548-5552.
- [82] KH Park; YD Park; JM Han; KR Im; BW Lee; Y Jeong; TS Jeong; WS Lee. *Bioorg. Med. Chem. Lett.*, **2006**, 16(21), 5580-5583.
- [83] CMM Santos; M Freitas; D Ribeiro; A Gomes; AMS Silva; JAS Cavaleiro; E Fernandes. *Bioorg. Med. Chem.*, **2010**, 18(18), 6776-6784.
- [84] EV Buravlev; OG Shevchenko; AV Kutchin. *Bioorg. Med. Chem. Lett.*, **2015**, 25(4), 826-829.
- [85] E Vieira; J Huwyler; S Jolidon; F Knoflach; V Mutel; J Wichmann. *Bioorg. Med. Chem. Lett.*, **2005**, 15(20), 4628-4631.
- [86] C Fernandes; L Oliveira; ME Tiritan; L Leitao; A Pozzi; JB Noronha-Matos; P Correia-de-Sa Madalena; M. Pinto. *Eur. J. Med. Chem.*, **2012**, 55, 1-11.
- [87] L Hu; H Hu; W Wu; X Chai; J Luo; Q Wu. *Bioorg. Med. Chem. Lett.*, **2011**, 21(13), 4013-4015.
- [88] L Piazza; F Belluti; A Bisi; S Gobbi; S Rizzo; M Bartolini; V Andrisano; M Recanatini; A Rampa. *Bioorg. Med. Chem.*, **2007**, 15(1), 575-585.
- [89] DN Tchamo; MG Dijoux-Franca; AM Mariotte; E Tsamo; JB Daskiewicz; C Bayet; D Barron; G Conseil; AD Pietro. *Bioorg. Med. Chem. Lett.*, **2000**, 10(12), 1343-1345.
- [90] Kumar; BK Singh NK; Sharma; K Gyanda; SK Jain; YK Tyagi; AS Baghel; M Pandey; SK Sharma; AK Prasad; SC Jain; RC Rastogi; HG Raj; AC Watterson; EV Eycken; VS Parmar. *Eur. J. Med. Chem.*, **2007**, 42(4), 447-455.
- [91] ME Sousa; MMM Pinto. *C. Med. Chem.*, **2005**, 12(21), 2447-2479.